Benthic invertebrate assemblages and sediment characteristics

of cold seeps in the Hikurangi Margin, New Zealand

Sheree Boyd

A thesis submitted to the Auckland University of Technology

in partial fulfillment of the requirements for the degree of

Master of Applied Science

1 May 2009

School of Applied Science

Primary supervisor: Dr Andrea Alfaro

Table of Contents

List of Tables

List of Figures

List of Appendices

Attestation of Authorship

I hearby declare that this submission is my own work and that, to the best of my knowledge and belief, it contains no material previously published or written by another person (except where explicitly defined in the acknowledgements), nor material which to a substantial extent has been submitted for the award of any other degree or diploma of a university or other institution of higher learning.

Acknowledgement

Abstract

Cold seep ecosystems in the deep sea are fuelled by chemosynthetic processes based on methane emission to the sediment surface from gas hydrate disassociation, methanogenesis or thermogenic processes. While cold seep ecosystems have been studied in the last three decades worldwide, little is known about New Zealand's cold seep habitats and associated fauna. A joint German-New Zealand cruise to the Hikurangi Margin in early 2007 enabled biological and sediment sampling to investigate the biological and sedimentological relationships and variability of seeps and their faunal diversity. Multi-disciplinary approaches were employed that included X-ray radiography, stratigraphic descriptions, lebensspuren traces analysis, sediment grain size analysis, determination of total organic content, carbonate content and its stable isotopic composition, and analysis of benthic invertebrate assemblages of seep habitats. The results of this study revealed three distinctive habitats and associated fauna based on the sediment characteristics and faunal type. Habitat 1 includes all sites pertaining to Omakere Ridge, a seep-related habitat comprised of layers of very poorly sorted, sandy silt, shell hash and bands of methane-derived authigenic aragonitic carbonate nodules with low total organic content (TOC). Due to the characteristics of the sediments and death assemblages of molluscs, it is inferred that Habitat 1 methane seepage is actively diffusive, waning or dormant. Habitat 2 describes sites that are either non-seep or relic and applies to those at Bear's Paw and Kaka. Habitat 2 constituted of shell hash overlain with very poorly sandy silt, and low carbonates content and low to medium TOC. Habitat 3 describes non-seep related habitats, and includes all sites of the Wairarapa region and one reference site from Kaka also falls into this category. Sediments for Habitat 3 constituted poorly sorted silt with high TOC and low carbonate

content which can be explained by their close proximity to land and converging sea currents. The mineral components of the background siliciclastic sediments for all sites studied originated in the Tertiary mudstone of the East Coast Basin. The characteristics of seep habitats of the Hikurangi Margin were comparable to that of the Northern Hemisphere modern seep counterparts, although the abundance and distributions of seep fauna were low. Results from this research have enhanced our understanding on the spatial and variability of methane fluxes and their affects on the duration of cold seep ecosystems, especially for New Zealand. However, more such studies are essential to increase our understanding of seep sediments and explain disturbance-sediment-benthic invertebrate interactions.

1. INTRODUCTION

Cold seep ecosystems are established on the continental margins where methane gas or pore fluid is released from deep within the seafloor by disturbances such as gas hydrate disassociation, seismic activity or subduction. That methane seepage provides energy for the microbial communities within the sediments, which in turn, support the chemosynthesis-based benthic communities. These communities thrive in extreme environments thus making them unique and worthy of study. However, the characteristics and functioning of the cold seep ecosystems are not fully understood despite many studies spanning almost three decades. The aim of this study is to report on the uniqueness of cold seep habitats by investigating various components that constitute such habitats and to compare findings between local regions and with Northern Hemisphere counterparts.

1.1 Background

Ocean makes up about 70% of the Earth's surface and about 50% of the ocean is deeper than 4,000 m below sea level (Bruun 1956). The sea floor is overlain with sediments, derived from continental rocks that undergo weathering, providing habitats for marine benthic communities. There are three major types of marine sediments comprising lithogenous, biogenous and hydrogenous (Seibold and Berger 1993).

1.1.1 *Lithogenous sediments*

Quartz is most abundant in lithogenous sediments; while clay minerals of chlorite, illite, kaolinite and montmorillonite make up the lithogenous sediments of the deep-sea (Futterer 2006). The grain size of lithogenous sediments is proportional to the energy required to lay the particles down and its proximity to the source. For example, high energy environments, such as exposed coastal shores in close proximity to the source,

have coarse grained particles (sand); whereas, at the deep-sea, where the energy level is low and farther from the land, fine-grained particles (silt and clay) are more evident. Wind can carry fine-grained particles of up to 80 μm in size, which results in silt and clay fraction (Futterer 2006). Lithogenous sediments make up ~ 70% of the volume of marine sediments (Leeder 1982), ~ 50% of these are clay minerals, and less than 1% of the sediments contain heavy minerals (Futterer 2006).

1.1.2 *Biogenous sediments*

The deposition of calcium carbonate on the seafloor is derived from the remains of organisms that constituted biogenous sediments, which make up ~30 % of the volume of marine sediments (Leeder 1982). Shells and skeletal remains of benthic organisms make up biogenous sediments on the continental shelves. Planktonic remains make up the biogenous of the deep sea beyond the continental shelves in the abyssal depth (Seibold and Berger 1993).

1.1.3 *Hydrogenous sediments*

Hydrogenous sediments are derived from the precipitation of minerals in the seawater or pore-water and make up a small part of marine sediments. Such minerals include metal sulfides, phosphate, manganese nodules and carbonates. Metal sulfides are associated with hydrothermal vents. Phosphates occur in areas with high primary productivity and upwellings. Manganese nodules associate with hydrothermal vents, the side of seamounts or in areas with marine sediments containing high concentrations of volcanic materials from the mantle (Judd and Hovland 2007). Carbonates come in various forms ranging from small nodules within the sediments to slabs or crusts on the seafloor. They are common features of the continental margins, especially in areas where active or relict methane seepage occurs. Carbonates are by-products of chemical reactions,

which take place in anoxic sediments as follows: methane reacts with sulfate ions to form bicarbonate ions, hydrogen sulfide ions and water. Subsequently, calcium ions from seawater react with bicarbonate ions to form calcium carbonate, carbon dioxide and water (Baker and Burns 1985; Judd and Hovland 2007). In addition, carbonates are produced by a consortium of methanotrophic archaea and sulphate-reducing bacteria involved in anaerobic oxidation of methane within the sediments or at the sediment-water interface at seeps. These are methane derived authigenic carbonates and their mineral content as well as carbon and oxygen isotopic composition varies depending on in situ conditions favouring the precipitation of minerals such as aragonite, calcite and magnesite (Greinert et al. 2001; Muralidhar et al. 2006; Naehr et al. 2007). Such conditions include pore-water chemistry, methane flux, sulphate concentrations, rate of microbial activities (Muralidhar et al. 2006) as well as sedimentation rate and benthic organisms' bioturbation/bioirrigation activities (Luff et al. 2004). Carbonate slabs on the seafloor, which were initially formed below the sediment surface, are brought to the surface by tectonic activity such as uplifting or by exposure due to sediment erosion (Naehr et al. 2007). These slabs provide a habitat for epibenthic invertebrates. .

1.1.4 *Classification of deep-sea sediments*

Murray and Renard (1891) were presumably the first to describe two types of marine sediments as terrigenous deposits and pelagic deposits based on their composition, proximity to source and nature of deposition. Terrigenous deposits refer to rock fragments or grains that were washed down from land and accumulated on the continental margins.   Pelagic deposits are formed as clay and oozes in the deep sea, farther from the land where sedimentation rates are low. Berger (1974) added the term 'hemipelagic deposits' to the classification of marine sediment by which deep-sea

sediments are subdivided into two types, pelagic deposits and hemipelagic deposits. Hemipelagic deposits are composed of muds, which are subdivided into calcareous muds ($CaCO_3$ content >30%), terrigenous muds ($CaCO_3$ <30%; quartz, feldspar, mica dominant) and volcanogenic muds ($CaCO_3$ content < 30%). The sedimentation rate varies between millimetres and 30 centimetres per a thousand years, which is dependant on the proximity to sediment source (Seibold and Berger 1993).

1.1.5 *Environmental conditions of the deep-sea*

Environmental conditions of the deep-sea are extreme with low temperature, high salinity, high hydrostatic pressure, low oxygen (~ 5 mL 1^{-1}), no light and low productivity. The ocean's temperature and salinity change with respect to depth, and temperature decreases from ~ 20°C to ~ 5°C as depth increases. Hydrostatic pressure increases with an increasing depth, and pressure increases 1 atmosphere (atm) for every 10 metres of water depth. That is, at a water depth of 1,000 metres, the pressure is 100 atm. Salinity changes very little with increasing depth and on an average, the salinity is 35 ‰. Oxygen is abundant in the photic zone, a sunlit region in the top ~100 metres of the ocean surface. However at deeper depths between 600 and 1100 metres below sea level, the concentration of oxygen is reduced to < 0.5 mL per litre. This level of oxygen is known as an oxygen minimum zone (OMZ). Below this zone, the oxygen concentration increases to 5 mL 1^{-1}. The degree of oxygen availability exerts control on the abundance, composition and diversity of benthic fauna and correlates with food availability (Levin et al. 1991 1991). Meiofauna and microorganisms tend to be more tolerant of low oxygen concentrations compared with macrofauna. Below the photic zone is a deep-sea devoid of sunlight necessary for photosynthesis-based primary production. Phytoplankton, free-floating photosynthetic organisms contribute to

primary productivity and oceanic food webs in the open sea. Their production occurs in the photic zone at a rate of 50 g C/m^{2}yr (Seibold and Berger 1993). However, the abundance and biomass of phytoplankton decreases exponentially with increasing depth. Only ~ 1% of the particulate organic matter derived from phytoplankton production reaches the deep-sea floor (Suess 1980). Zooplankton consumes phytoplankton and in turn is consumed by small fishes followed by large carnivorous fishes, cephalopods, mammals and marine birds. These form the food web of the photic realm of the open sea and the scarcity of food source increases with increasing depth and distance from the land. The main food source available in the deep-sea is the marine snow, an aggregation of organic detritus from the food webs, which provides energy for the mesopelagic organisms (Burd and Jackson 2009). The remainder of marine snow blankets the deep-sea sediments as oozes, which are used by microorganisms and some deposit feeder invertebrates. The scarcity of food source may be responsible for the low densities of benthic communities of the deep-sea homogeneous sediments. However, the deep-sea floor hosts a variety of habitats and associated benthic communities and these rely on chemosynthetic processes for an energy source (Van Dover 2000; Judd and Hovland 2007). The fate of organic matter incorporated into sediments is discussed below.

1.1.6 *Early diagenesis and biogeochemical zonation*

Early diagenesis as defined by Berner (1980) is the transformation by which, following deposition, the marine sediments incorporated with organic matter undergo changes by physical, chemical and biological processes. Physical processes include 1) the compaction and dewatering of deposited sediments due to the pressure from burial; 2) slumping caused by gravity, seismic activities or upward expulsion of hydrocarbon

seepages; and 3) erosion from the uplifting of seafloor by tectonic activity. Chemical processes include microbial metabolic reactions in the degradation of organic matter, the dissolution and precipitation of minerals (reduction-oxidation reactions) and the formation of methane derived authigenic carbonates. The biological process includes bioturbation activities by benthic organisms that alter the formation of layers in sediments.

Due to these processes, the biogeochemical zonation of sediments is formed comprising three layers. These stratums, starting downward from the sediment surface, are oxic, suboxic and anoxic zones (Froelich et al. 1979) and these correspond with the microorganisms' use of oxygen, sulphate and methane as oxidants for their metabolism (Judd and Hovland 2007). As the sediment depth increases, the oxygen supply diminishes and is replaced with sulphate followed by methane. The sulphate-methane transition zone (SMTZ) is a region in the subsurface where the concentration of sulphate is balanced by concentration of methane. However, below SMTZ, the methane concentration increases with increasing depth. Likewise, aerobic microorganisms give way to sulphate reducing bacteria and then to methanogens (methane-producing microorganisms such as methanotrophic archaea). Early diagenesis of marine sediment occurs in the first few hundred metres below seafloor where the temperature does not exceed 25°C (Berner 1980). This enables microbial activity to take place at these depths and this is discussed in the following sections.

Oxic zone
The oxic zone is in the upper part of the sediments column overlain by oxygenated seawater. Its depth varies from millimetres to centimetres depending on sedimentation rate, organic matter supply, biological oxygen demand (BOD – a measure of the amount

of oxygen consumed by microorganisms in aerobic oxidation of organic matter) and the rate of microbial activity (Judd and Hovland 2007). In addition, bioturbation and/or bioirrigation activities by benthic organisms oxygenate sediments and these have effects on the oxic zone depth. Oxygen is introduced into the seawater via photosynthetic processes in the photic regions of the ocean and also by input from the atmosphere across the ocean-atmosphere interface. This oxygen-rich water is brought to the deep-sea floor by deep water circulation. Organic matter in the sediments not used by benthic invertebrates is degraded by microbial activity in the presence of oxygen. From this activity, carbon dioxide, nitrate and phosphate are released as products. In the oxygen minimum zone (OMZ) where oxygen is a limiting factor or below the oxygen penetration depth in the sediments, microorganisms use nitrate as an electron acceptor in the degradation of organic matter (Hensen et al. 2006).

Suboxic zone

The suboxic zone is at the oxic-anoxic interface where the concentration of oxygen and sulphide is low. Dissolved iron and manganese accumulate in this zone in the absence of nitrate. Manganese and iron are the next electron acceptors used by manganese- and-iron-reducing microorganisms involved in the decomposition of organic matter (Froelich et al. 1979).

Anoxic zone

The anoxic zone is an oxygen-depleted region below the suboxic zone where aerobic microorganisms give way to anaerobic microorganisms. The sulphate reduction zone is in the upper part of the anoxic layer followed by the sulphate-methane transition zone and methanogenesis zone. In anaerobic respiration, organic matter in the sulphate-rich sediments undergoes mineralisation by sulphate reducing bacteria that convert sulphate

to hydrogen sulphide. Sediments containing high concentration of hydrogen sulphide are black and have the characteristic smell of rotten eggs. Methanogenesis is a process by which methanotrophic archaea produces methane and is the last step in the breakdown of organic matter by microorganisms. Methanotrophic archaea use carbon dioxide, derived from the degradation of organic matter by sulphate reducing bacteria (SRB), and hydrogen to form microbial methane. Methane from the methanogenesis zone migrates upward into the SMTZ where anaerobic oxidation of methane (AOM) takes place (Iversen and Jorgensen 1985). Aggregates of methanotrophic archaea overgrown by sulphate reducing bacteria use hydrogen as an intermediate electron carrier in AOM where methane is oxidised to bicarbonate and sulphate is reduced to hydrogen sulfide (Boetius et al. 2000; Treude et al. 2003). The balanced equations for the reaction in AOM are as following:

$$CH_4 + 2H_2O \rightarrow CO_2 + 4H_2$$
$$\frac{SO_4{}^{2-} + 4H_2 + H^+ \rightarrow HS^- + 4H_2O}{CH_4 + SO_4{}^{2-} \rightarrow HCO_3{}^- + H_2O}$$
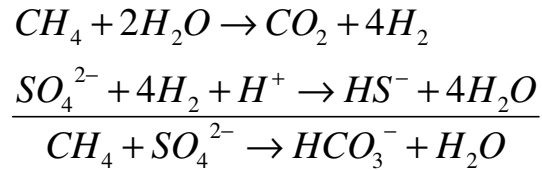
However, methyl sulphides are used as intermediate electron carriers in AOM through which methanotrophic archaea oxidise methane and reduce carbon dioxide to produce methyl sulphide, which is then used by SRB in their metabolic pathway (Moran et al. 2008). As burial of organic matter deepens, any remains of organic matter not used by methanogens undergo fermentation to form kerogens in the presence of high temperature. Petroleum and natural gas (e.g. thermogenic methane) are products of kerogens by means of thermal cracking when bonds between atoms are destroyed by heat. Thermogenic methane may migrate upwards to the sediment-water interface via fissures and faults. Microbial activities play a vital role in nutrient recycling that fuel

chemosynthesis-based ecosystems of the deep-sea. Chemosynthetic processes are dependent on the availability of organic matter and microbial degradation of organic matter, and these are indirectly linked with photosynthetic processes from the photic realm (Tunnicliffe et al. 2003). Moreover, without photosynthetically produced organic matter, life in the deep-sea may not exist.

1.2 Past discoveries of deep-sea habitats and associated benthic communities

The first oceanographical and biological works on the deep-sea floor were carried out by Challenger Expedition (1872 – 1876) between 180 and 4,500 metres below sea level (Murray and Thomson 1895) and these laid the foundation for all subsequent researches in these fields (Seibold and Berger 1993). Petersen grabs, trawls and dredges were used for quantitative samplings of benthic fauna and sediment samplings. Galathea Expedition (1950 – 1952) was the first to sample the deep-sea floor at greater than 10,000 metres below sea level and the first to carry out microbiological work on deep-sea sediments (Zobell and Morita 1956). The Challenger Expedition was the culmination of the era of 'heroic' deep-sea exploration (Tyler 2003). As technology advanced, more sophisticated research projects were carried out and contributed to the expanding knowledge on deep-sea ecology. Initially, it was assumed that no primary production occurred within the deep-sea and that the deep-sea benthic ecosystem was fuelled by food rained down from surface waters, and that deep-sea diversity was low (Tyler 2003). However, these notions were abandoned following the first discovery of the chemosynthetic communities of hydrothermal vents at the Galapagos Ridge in the seventies. These vents were discovered by Corliss and his colleagues aboard *Alvin,* a three-person deep submergence vehicle (Corliss et al. 1979). Subsequently, more hydrothermal vents were discovered in a variety of geological settings in the deep-sea,

especially along the tectonic plate boundaries (Hessler and Kaharl 1995; Campbell 2006) as well as in the shallow water counterparts (Miura et al. 2002; Tarasov et al. 2003). Deep-sea hydrothermal vents provide habitats among the barren seascapes analogous to the desert oases. Such oases are found along the mid-oceanic ridges in the Northeastern Pacific (Levesque et al. 2006), Western Pacific (Desbruyeres et al. 1994), East Pacific Rise (Shank et al. 1998; Van Dover 2002), Mid-Atlantic Ridge (Desbruyeres et al. 2001) and Indian Ocean (Hashimoto et al. 2001). Hydrothermal vents spout extremely hot sulfide-rich water from within the oceanic floor like a geyser or by diffuse emission. Free living and symbiotic chemoautotrophic bacteria convert these sulfide compounds to energy by chemosynthetic process which sustains vent communities (Van Dover and Lutz 2004).

Deep-sea currents facilitate larval dispersal giving rise to vent-seep fauna in a variety of geological settings (Van Dover 2002). Recent evidence showed the similarity of seep-specific fauna in the Indian Ocean to that of Pacific and Atlantic counterparts which may be attributed to global dispersal via the spreading ridge corridors (Hashimoto et al. 2001). Whale carcasses also provide a stepping-stone for settlement, recruitment and larval dispersal for benthic invertebrates (Bennett et al. 1994; Butman et al. 1995). The distance to which larvae disperse is dependent on the species' larval development and dispersal capability.

1.3 Cold seeps

Paull (1984) aboard Alvin was the first to discover cold seeps and their associated fauna on the Florida Escarpment adjacent to the abyssal Gulf of Mexico, at a depth greater than 3000 metres below sea level (bsl). These fauna were benthic invertebrates comprised of bivalves, gastropods, vestimentiferans, galatheids, holothurians,

ophiuroids and limpets that were similar to hydrothermal vent communities. Subsequently, cold seep communities were discovered in depth between 400 metres (e.g. Sea of Okhotsk, Sahling et al. 2003) and 6,000 metres bsl (e.g. Japan Trench, Li et al. 1999) worldwide in a variety of geological settings.

Cold seeps are oasis-like sulfide and methane rich habitats with soft bottom and carbonate concretions that support chemosynthesis based ecosystems (Carney 1994). These seeps are features of the continental margins, both active and passive as well as abyssal plains where seepage of methane-rich fluids and/or methane gas from deep within through faults, fissures or by diffusion occurs. For instance, in the continental active margins, the methane seepages usually take place in the subduction region where an accretionary prism is formed (Tunnicliffe et al. 2003). As the oceanic plate subducts beneath the continental plate, the overlying sediments compress to form a wedge hence an accretionary prism. Since methane is buoyant, this tectonic process induces high pore fluid pressure, causing the upward expulsion of methane. The origin of methane may be microbial or thermogenic and stable carbon isotope analysis is used to discriminate its origins (Judd and Hovland 2007). There are two types of seepage activity, active seeps and passive seeps (Abrams 1996). Active seeps are areas where high concentrations of methane or other hydrocarbons are actively seeping through the sediment-water interface. They may be found in regions containing gas hydrates (e.g. Northeast Pacific, Sahling et al. 2002), pockmarks (e.g. West Africa, Olu-Le Roy et al. 2007) or gas bubbles (e.g. New Zealand, Lewis and Marshall 1996). In contrast, passive seeps are areas where hydrocarbons are not actively seeping and they may be relict, sporadic, or inhabited by a migration barrier such as carbonate concretions. The succession of benthic communities of cold seeps is linked with the seepage activity and

this is discussed further in the next section.

1.3.1 *Environmental conditions regulating benthic invertebrates assemblages of cold seeps*

Benthic invertebrates of cold seeps have physiological adaptations that enable them to exploit sulphide from sulfide-rich sediments, which would otherwise be toxic to aerobic invertebrates (Van Dover 2000). Since these benthic invertebrates have no digestive system, they host chemoautotrophic symbionts in their tissues that provide nutrition to the hosts. Members of the bivalve families of Mytilidae, Vesicomyidae, Solemyidae and Lucinidae as well as members of the tubeworm families of Vestimentifera host chemoautotrophic symbionts and these are part of chemosynthesis-based communities inhabiting cold seep habitats.

Bathymodiolus sp. (large mussels) of Mytilidae harbour two types of chemoautotrophic symbionts in their gills, methanotrophic and thiotrophic (Duperron et al. 2005). *Bathymodiolus* sp. is known for its aggregation in large numbers in seep habitats with high methane supply and carbonate concretions (Sibuet and Olu 1998). While, *Idas* sp., a close relative of the genus *Bathymodiolus* has multiple symbionts including one methanotroph, two thiotrophs, one methylotroph and two other symbionts – marine gamma proteobacteria and Bacteroidetes (Duperron et al. 2008).

Calyptogena spp. (clams) of Vesicomyidae have symbiotic sulphur-oxidising bacteria in their gill tissues and require high concentrations of sulphide in their habitats (Fiala-Medioni et al. 1993; Barry et al. 2007). Sulphide from the sediments is taken up by the vascularised foot of *Calyptogena* spp. and sulphide binds to lipoprotein in the blood to be transported to the gill tissues where it is used by symbiotic sulphur-oxidising bacteria (Pruski and Fiala-Medioni 2003).

Acharax sp. of Solemyidae is a deep burrowing clam that hosts symbiotic sulphur-oxidising bacteria (Imhoff et al. 2003) and these symbionts rely on sulphide production from anaerobic oxidation of methane in the anoxic sediments (Boetius and Suess 2004). Further, *Acharax* sp. occupies sediment with a lower supply of sulphide than those of *Calyptogena* spp. (Sahling et al. 2002), and requires digging deeper into the sediments to exploit sulphide presumably from the SMTZ.

Deep burrowing lucinid clams of Lucinidae host symbiotic sulphur-oxidising bacteria and commonly inhabit the sulphide-rich suboxic zone of marine sediments (Carney 1994; Taylor and Glover 2006) both in deep-sea and shallower counterparts. There appears to be no literature on these clams inhabiting sediments surrounding hydrothermal vents. This may be due to their intolerance for high temperature and salinities in these habitats. Therefore they may be restricted to cold seep environments as well as non-seep reducing environments.

Lamellibrachia sp., (tubeworm) of Vestimentifera has a long sinuous, chitinous tube that attaches permanently to the substratum. Its basal (posterior) end of the tube takes up sulphide from deep in the sediment and binds sulphide to haemoglobin in its blood, then transports it to the trophosome where it is taken up by sulphide-oxidising symbiotic bacteria, and in turn provides nutrition to the host (Julian et al. 1999). This enables the tubeworm to flourish under conditions where there is minimal supply of sulphide in the sediment/water interface.

Seep communities' structure and composition are determined by the rate of sulphide supply and are dependent on the methane gas/fluid flow regime (Sahling et al. 2002; Haeckel et al. 2008). In addition, constant supply of sulphide to maintain the chemosynthetic communities is more important than the absolute concentration of

sulphide (Dubilier et al. 2008). Therefore, there are variations in the assemblages of benthic invertebrates inhabiting seeps between sites. For example, *Beggiatoa* communities, *Calyptogena* communities and *Acharax* communities which have been observed at Hydrate Ridge, Cascadia convergent margin (Sahling et al. 2002), *Bathymodiolus* communities at Blake Ridge, Atlantic continental rise (Van Dover et al. 2003) and *Vestimentiferan* communities in the Gulf of Mexico (Bergquist et al. 2003).

There are similarities of taxa of seep-related benthic invertebrates between seep habitats in various tectonic settings and water depths worldwide and these are indicative of the seep settings (Sibuet and Olu 1998). The persistence of seep ecosystems depends on the continuous supply of sulphide and methane, which are controlled by the influx of methane into sedimentary pore fluids from the deep (Levin 2005). Moreover, the seep sites serve as a gateway for the release of methane of thermogenic or biogenic origins, or from hydrate dissociation into the water column (Judd and Hovland 2007). In addition, authigenic carbonates are common features of the seep habitats and the density of carbonates depends on the duration and rate of methane influx, and environmental conditions at the time of precipitation (Luff et al. 2004). The carbonate formation affects the chemosynthesis-based communities that inhabit those sites. As the carbonate crust forms, it restricts the supply of methane-rich pore fluids to the sediment surface. Subsequently, microbial activities involving anaerobic oxidation of methane and the production of sulphide are reduced, which in turn affects the abundance and distribution of benthic invertebrate communities (Orphan et al. 2004). Therefore, the species diversity of cold seep communities vary between sites, which reflects the temporal and spatial variability of seabed fluid flow.

1.4 New Zealand deep-sea benthic invertebrate research

Past studies on the New Zealand's deep-sea benthic diversity were predominantly based on the Chatham Rise (McKnight and Probert 1997; Probert et al. 1997), and on the continental shelf and upper slope off the west coast of South Island (Probert and Grove 1998; Probert et al. 2001). Other areas that have been investigated include part of Cook Strait, Foveaux Strait and the continental shelf off the west coast of the North Island (McKnight 1969). These studies employed sampling gear that included dredges, trawls and grabs for benthic invertebrates and sediment samplings. Results from these studies identify the paucity of published data on New Zealand deep-sea benthic invertebrates, especially on chemosynthesis-based seep ecosystems.

1.5 New Zealand cold seep research

Benthic invertebrates within cold seeps are not well understood in the New Zealand region compared with other parts of the world. However, in the late 1980's a trawler harvested a block of cemented shells from the continental slope seabed off the east coast of New Zealand which was later identified to be of seep fauna (Lewis and Marshall 1996). This was the first discovery of seep fauna in the Hikurangi Margin. Flare (gas bubbles) was first reported in the area by fishermen in 1994, which indicated possible methane seepage (Lewis and Marshall 1996). These findings generated interest among scientists both in New Zealand and overseas which lead to multidisciplinary researches on gas hydrate resources (Henrys et al. 2003; Pecher et al. 2005; Faure et al. 2006) and seep fauna (von Cosel and Marshall 2003 and references therein) on the Hikurangi Margin. In late 2006, as part of the Census of Marine Life's Chemosynthetic Ecosystems programme (ChESS), New Zealand's National Institute of Water & Atmospheric Research (NIWA) conjoined with three research institutes from the United

States of America, to explore seeps in the Hikurangi Margin and collect biological and sediment samplings (Proffitt 2006). The objective of ChESS was to form a database for all species from the deep-sea's chemosynthesis-based benthic communities. Recent studies on the ancient seeps of the East Coast Basin adjacent to the Hikurangi Margin revealed fossilized chemosynthesis-based fauna, which appeared to be similar to that of the present day seep benthic communities (Campbell et al. 2008).

1.6 RV SONNE SO191 expedition to the Hikurangi Margin

The Hikurangi Margin was one of the sites chosen by the Leibniz Institute of Marine Sciences of the University of Kiel, Germany (IFM-GEOMAR) as part of their research project COMET called "New Vents" for investigating the role of oceanic methane seepage on the local, regional and global methane (Greinert and Bialas 2008). Auckland University of Technology (AUT) was one of the twelve institutes from around the world involved in this multidisciplinary research. During the first three months of 2007, an expedition to the Hikurangi Margin aboard IFM-GEOMAR's RV SONNE SO191, a research cruise, involved surveying which included bathymetric mapping (Klaucke et al. 2008; Liebetrau et al. 2008), flare imaging (Jones et al. 2008) and ocean floor observation for sediment and biological samplings as well as in situ measurements (Naudts et al. 2008). These assisted in biogeochemical and microbiological samplings (Niemann et al. 2008; Sommer et al. 2008), water column samplings (Faure et al. 2008; McGinnis et al. 2008), pore fluid samplings (Haeckel et al. 2008), seep sediments (this study; Campbell et al. in press) and associated gas hydrates and carbonates samplings (Liebetrau et al. 2008; Campbell et al. in press), benthic invertebrates samplings (this study; Thurber et al. 2008; Campbell et al. in press) and benthic foraminifera samplings (Martin et al. 2009).

This expedition has given AUT a window of opportunity to explore the uncharted seeps and to investigate their unique chemosynthesis-based ecosystems. In addition, AUT had the opportunity to try out a new methodology which has not been employed by past studies, using X-radiographic images of the seep sediments. While sample numbers were limited, they provided qualitative data concerning the spatial variability of faunal assemblages of seeps. Other environmental factors examined in the study include grain size diversity, total organic content, carbonate content, mineralogy and origins contributing to the stratified layers of sediment as shown in the X-radiography of core samples. In addition to the biological and sedimentological aspects of this study, the application of ichnology, ethology and taphonomy were applied. Ichnology is the study of trace fossils in sedimentary rock; while ethology is the study of organisms' behaviour in their natural habitats and these combined concepts were used to assist in the interpretation of X-radiographic images of burrow structures in sampled unconsolidated sediments from seep sites. Taphonomy is the study of the nature of shell remains following death and burial. The general information gained from this study should further our understanding of the formation of chemosynthesis-based seep ecosystems.

2 METHODS OF STUDY

2.1 Geological setting of study sites

The Hikurangi Margin on the eastern North Island, New Zealand is an active convergent margin that lies at the southern end of the Kermadec Volcanic Arc, where the oceanic crust of the Pacific Plate is subducting beneath the continental crust of the Australian Plate at a velocity of 50 mm per year (1996). This tectonic activity forms an accretionary prism overlain with hemipelagic sediments at a sedimentation rate of ≥ 29 cm/ka (Carter et al. 2002). However, there are variations in sediment thickness along the margin making it difficult to determine the age of sediments at various sites (Henrys et al. 2003). According to seismic surveys, approximately 40,000 km^2 of the Hikurangi Margin contains gas hydrate (Henrys et al. 2003). Gas hydrate is a crystalline solid comprising a gas molecule (e.g. methane) trapped within the structure of water molecules which formed at high pressure (> 30 ATM) and low temperature (0°C) (Kvenvolden and Lorenson 2001). Moreover, gas hydrate may be formed on the ocean floor or within sediment up to 1,000 metres in depth where excess of methane exceeds its solubility in water. Hydrate may contains methane derived from methanogenesis or thermogenic source (Kvenvolden and Lorenson 2001). When hydrate is destabilised, methane is released and used by methanotrophic microorganisms involved in anaerobic oxidation of methane, which in turn supports chemosynthesis-based benthic ecosystems.

The East Cape Current brings nutrient-rich subtropical water along the east coast of the North Island from the north. In addition, the Wairarapa Coast Current (WCC), flows along the Wairarapa Coast from Cape Palliser, the southern tip of the North Island and joins the East Cape Current from the north (Chiswell 2000). The WCC contains a

mixture of nutrient-rich subtropical waters derived from the Southland Current and D'Urville Current. These currents bring marine organic matter to the seafloor.

2.2 Sampling sites

During the cruise of RV SONNE 191 leg 2 in February 2007 and leg 3 in March 2007, a video-guided box corer and video-guided multi-corer were deployed for sediment samplings and semi-quantitative sampling of benthic invertebrates of the cold seep habitats in the Hikurangi margin. Sites were chosen for sampling according to the cruise scientists' discretion using the Ocean Observation System (OFOS), a towed video camera sled that surveyed the sea bed. The number of samples obtained depended on the success of the various deployments. Moreover, the samplings could not be conducted in the middle of the active seeps because the sediments were too indurated; therefore all samplings were performed either on the periphery of active seeps or farther out. During leg 2, seven sites were selected, and seven were also selected during leg 3 (Table 1, Figure 1).

Table 1. Sites selected for samplings

Station No. and region	Site	Gear Type	Ship position (Gear at bottom)		Depth (m)
Omakere Ridge					
SO191/2-51	LM9	TV-BC	40°1.076'S	177°51.631'E	1155
SO191/2-66	LM9	TV-BC	40°3.223'S	177°49.293'E	1097
SO191/2-96	LM9, south	BC	40°3.223'S	177°49.256'E	1096
SO191/2-98	LM9, south	BC	40°3.205'S	177°49.187'E	1101
SO191/2-173	LM9, Bear's Paw	TV-MUC	40°3.197'S	177°49.190'E	1106
SO191/3-186	Bear's Paw	TV-MUC	40°3.18'S	177°49.20'E	1078
SO191/3-232	Kaka	TV-MUC	40°02.15'S	177°47.95'E	1172
SO191/3-242	Kaka – raindrop site	TV-MUC	40°02.14'S	177°47.91'E	1175
SO191/3-261	Kaka – raindrop site	TV-MUC	40°02.15'S	177°47.96'E	1171
SO191/3-262	Kaka – NSR	TV-MUC	40°02.15'S	177°47.95'E	1167
Rock Garden					
SO191/3-224	Rock Garden	TV-Grab	40°1.025'S	178°10.047'E	610
Wairarapa					
SO191/2-156	North Tower	TV-MUC	41°46.915'S	175°24.228'E	1072
SO191/2-158	North Tower	TV-MUC	41°46.850'S	175°24.192'E	1060
SO191/3-305	Wairarapa - NSR	GC	40°46.69'S	177°25.23'E	1051

* TV-BC = video guided box core, BC = box core, TV-MUC = video guided multi-core, GC = gravity core, TV-Grab = video guided grab; NSR = non-seep reference site
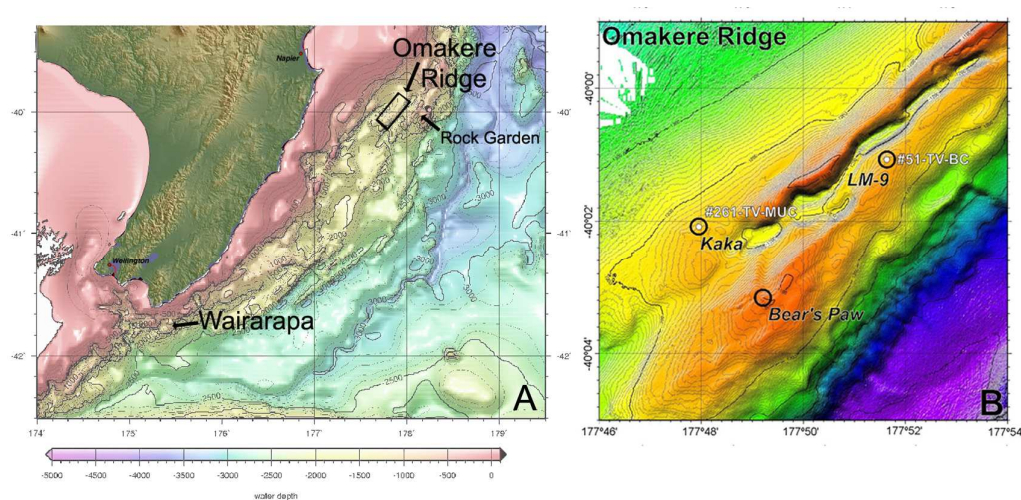
Figure 1. A) Map showing sites selected for samplings. Omakere Ridge includes Kaka: SO191-3/232, 242, 261-262; LM9: SO191-2/51, 66, 98; and Bear's Paw: SO191-3/173, 186. Rock Garden: SO191-3/224. Wairarapa: SO191-2/156, 158 and SO191-3/305. B) Close up of Omakere Ridge.

2.3 Field methods

Early in the expedition (leg 2), video guided box core samplings were carried out at two sites, SO191/2-51 and SO191-2/66. At another two sites (SO191/2-96 and SO191-2/98) box core samplings were taken without a video camera. The box core sampling method was later aborted due to technical problems and a video-guided multi-corer (Figure 2) was used for the remainder of the expedition. A total of 4 box core samples from leg 2, 12 multi-core samples (3 samples from leg 2 and 9 samples from leg 3) and 1 gravity core from leg 3 were obtained (Table 2). The size of the box core was 50 x 50 x 50 cm, and plastic containers sized 21 x 30 x 8.5cm were used for sub-samplings containing two or more slabs from each box core sampling per site (Figure 3). The size of cylindrical cores of multi-core samplings was 34.55cm in circumference (11 cm in diameter) and the length of each core varied, depending on the success of the multi-corer deployment. The length of the gravity core sample was 81 cm and its diameter

20

was slighter wider than those of the multi-corer. These samples were used for biological and sedimentological analyses. In addition, a video-guided grab (Figure 2) was used to collect carbonate rocks containing epifauna from site SO191/3-224. All organisms collected from the core samples on board the ship were preserved in appropriate fixture according to National Institute of Water & Atmosphere Research's (NIWA) protocol. Buffered 10% formalin (4% formaldehyde) was used to fix worm specimens and 95% ethanol was used to fix molluscs, arthropods, cnidarians and echinoderms. These specimens were used for taxonomic identification and assessment of faunal diversity among sites.
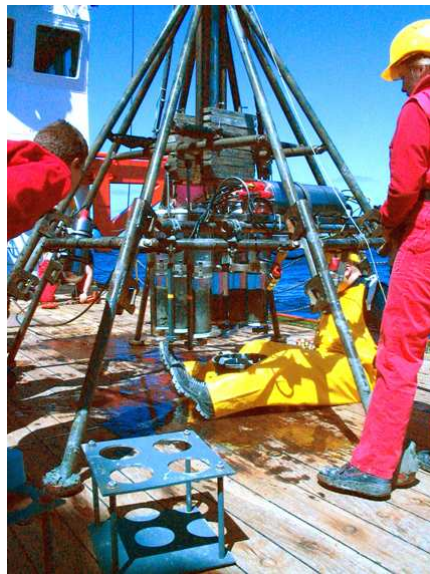
Figure 2. Video-guided multicorer (left) and video-guided grab
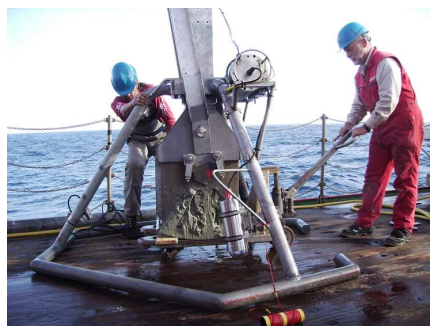
Figure 3. Video guided box core sampler (left) and plastic container used for sub-samplings of sediments

Table 2. List of core samples (*cylindrical core)

Station No.	Core type	Core recovery (cm)	No. of samples	No. of sub-samples	Sample label
SO191-2/51	slab	30	1	5	51-1B, 51-2B, 51-3B, 51-4B, 51-5B
SO191-2/66	slab	30	1	2	66-1B, 66-2B
SO191-2/96	slab	30	1	2	96-1B, 96-2B
SO191-2/98	slab	30	1	2	98-1B, 98-2B
SO191-2/156	*	9	1		156
SO191-2/158	*	18, 23	2		158A, 158B
SO191-3/173	*	12	1		173B
SO191-3/186	*	6	1		not used for analysis
SO191-3/232	*	25, 27	2		232-1A, 232-1B
SO191-3/242	*	18, 22	2		242, 242B
SO191-3/261	*	16	1		261
SO191-3/262	*	28, 33	2		262, 262B
SO191-3/305	*	81	1	4	305-1, 305-2, 305-3, 305-4

2.4 Laboratory methods

All multi-core and box core slabs were imaged using a diagnostic x-ray machine,

Toshiba KXO-15E, at Radiology Clinic, Auckland. Radiographs of these were made

using a standard 30 x 40 cm Fuji film and no magnification. X-ray tubes were housed

in oil to keep them cool and ran according to normal standards. Further, radiographs

were scanned using a film digitiser and stored on compact disk for sedimentological

analyses, specifically for ichnology and stratigraphy descriptions. All cores were

divided in half lengthwise, the left side used for biological analyses and the right side

for sedimentological analyses. The biological analyses entailed sieving and sorting the

sediments to retrieve all benthic invertebrates, and these were preserved either in

buffered 4% formalin or 95% ethanol depending on the type of specimens (see Section

1.3). These specimens were photographed for taxonomic identification. All carbonate

nodules and shells retrieved from sediment samples were air dried and photographed.

Also, carbonate rocks containing epifauna retrieved from the Rock Garden site

(SO191/2-224) were air dried and photographed. The digital images of all organisms

found on the rocks were obtained using a Leica Wild M3C stereomicroscope and these

were used for the identification of the epifauna to the lowest taxonomic order as far as

possible. The purposes of taxonomic identification are to assess the benthic invertebrate assemblages of cold seeps and to determine whether these organisms are cosmopolitan, endemic to seep settings, restricted to New Zealand region, or new to science. The sedimentological analyses involved total organic carbon and carbonate content as well as grain size analysis. In addition, carbonate mineralogy and stable isotopic analysis for carbonates are also included.

2.4.1 *Grain size analysis*

Grain size is one of the basic physical properties of sediments and provides clues concerning the depositional environment and early diagenesis of sediment. Grain size analysis is used by sedimentologists to characterise the sediment texture and its relation to environmental conditions. Biologists use this information to examine the interactions between benthic invertebrates and sediment texture. Malvern's Mastersizer 2000 particle size analyzer was used to determine the background unconsolidated sediment grain size gradient on each core sample, totalling 77 subsamples. Grain size data were given in micron units after Udden (1914) and Wentworth (1922) and modified by Blott (2000) in which the volume percentage of grains falls into each size fraction (Table 3). The results from these analyses were processed using a GRADISTAT Version 4.0 (Blott 2000), a software used for the statistical analysis of grain size distribution for unconsolidated sediments. Afterwards, these results were transferred to Microsoft Excel for graphing. Four statistical measurements comprising central tendency (mean and mode), sorting (standard deviation), skewness and kurtosis were used for sediment grain size analysis. Sorting is a measure of uniformity of grain sizes. Note that the grain size distribution for some sediment samples of this study was not normal, but produced a bimodal distribution. As a result, some statistical measurements may not be

reliable. Nevertheless, these measurements were included this study. Physical

descriptions of the sediment were based on grain size distribution as presented in Folk

and Ward (1957) (Table 4). Ternary plot was constructed for each core sample based

on Folk's (1954) classification of textural groups for terrigenous sediments (Appendix

2). This provided a quick overview of sediment textural class between sampling sites.

Table 3. Sediment grain size classification after Udden (1914) and Wentworth (1922) which was modified and applied in the GRADISTAT programme

Grain size Phi (Φ) unit:	Grain size (mm/µm)	Class terms:
< -10	< 1024 mm	Very large boulder
-10 to -9	1024 to 512	Large boulder
-9 to -8	512 to 256	Medium boulder
-8 to -7	256 to 128	Small boulder
-7 to -6	128 to 64	Very small boulder
-6 to -5	64 to 32	Very coarse gravel
-5 to -4	32 to 16	Coarse gravel
-4 to -3	16 to 8	Medium gravel
-3 to -2	8 to 4	Fine gravel
-2 to -1	4 to 2	Very fine gravel
-1 to 0	2 to 1	Very coarse sand
0 to 1	1 mm to 500 µm	Coarse sand
1 to 2	500 to 250	Medium sand
2 to 3	250 to 125	Fine sand
3 to 4	125 to 63	Very fine sand
4 to 5	63 to 31	Very coarse silt
5 to 6	31 to 16	Coarse silt
6 to 7	16 to 8	Medium silt
7 to 8	8 to 4	Fine silt
8 to 9	4 to 2	Very fine silt
> 9	> 2	Clay

Table 4. Modified geometric geographical measures after Folk and Ward's method (1957) which was adopted in the GRADISTAT programme (Blott 2000; Blott and Pye 2001). Please note, Px is grain diameter in metric at the cumulative percentile value of x.

Mean	Standard Deviation
$M_G = \exp \dfrac{\ln P_{16} + \ln P_{50} + \ln P_{84}}{3}$	$\sigma_G = \exp\left(\dfrac{\ln P_{16} - \ln P_{84}}{4} + \dfrac{\ln P_5 - \ln P_{95}}{6.6}\right)$

Skewness	Kurtosis
$Sk_G = \dfrac{\ln P_{16} + \ln P_{84} - 2(\ln P_{50})}{2(\ln P_{84} - \ln P_{16})} + \dfrac{\ln P_5 + \ln P_{95} - 2(\ln P_{50})}{2(\ln P_{25} - \ln P_5)}$	$K_G = \dfrac{\ln P_5 - \ln P_{95}}{2.44(\ln P_{25} - \ln P_{75})}$

Sorting (σ_G)		Skewness (Sk_G)		Kurtosis (K_G)	
Very well sorted	< 1.27	Very fine skewed	⁻0.3 to ⁻1.0	Very platykurtic	< 0.67
Well sorted	1.27 – 1.41	Fine skewed	⁻0.1 to ⁻0.3	Platykurtic	0.67 – 0.90
Moderately well sorted	1.41 – 1.62	Symmetrical	⁻0.1 to ⁺0.1	Mesokurtic	0.90 – 1.11
Moderately sorted	1.62 – 2.00	Coarse skewed	⁺0.1 to ⁺0.3	Leptokurtic	1.11 – 1.50
Poorly sorted	2.00 – 4.00	Very coarse skewed	⁺0.3 to ⁺1.0	Very leptokurtic	1.50 – 3.00
Very poorly sorted	4.00 – 16.00			Extremely leptokurtic	> 3.00
Extremely poorly sorted	> 16.00				

2.4.2 *Total organic carbon and carbonate content*

Total organic carbon is a measure used to assess the vertical distribution of organic matter in the sediment columns. Total organic carbon and carbonate contents of bulk sediment samples, totaling 77 subsamples, were determined using a Carlo Erba NA 1500 elemental analyser which was conducted by IFM-GEOMAR. Each sample was combusted at 1050°C, releasing carbon dioxide, and carbonate was removed from each sample by acidification using hydrochloric acid. Organic carbon is measured as the difference in total carbon (TC) before and after combustion. Carbonate content is measured as the difference between TC and total organic carbon (TOC) after acidification. These are expressed as weight percent (wt%). Further, these samples were used for the analysis of carbon isotopic composition of organic matter. The results of $\delta^{13}C$ ‰ values assisted in the interpretations of the organic matter sources and their profiles in the sediment column. In normal marine sediment, the organic carbon content decreases with increasing depth due to microbial degradation and early diagenesis of organic matter (Rullkotter 2006).

2.4.3 *Stable isotopes of carbonate and carbonate mineralogy*

Analyses of stable carbon and oxygen isotopes and mineral content of carbonates were used to differentiate the diagenetic/biogeochemical processes responsible for the formation of carbonates. Factors influencing the precipitation of different carbonate minerals are ambient temperature, seawater and sediment pore water chemistry, as well as the level and type of microbial activities (Naehr et al. 2007). Moreover, the prerequisites for carbonate formation include: suitable substrate for the formation of crystals; no mechanical abrasion; bicarbonate-supersaturated seawaters; high exchange rates of water between seawater and pore water; oxygenated pore water; and time

(Tucker 1990). The measurements for carbon and oxygen were expressed in delta notation relative to Pedee Belemnite standard, $\delta13C$ ‰ and $\delta18O$ ‰ respectively. These provided a basis for the interpretation of the carbonate origin. For example, based on Campbell's (1992) compilation of data on carbon and oxygen isotopic composition of seep carbonates from literatures, there are six categories of carbon sources comprising methanogenesis (+5 to +15 $\delta^{13}C$ ‰), seawater inorganic carbon (+2 to -2 $\delta^{13}C$ ‰), sedimentary organic diagenesis (-15 to -35 $\delta^{13}C$ ‰), oil fractions (-20 to -35 $\delta^{13}C$ ‰), thermogenic methane (-40 to – 50 $\delta^{13}C$ ‰) and biogenic methane (-50 to <-60 $\delta^{13}C$ ‰). Concerning the precipitation of particular carbonate minerals, high temperature coupled with high concentrations of sulphate and high alkalinity in pore waters favour the precipitation of aragonite; while low concentrations of sulphate and low alkalinity favours precipitation of magnesian calcite (Greinert et al. 2001). Carbonate nodules, which were extracted from selected bulk sediment samples containing carbonate horizons, totally 14 subsamples, were washed and later oven dried at 80°C overnight. The dried samples were then pulverised by crushing in a rolling motion using mortar and pestle. Approximately 3 mL of powdered carbonates from each subsample were used for stable isotopes analysis and 15 mL of each subsample for carbonate mineralogy analysis. Analyses of carbon and oxygen isotopic composition of carbonates were conducted at IFM-GEOMAR. Carbonate mineralogy analysis by X-ray diffraction method was carried out by the Geology Department of the University of Auckland using goniometer (Philips PW1050/25) with a high voltage X-ray generator (Philips PW1130). For X-ray diffraction method, samples of powdered carbonates was analysed separately by pressing it into an aluminum holder and placing it in a diffractometer to be measured for angle of crystals. The University of Auckland provided data for these two

analyses and the results from these assisted in the carbonate descriptions and interpretations.

2.5   Box core and multicore descriptions

X-ray images of box core and multicore samples were used for the visual description and analysis of bioturbation, invertebrate ethological patterns, stratigraphy and taphofacies. Bioturbation was described in terms of diameter of burrow structures and their orientation, as well as the degree of bioturbation based on Taylor & Goldring's (1993) bioturbation index (Table 5). The description of invertebrates' behavioural patterns was based on the Pemberton et al.'s (1992) and Bromley's (1996) ethological classification of trace fossils (Table 6). The morphology of the trace fossils served as a guide to assisted in identifying the lebensspuren (living) traces in modern marine sediments. Moreover, these lebensspuren traces were assigned with trace fossil names. The purpose of these studies on traces was to evaluate their density, abundance and ichnofacies associations of seep habitats and wherever possible to compare these findings with other non-seep habitats of the marine environments. There are nine categories of behavioural patterns comprising feeding traces (*fodinichnia*), dwelling traces (*domichnia*), escape traces (*fugichnia*), farming traces (*agrichnia*), grazing traces (*pascichnia*), locomotion traces (*repichnia*), resting traces (*cubichnia*), predation traces (*praedichnia*) and equilibrium traces (*Equilibrichnia*). However, only four traces, *domichnia, fodinichnia, repichnia* and *cubichnia* were recognised in this study and the key legend was used to differentiate the burrow types (Table 7, Figure 4). There was one other trace, 'probing' trace, not included in Pemberton et al.'s (1992) or Bromley's(1996) ethological classification of trace fossils, and this is included in this study. Its significance will be discussed in Section for Discussion.   Bed thickness,

bedding contact and bedding types were noted in the stratigraphy description of the box core samples. Visual descriptions of carbonates based on X-ray images of core subsamples were made and some visual inspections of carbonates retrieved from sieving and sorting were also noted. The depth of subsurface carbonate horizon was measured in centimetres below sea floor (cm bsf). Taphofacies analysis was based on two processes, the taphonomic characteristic of shells and their relationship to the environment (Davies et al. 1989). Criteria used for taphonomic analysis included degree of discoloration of the shell surface, wholeness (whole or fragment), and cementation of shell and assemblage formation (e.g. parautochthonous, allochthonous and autochthonous). All shell specimens retrieved from the core samples were identified to the lowest taxonomic order possible, and where applicable, systematic descriptions were provided. Adobe® Creative Suite® 3 Design Standard was used to produce stratigraphy and ichnofacies descriptions of X-ray images of core samples. A key legend for the stratigraphic column is provided (Figure 5). In the results section, a systematic diagnosis of each core subsample is presented beginning with core stratigraphic descriptions (see Section 2.5 for methods) followed by results from total organic content, stable isotopic and mineralogic analysis of the carbonates, and finally benthic invertebrate assemblage analyses. For the core stratigraphic descriptions, core photos, X-radiographs, drawings of stratigraphic columns, graphs of grain size distribution and carbonate content and TOC were laid out in columns on a single page for each core subsample. This presentation provided a "snapshot" of each core's physical parameters interpretations of sediment texture, burrow structures, carbonates and shells for each horizon. The analytical results for TOC and carbonate content were obtained for selected core subsamples. The relationship between sediment grain size and TOC for selected core samples is discussed in Sections 3.13 and 4.1.3. The

statistical data of grain size distribution for all horizons of all subsamples are listed in Appendix 1 and these assisted in the interpretation of the graphical outputs. The mode of distribution, sorting, skewness and kurtosis are described in the text for sediment texture. The stratigraphic column is a symbol diagram to be used in conjunction with X-radiographs to describe the coers physically. Each log was divided into labelled horizons to reflect sediment texture and presence of carbonate nodules/bands, shells and burrow structures (see Figure 5 for key legend). Each burrow structure shown on the X-radiograph revealed dark grey shading relative to the background and was labelled with burrow type based on its ethological pattern (see Table 7 for key legend). Other observed physical characteristics included water features and cracks that are shaded in dark grey compared with the background, and these features resulted from the impact of sampling gear on the sea floor and handling of the cores. The horizons containing extensive or dispersed carbonate nodules as well as shells illuminated as white on the X-radiographs. Each shell that appeared on the X-radiograph was labelled with 'S' and a serial number placed beside it. This labelling scheme allowed cross-referencing for the digital images of the shells.

Table 5. Bioturbation Index (BI) from Taylor & Goldring (1993)

Grade	Percent bioturbated	Classification
0	0	No bioturbation
1	1-4	Sparse bioturbation, bedding distinct, few discrete traces and/or escape structures
2	5-30	Low bioturbation, bedding distinct, low trace density, escape structures often common
3	31-60	Moderate bioturbation, bedding boundaries sharp, traces, discrete, overlap rare
4	61-90	High bioturbation, bedding boundaries indistinct, high trace density with overlap common
5	91-99	Intense bioturbation, bedding completely disturbed (just visible), limited reworking, later burrows discrete
6	100	Complete bioturbation, sediment reworking due to repeated overprinting

Table 6. Trace fossil ethology descriptions (Pemberton et al. 1992; Bromley 1996)

Category	Structure morphology
Crawling traces (*Repichnia*)	Sinuous or linear trails created by a wandering organism along the bedding planes, both on or within the sediments.
Dwelling traces (*Domichnia*)	Residential U-shaped or forked lined burrows, both vertical or obliquely inclined; or branched burrows both vertically and horizontally.
Escape traces (*Fugichnia*)	Vertical burrows with backfill created by an organism escaping upward or downward in response to sudden aggradation or degradation of sediments, respectively; or horizontal burrow subsurface formed by an organism escaping a predator.
Farming traces (*Agrichnia*)	Complex horizontal burrow systems combining dwelling and feeding purposes; feeding strategies involve microbial farming, trapping meiofauna or sulfide pumps.
Feeding traces (*Fodinichnia*)	Unlined or mucus lined burrows created by deposit feeders. Burrows may be single, branched or unbranched, concentric, cylindrical, sinuous or U-shaped, depending on the ichnogenus type.
Grazing traces (*Pascichnia*)	Unbranched meandering or spiral furrows on the sediment surface or burrows in the subsurface created by deposit feeders.
Predation traces (*Praedichnia*)	Various form of structures depending on the predator-prey type. Structures tend to be isolated.
Resting traces (*Cubichnia*)	Small depression in the sediment surface by mobile organism digging in to temporarily rest. The structure may be isolated or with crawling traces or escape traces.
Equilibrium traces (*Equilibrichnia*)	Shifting of burrows in response to changes in the sea floor level. Upward shift of burrow forms when sedimentation occurs or downward shift of burrow forms when erosion occurs.

Table 7. Descriptions of X-ray burrow structures

Ethology	Burrow type	Characteristic morphology	Ichnogenus (if known)
1. Dwelling trace (Domichnia)	br 1a	Vertical or obliquely inclined, slightly j-shaped, wall not lined, 1 mm in diameter, length range between 30 mm and 60 mm, dark grey X-ray shade	cf. *Skolithos*
	br 1b	Vertical or obliquely inclined, cylindrical to sinuous structure, wall not lined, 2 mm in diameter, medium grey X-ray shade.	cf. *Skolithos*
	br 1c	Obliquely inclined, slightly j-shaped, wall not lined, segmented burrow filled with carbonate nodules, 4 mm in diameter, white X-ray shade.	?
	br 1d	Vertical or opliquely inclined, lined with black H_2S stained sediment, 4 to 6 mm in diameter, dark grey X-ray shade	cf. *Spongeliomorpha*
	br 1e	Obliquely inclined, slightly j-shaped, wall not lined, 8 to 10 mm in diameter, dark grey X-ray shade.	?
	br 1f	A simple trace (1 mm in diameter) occupied by worms living in it, medium grey X-ray shade.	Worm trace
2. Feeding-dwelling trace	br 2a	Horizontal undulating burrow, wall lined, 2 mm in diameter, filled dark grey X-ray shade with halo appearance on the wall margin with light grey X-ray shade.	cf. *Palaeophycus*
Feeding-crawling trace	br 2b	Horizontal undulating burrow, wall not lined, 4 to 6 mm in diameter, faint dark grey X-ray shade.	cf. *Planolites*
Feeding-dwelling trace	br 2c	U-shaped burrow, 3 mm in diameter, created by juvenile cf. *Acharax clarificata*, dark grey X-ray shade.	cf. *Solemyatuba*
3. Resting trace (Cubichnia)	br 3	Unlined burrow occupied by a sea anemone (*Isoparactis farex*), 2 mm in diameter, light to dark grey X-ray shade.	*Bergaueria*
4. 'Probing' trace	br 4	Radiating 'root-like' traces beneath mollusc formed by mollusc' extensible foot.	cf. *Chondrites* (Seilacher 2007)
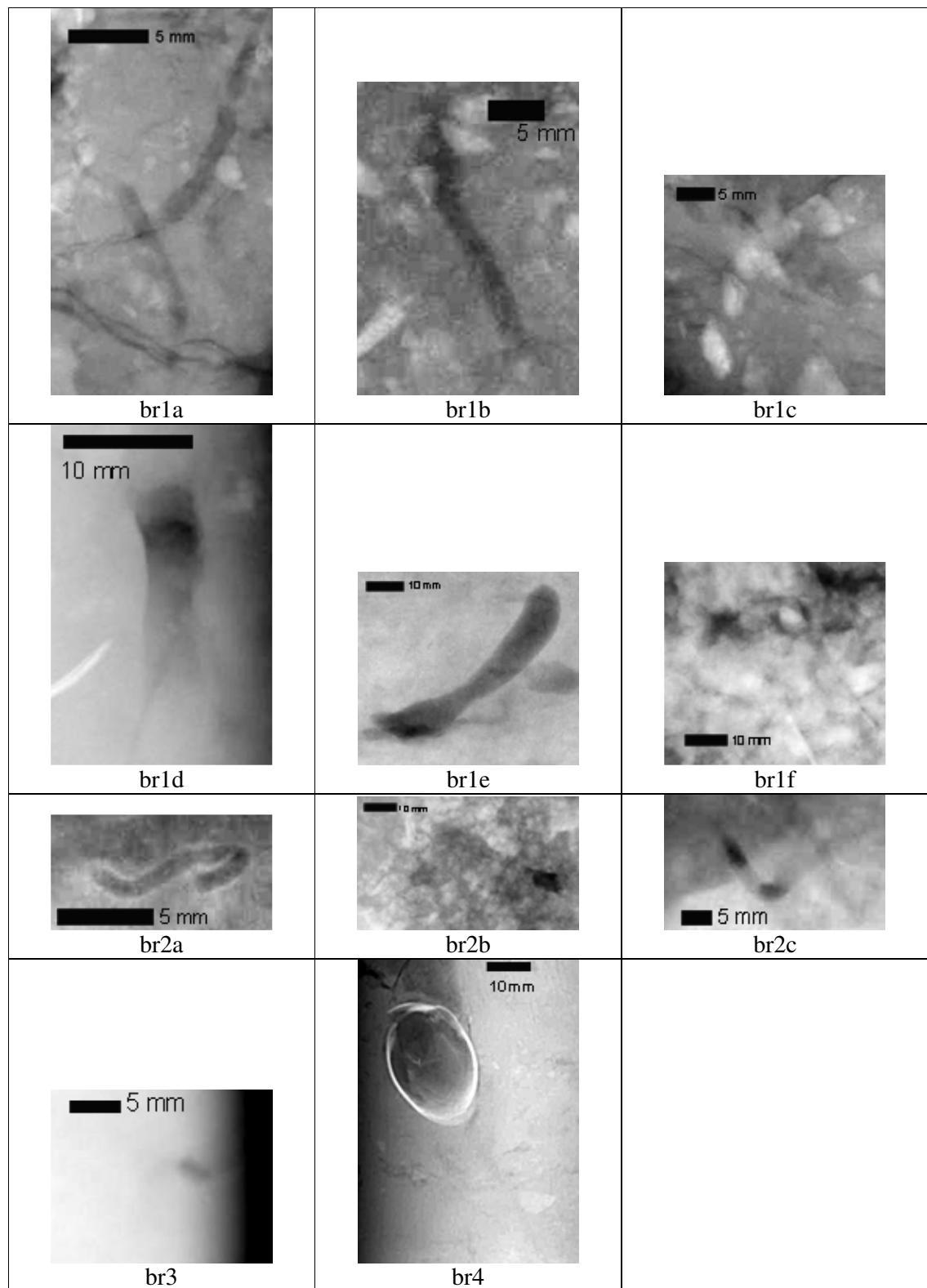
Figure 4. X-radiographs of burrow types (refers to Table 7 for details)
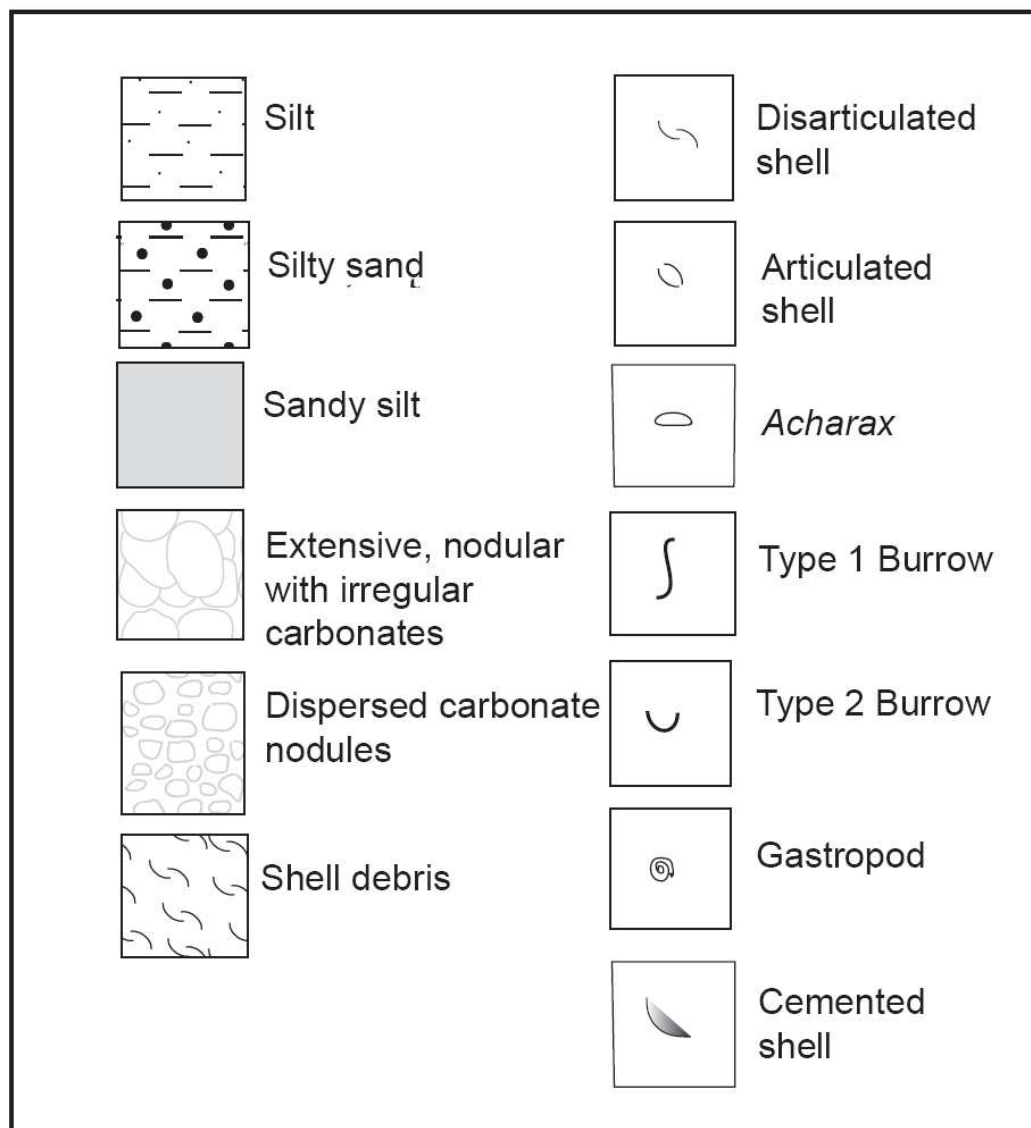
Figure 5. Key legend for the stratigraphic columns

3 RESULTS

This section covers the systematic analysis of cores beginning with the box core samples followed by multicore samples and gravity core samples. These are mirrored in the station numbers associated with expedition sampling sites. The results from total organic content, carbonate content, and the stable isotopic composition and mineral content of carbonates are subsequently analysed. Finally, the analysis of benthic invertebrate assemblage is made. Following is an overview of the results, which are further explored under appropriate headings.

The results of grain size analysis, total organic carbon (TOC) and carbonate content for the core 'background' sediments showed two end-members between very poorly sorted sandy silt containing high carbonate contents and low TOC (Omakere Ridge sites) and poorly sorted silts containing low carbonate contents and high TOC (Wairarapa sites). These variations reflected the spatial and temporal variability of seepage activity for all sites containing carbonate nodules. However, multicore 158A (North Tower, Wairarapa) and the two reference sites, gravity core 305 (Wairarapa) and multicore 262 (Kaka of Omakere Ridge), were taken outside of seep areas contained poorly sorted silt.

The results of mineralogy and stable isotopic composition of carbonate nodules of the core samples containing bands of carbonate nodules (20 to 30 cm thick, Omakere Ridge sites 55, 66 and 98) showed a range of $\delta^{13}C$ values, between -46.68 and -50.3 ‰ PDB and a range of $\delta^{18}O$ values, between 2.7 and 3.17 ‰ PDB (see Section 3.14 and Appendix 3). Aragonite was the dominant mineral species of these high carbonate content nodules and bands (62.5 to 78.0 % wt carbonate), while various mineral species: quartz, magnesian-calcite and plagioclase were minor. The variation in mineral contents reflected the environmental conditions at the time of precipitation.

Furthermore, the stable isotopic composition of these carbonates indicates their methane-derived pore fluids. These results are further addressed in the discussion section (Section 4.1.5).

The results of the mineralogy and stable isotopic composition for the background sediments, that is, low carbonate content (0.8 to 33.6 % wt carbonate) showed a range of δ^{13}C values, between 1.5 and -44.39 ‰ PDB and a range of δ^{18}O values, between 0.04 and 2.92 ‰ PDB (see Section 3.14 and Appendix 3). These results indicate the carbon sources of the carbonate in these sediments were derived from seawater, sedimentary organic diagenesis and/or early influx of methane into sedimentary pore fluids. The sediments showed a wide range of mineral contents with quartz being the dominant mineral species; while the minor mineral species, in decreasing order of abundance, included plagioclase, magnesian-calcite, aragonite and potassium feldspar. The results of the mineral contents are further addressed in the discussion (Section 4.1.5).

3.1 Station SO191-2/51, LM9 (1155 m bsl)

Figure 6 is a representative of the box core sample from Station 51. The side view of the box core shows a gap in the centre which was caused by the impact of the box core with the sediments (Figure 6A). The cross-section view of the slab shows sediment texture (Figure 6B). The top view of the box core shows an undulating surface of the sediment mixed with carbonates (Figure 6C). There was evidence of some radiating grooves on the sediment surface, which were produced probably by detritus feeding worms such as sipunculids. The carbonate-cemented tubes in this box core sample (Figure 6D) are representative of many others found in this study. A three-dimensional view of the box core shows five sub-sampled slabs and each of these slabs were

analysed separately (Figure 6E). Note, only two slabs were obtained for all subsequent

box core samples. Multiple box core slabs were used to reconstruct a three-dimensional

view of sediment texture, carbonates, and benthic invertebrate distributions, and to show

the variation in layers between sub-sampled slabs. Furthermore, physical characteristics

of the deposits vary both laterally and vertically, and this is attributed to fluctuations in

hydrocarbon seeps influencing the interaction between benthic invertebrates and seep

environments (Campbell 2006).

3.1.1 *Station SO191-2/51, subsample 51-1B (Figure 7)*

Sediment description

The analysed sediment was divided into four horizons: A (28-30 cm bsf), B (15-28 cm

bsf), C (3-15 cm bsf) and D (0-3 cm bsf) with gradational transitions between horizons.

The grain size distribution for both Horizon A and B was bimodal, coarse skewed and

mesokurtic, and Horizons C and D were bimodal, coarse skewed and platykurtic.

Horizon A was very poorly sorted, very fine sandy medium silt; while Horizons B to D

were very poorly sorted fine sandy medium silt.   In the lower part of Horizon D, the

sediment was firm and black. Additionally, in Horizon B, a water feature as shown in

the X-ray image contained some firm black sediment (Figure 7, X-radiograph).

Total organic carbon (TOC) and carbonate contents of sediments

There was a slight decrease in TOC as depth increased within slab 51-1B. In contrast,

carbonate content of the background sediments increased from 11 to 24 % wt (Figure

7). However, the carbonate content of the carbonate nodules for Horizons C and A was

64.7 and 75.4% wt, respectively (Appendix 3).

Burrow feature descriptions

There was some evidence of bioturbation throughout the horizons except for Horizon A.

Horizon D had moderate bioturbation (BI = 3) containing a strong fabric of crawling traces of *Planolites* (br2a) overall. Horizon C had sparse bioturbation (BI = 1) with some dwelling traces of *Skolithos* (br1b) occurring toward the contact with Horizon D. Horizon B had low bioturbation (BI = 2) containing some dwelling traces of *Skolithos* (br1a) and one segmented burrow filled with carbonate nodules (br1c).

Carbonate descriptions

Carbonates occurred in three horizons, A, C and D. There was a large carbonate nodule that contained carbonate sand with shell cemented in the upper part of Horizon C, between 3 and 8 cm subsurface which is as shown in white on the X-ray image. Overall, both Horizons A and C had some medium grey small carbonate nodules, up to 1.5 cm in diameter.

Shell descriptions

Shell hash with some articulated shells but mostly fragments (bivalves and gastropods) was present in Horizon C. There were two empty, parautochthonous, articulated bivalve shells identified as *Lucinoma galathea* (Marwick, 1953) which were found at 6 cm and 8 cm subsurface (S1-2, Figures 7 and 8). The shell surface of S1 (Figure 8) was covered with a thin layer of carbonate sand. In contrast, the shell surface of S2 (Figure 8) was almost free of carbonate sand. There was an empty parautochthonous gastropod, the shell surfaceof which was eroded and quite chalky, which was found at 6.5 cm subsurface, identified as *Falsilunatia sp.* (S3, Figures 7 and 8).
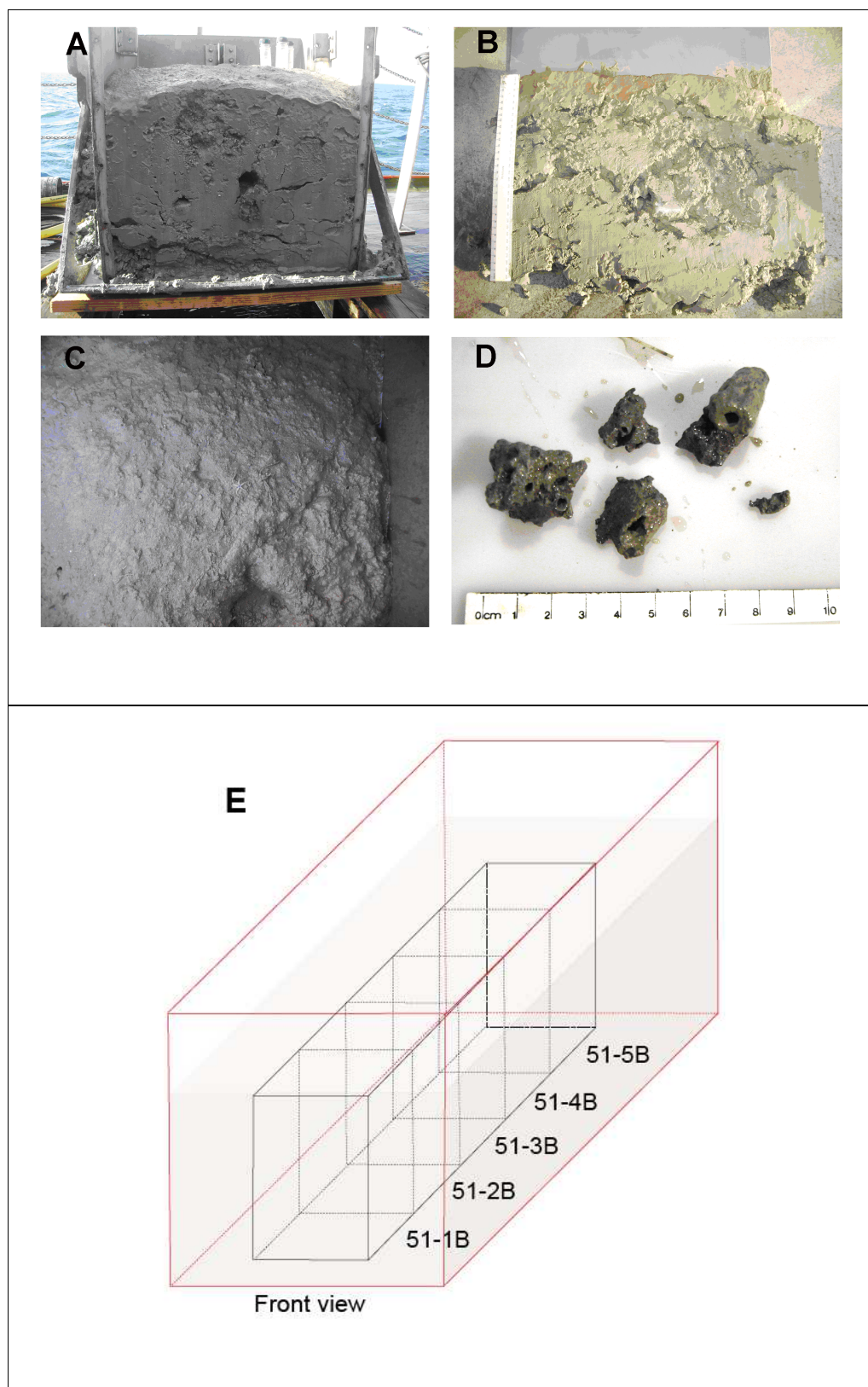
Figure 6. Station SO191-2/51 A) box core sample showing side view, B) cut away slab, C) top view, D) carbonate-cemented tubes, and E) box core subsample slabs in 3-D.

Figure 7. Core slab of the box core sub-sample 51-1B from Station SO191-2/51, 30 cm recovery. Key for X-radiograph: br1a-c (dwelling), br2a (crawling) are burrow types, wf = water feature, bm = burrow mottling, sh = shell hash, sb = shell bed, S1 and S2 = *Lucinoma galathea*, S3 = *Friginatica* sp. (refer to Figure 8 for shells).
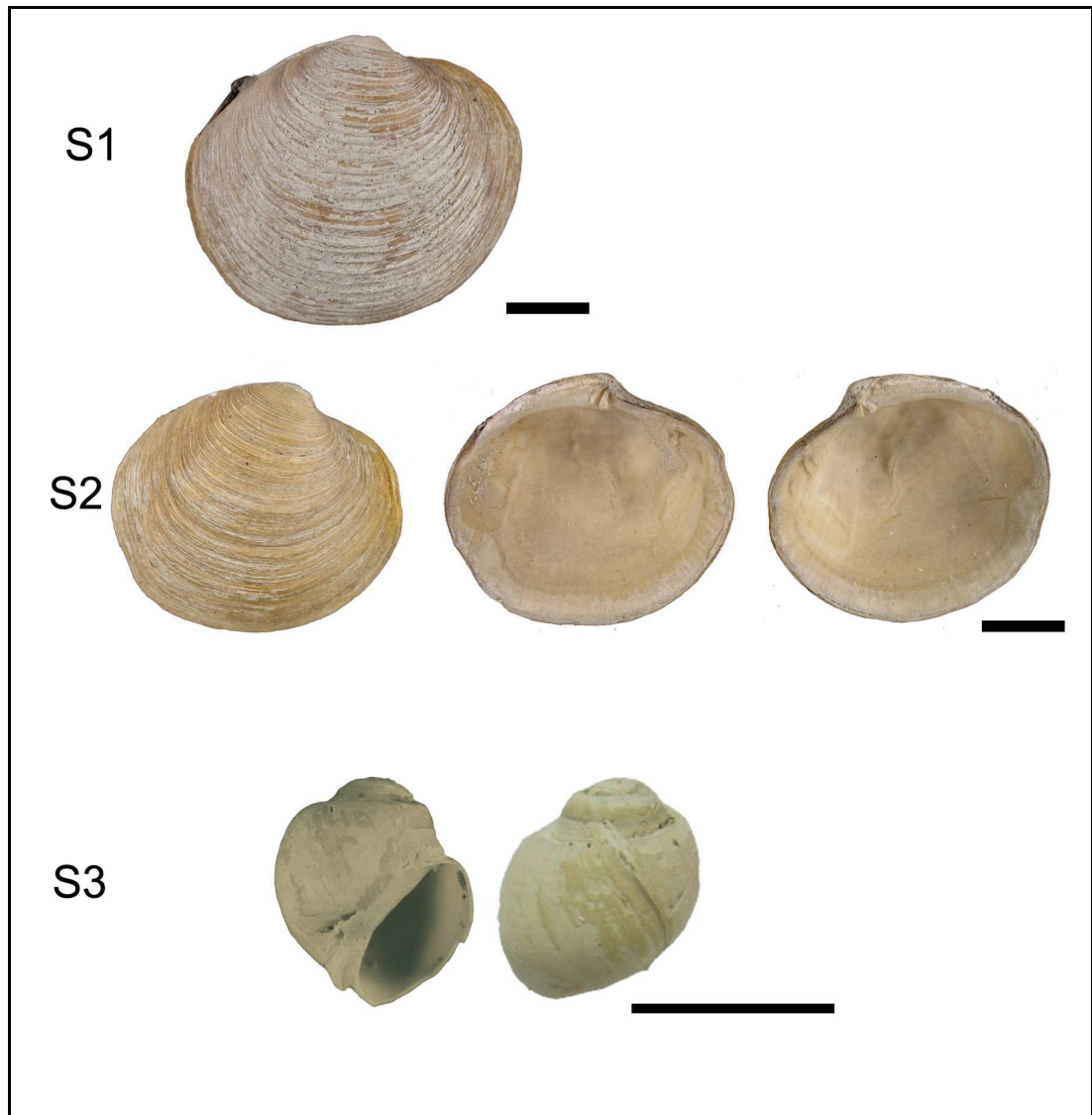
Figure 8. 51-1B shell specimens: S1 exterior of right valve, S2 exterior of right valve and interior of both valves of *Lucinoma galathea.* S3 *Falsilunatia* sp. All scale bars = 1 cm.

3.1.2 Station SO191-2/51-2B (Figure 9)

Sediment descriptions

The box core sediment was divided into five horizons: A (24-30 cm bsf), B (16-24 cm bsf), C (4-16cm bsf), D (1-4 cm bsf) and E (0-1 cm bsf). The bedding contact between each horizon was gradational. The grain size distribution for all horizons was bimodal, very poorly sorted, and coarse skewed, with a peakness variation between mesokurtic and platykurtic. The sediment texture changed from very fine sandy medium silt (Horizon A) to medium sandy fine silt (Horizon C) and then to fine sandy medium silt (Horizons D to E). The colour of the sediment progressively changed with increasing depth below sea floor, from olive brown to greyish brown and then to grey.

Total organic carbon (TOC) and carbonate contents of sediments

There was a slight decrease in TOC with increasing depth while the carbonate content increased with increasing sediment depth. However, the carbonate content of Horizon B was slightly less than that of Horizon C due to the low content of carbonate nodules in Horizon B.

Burrow feature descriptions

There was evidence of low bioturbation (BI = 1) throughout all horizons except for Horizon A. Horizon B had a faint fabric of burrow mottling and a large water feature with associated cracks. Horizon C had some horizontal undulating burrows 4 mm in diameter (br2b) which were interpreted as crawling traces of *Planolites.*   Horizon D contained some horizontal undulating burrows 2mm in diameter (br2a) inferred as feeding-dwelling traces of *Palaeophycus.*

Carbonate descriptions

Medium grey small carbonate nodules ≥ 1 cm in diameter occurred in all horizons. The density of carbonates varied considerably among these horizons. However, it appears that the carbonate density progressively decreased with increasing depth below the sea floor.

Shell descriptions

There was a living brown gastropod (height 3.5 mm, width 1.9 mm) found at 29 cm subsurface (Horizon A) (S9, Figures 9 and 10). It was identified as *Provanna* sp. (Lewis & Marshall, 1996; Waren & Ponder, 1991) in Family *Provannidae*. In Horizon B, there was a parautochthonous disarticulated shell with left valve missing belonging to *Lucinoma galathea* which was oriented adjacent to the crack on the left side of the core slab (S4, Figures 9 and 10). A parautochthonous, empty gastropod shell belonging to *Nassarius ephamillus* was found in Horizon B at 20 cm subsurface (S8, Figures 9 and 10). Its surface sculpture was fairly eroded. Horizon C had shell hash comprising some bivalves and gastropods. An autochthonous, articulated, cemented shell belonging to *Calyptogena* sp. was found at the contact between Horizons D and C (S7, Figures 9 and 10). Its sculptured surface was eroded and there was extensive pitting near the shell margin. A fragment of a right valve belonging to the same species was also found at the contact between Horizons D and C (S5, Figures 9 and 10). A single left valve of *Calyptogena* sp. (S5) and a patelliform gastropod (Figure 10A) of height 2.9 mm and length 5 mm, respectively, were retrieved from Horizon C through sieving and sorting. The *Calyptogena* shell was partly covered with brown periostracum and some borings. There was a minor dissolution near its umbo. Another parautochthonous, empty gastropod belonging to *Nassarius ephamillus* was found in Horizon C at 11 cm

44

subsurface. Its sculptured surface was severely eroded and extensively pitted.

Figure 9. Core slab of the box core sub-sample 51-2B from Station SO191-2/51, 30 cm recovery. Key legend for X-radiograph: br2a-b = crawling traces; wf=water feature, cr=crack, sb=shell bed, sh=shell hash, bm=burrow mottling, S4 = *Lucinoma galathea*, S5 & 7 = *Calyptogena* sp., S6 & S8 = *Nassarius ephamillus*, S9 = unidentified gastropod (refer to **Figure 10** for shells).
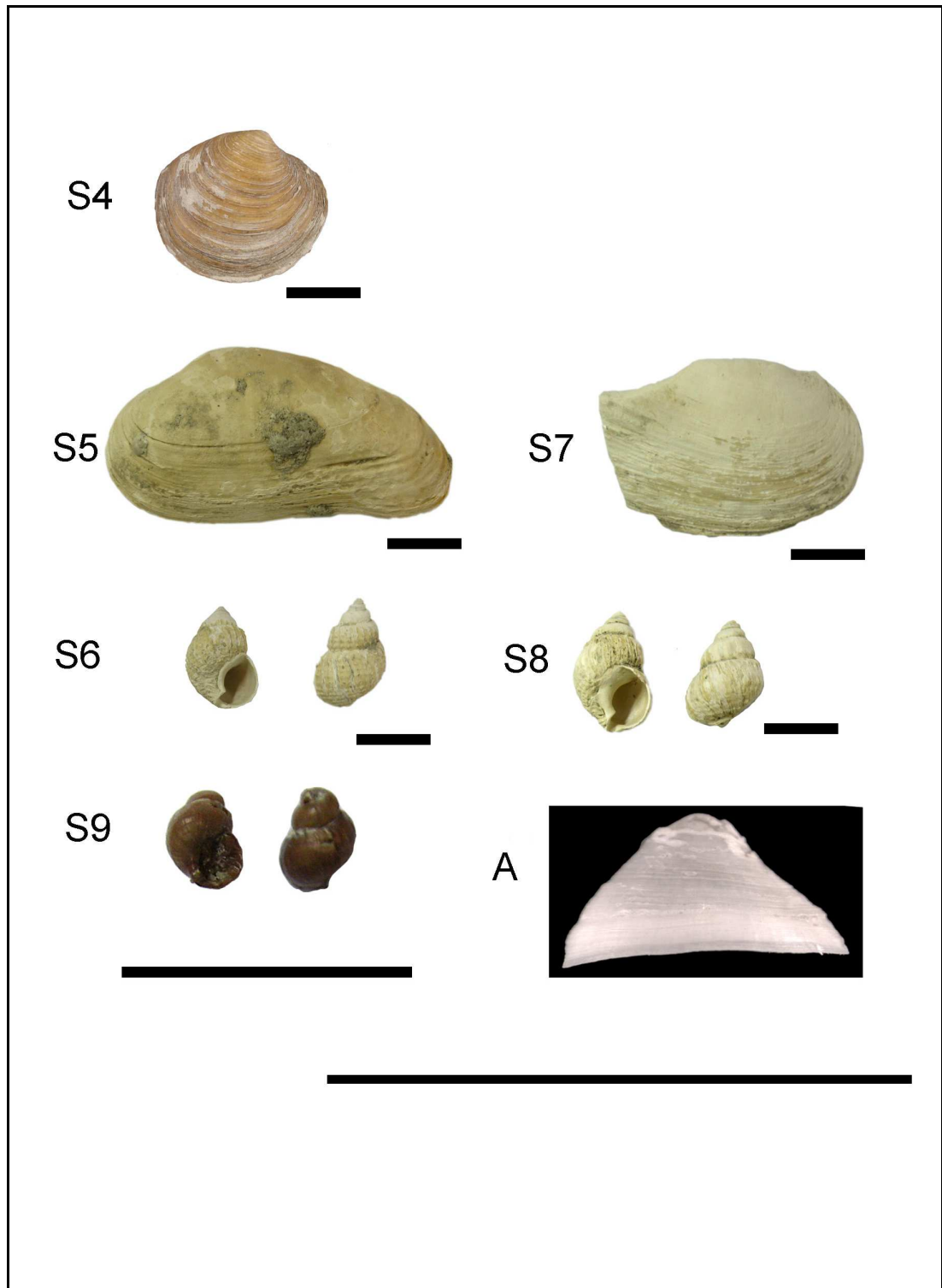
Figure 10. 51-2B shell specimens: S4 exterior of right valve of *Lucinoma galathea*; S5 exterior of left valve of *Calyptogena* sp.; S7 exterior of right valve of *Calyptogena* sp.; S6 and S8 *Nassarius ephamillus*; S9 *Provanna* sp.; and A patelliform gastropod. All scale bars = 1 cm.

3.1.3 *Station SO191-2/51, subsample 51-3B (Figure 11)*

Sediment descriptions

The box core sediment comprised three horizons: A (16-30 cm bsf), B (5-16 cm bsf) and C (0-5 cm bsf). The grain size distributions for all horizons were bimodal, very poorly sorted, coarse skewed and mesokurtic. Horizon A constituted very fine sandy fine silt; while both Horizons B and C contained fine sandy medium silt. There was a sharp and slightly undulating contact between Horizon B and C due to the change in the composition of sediment from muddy texture to clotted carbonate fabric.

Total organic carbon (TOC) and carbonate contents of sediments

There was a slight decrease in TOC with increasing depth while the carbonate content increased with increasing sediment depth. However, the carbonate content of Horizon B was high compared with Horizons A and C, which was attributed to a large amount of carbonate nodules in that horizon.

Burrow feature descriptions

There was low bioturbation (BI = 1) throughout the horizons. Horizon A had two types of burrows, crawling traces (br2b) of *Planolites* and dwelling traces (br1c) consisting of burrows filled with carbonate nodules (Figure 11, X-radiograph). There was a water feature in this Horizon. Horizon C had some dwelling traces (br1b) of *Skolithos.*

Carbonate descriptions

Horizon A contained some medium grey, small, sandy carbonate nodules (~ 0.5 cm diameter) dispersed throughout, whereas Horizon B contained extensive, medium grey, small, sandy nodules with irregular margins (~ 2 cm in diameter). Their density decreased with increasing depth between 6 cm and 30 cm subsurface.

48

Shell descriptions

Horizon B had a shell bed containing three parautochthonous, empty, articulated shells at between 5 and 10 cm subsurface (S10-12, Figures 11 and 12), and one autochthonous, empty articulated shell (S13, Figures 11 and 12) near the contact between Horizon C and B (S14, Figures 11 and 12). In Horizon A, there was an autochthonous, empty, articulated shell oriented adjacent to the water feature at 23-25 cm subsurface (S14, Figures 11 and 12). All these shells belong to *Lucinoma galathea*. The degree of discoloration on the shell surface varied among these shells, and all have some cemented sediments adhered to their surfaces (Figure 12). Based on a low degree of discoloration and its highest stratigraphic position, shell S13 appears to be the youngest of the group.
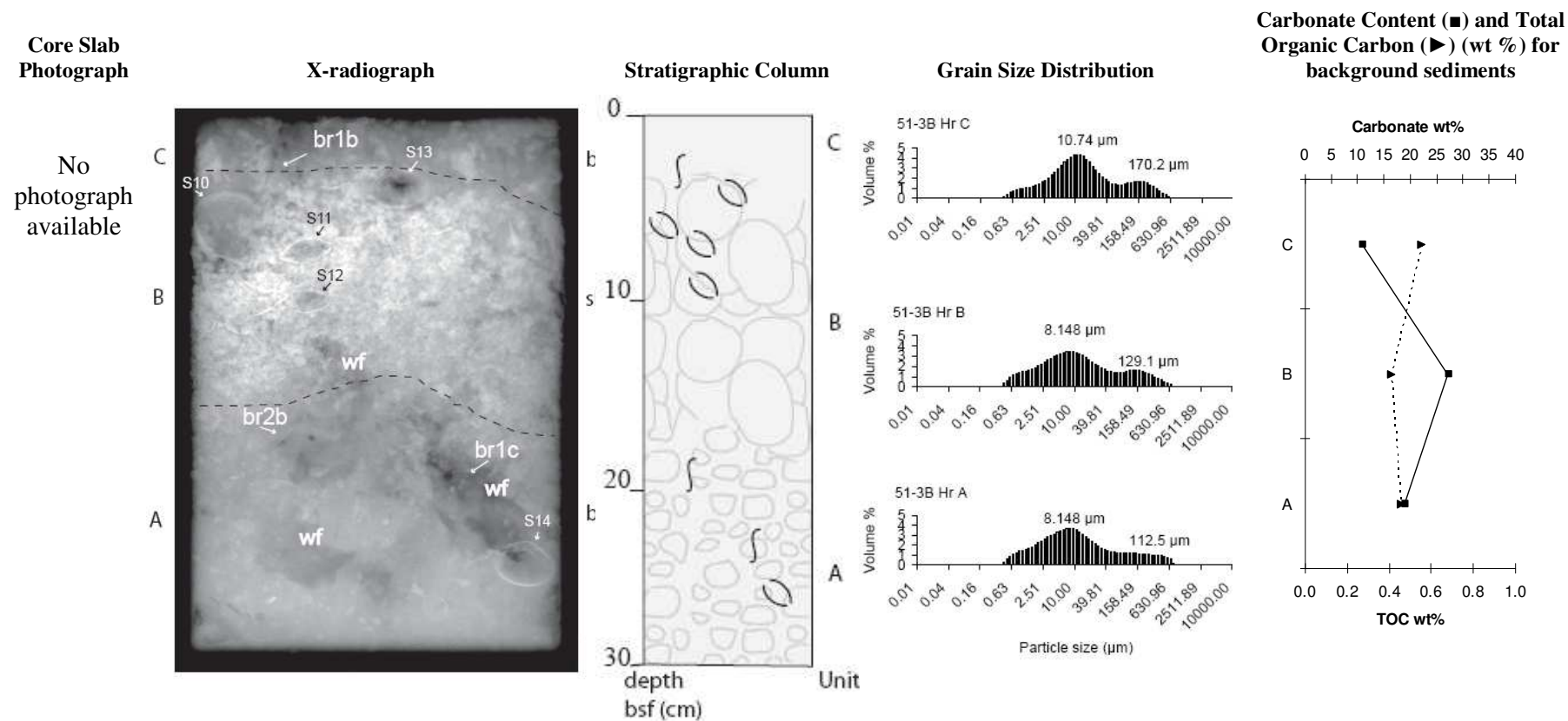
Figure 11. Core slab of the box core sub-sample 51-3B from Station SO191-2/51, 30 cm recovery. Key legend for X-radiograph: br1b-c (dwelling), br2b (crawling) = burrow types, wf=water feature, bm=burrow mottling, sb=shell bed, S10-14 = *Lucinoma galathea* (refer to **Figure 12** for shells).
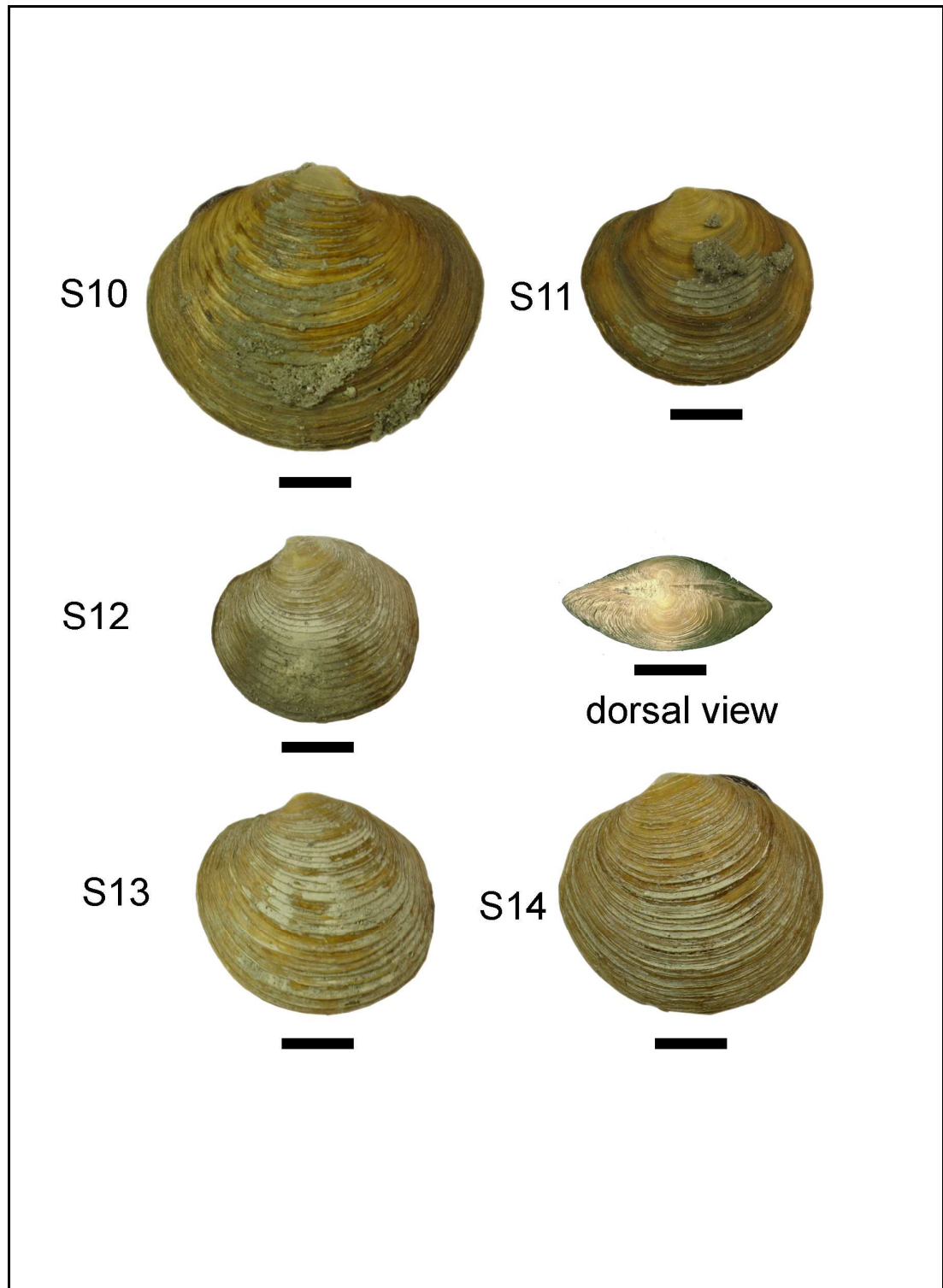
Figure 12. 51-3B shell specimens: *Lucinoma galathea*, S10 right valve, S11-14 left valve. All scale bars = 1 cm.

3.1.4 *Station SO191-2/51, subsample 51-4B (Figure 13)*

Sediment descriptions

The box core sediment was composed of three horizons: A (18/22-30 cm bsf), B (1.5-18/22 cm bsf) and C (0-1.5 cm bsf), with gradational contacts between each horizon. The grain size distribution for all horizons was bimodal, very poorly sorted, coarse skewed, and mesokurtic for Horizon A and platykurtic for Horizons B and C. Horizon A comprised grey fine sandy fine silt. Horizon B consisted of grey, fine sandy fine silt. Horizon C constituted light brownish grey fine sandy medium silt.

Total organic carbon (TOC) and carbonate contents of sediments

There was no trend in TOC or carbonate content with increasing depth within the sediment column.

Burrow feature descriptions

There was low bioturbation (BI=1) throughout the core. Horizon A had two types of burrows comprising dwelling traces (br1b) of *Skolithos* and crawling traces (br2b) of *Planolites.* Horizon B had some crawling traces (br2b) of *Planolites* and a water feature (Figure 13, X-radiograph).

Carbonate descriptions

Horizon B contained some medium grey, small sandy carbonates nodules, fine to gritty (1.5 cm in diameter) throughout. Horizon A contained some medium grey, large carbonate nodules with irregular margins dispersed throughout. There was a large clump of carbonates in a triangular shape in this horizon at 30 cm subsurface which is shown as the white X-ray shade. This clump was made up of some medium grey, large carbonate nodules with irregular margins (~ 3 cm in diameter).

Shell descriptions

Horizon B had some shell hash consisting of some shell fragments and sponge

fragments, which were retrieved through sieving and sorting (Figure 14). These shell

fragments were unidentified because of the high dissolution of shell surfaces and

fragmentation of the shells. The sponge fragments may be part of a glass sponge

belonging to class Hexactinellida; however, its taxon is indeterminate.

Figure 13. Core slab of the box core sub-sample 51-4B from Station SO191-2/51, 30 cm recovery. Key legend for X-radiograph: br1b (dwelling), br2b (crawling) = burrow types, wf=water feature, sh=shell hash.
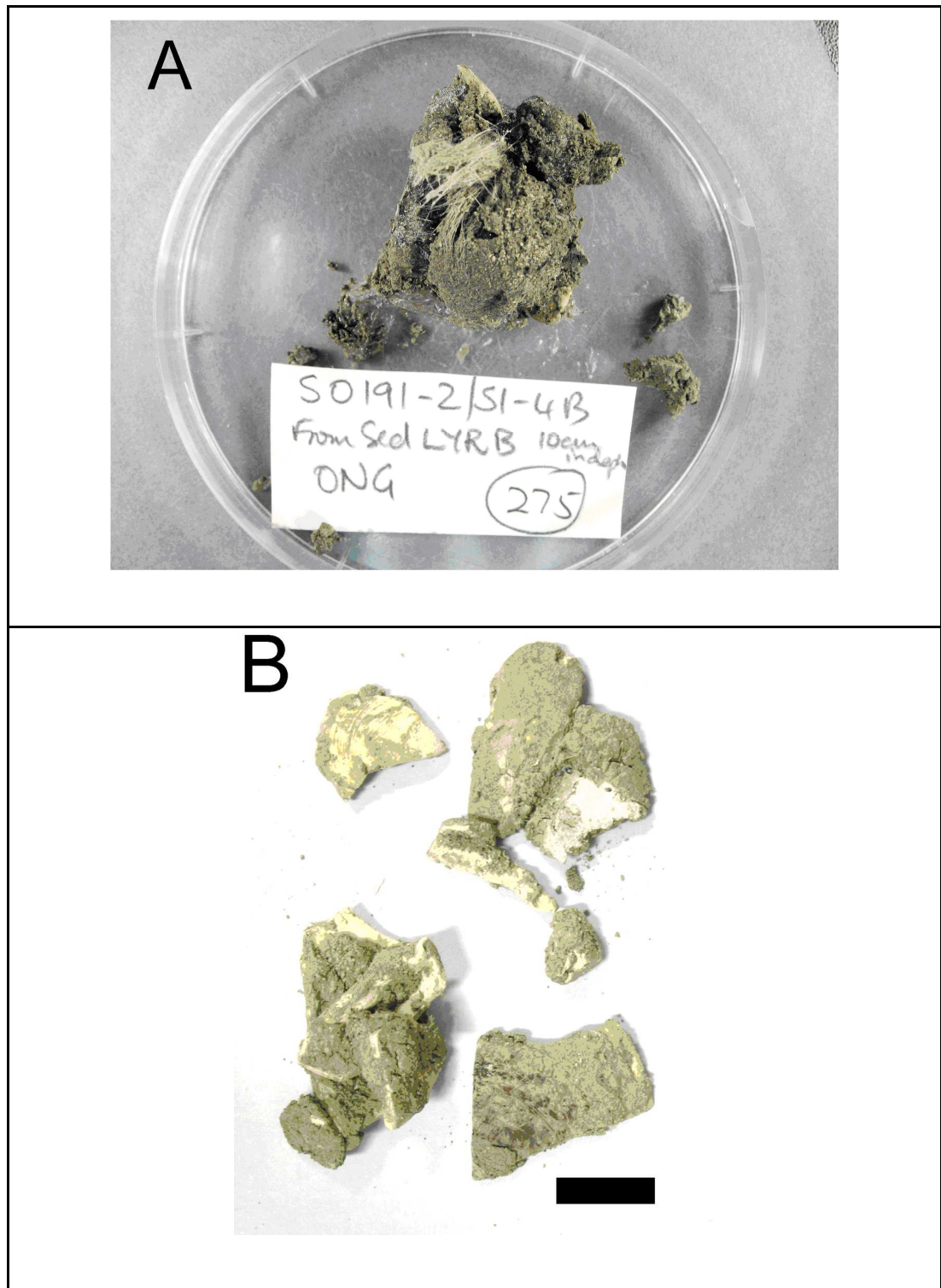
Figure 14. 51-4B: A) sponge fragment, circular dish diameter = 8.7 cm; and B) unidentified shell fragments, scale bar = 1 cm.

3.1.5 *Station SO191-2/51, subsample 51-5B (Figure 15)*

Sediment descriptions

The box core sediment consisted of three horizons: A (12-30 cm bsf), B (4-12 cm bsf) and C (0-4 cm bsf). There was a non-planar boundary between Horizon B and A which is attributed to a change in sediment composition. The bedding contact between Horizon B and C was gradational. The grain size distribution for Horizon A was unimodal, coarse skewed and mesokurtic; for Horizon B, unimodal, coarse skewed and leptokurtic; and for Horizon C, bimodal, coarse skewed and platykurtic. Horizons A and B had very poorly sorted, grey, very fine sandy medium silt; while Horizon C comprised very poorly sorted, olive-grey, fine sandy medium silt.

Burrow feature descriptions

There was some bioturbation (BI = 1) throughout all horizons. Horizon A hosted three types of dwelling traces: obliquely inclined cylindrical structures belonging to *Skolithos* (br1b); obliquely inclined, slightly j-shaped, segmented burrows filled with carbonate nodules (br1c); and another type of crawling trace (br2b) attributed to *Planolites.* Horizon B had some crawling traces (br2b) of *Planolites* (Figure 15, X-radiograph).

Carbonate descriptions

Horizon A contained some dispersed carbonate nodules, the density of which decreased with increasing depth. Horizon B contained extensive, medium grey, small sandy nodules with irregular margin.

Shell descriptions

Horizon B had some bivalve shell debris. A parautochthonous, disarticulated, *Calyptogena* shell, which was heavily cemented and partly fragmented, was found at the contact between B and C (S15, Figures 15 and 16). A remnant of *Acharax clarificata*

with some periostracum intact was found in Horizon A at 28 cm subsurface (S16,

Figures 15 and 16).

Core Slab Photograph	X-radiograph	Stratigraphic Column	Grain Size Distribution	Carbonate Content (■) and Total Organic Carbon (►) (wt %) for background sediments
				N/A

Figure 15. Core slab of the box core sub-sample 51-5B from Station SO191-2/51, 30 cm recovery. Key legend for X-radiograph: br1b-c (dwelling) br2b (dwelling) = burrow types, wf=water feature, 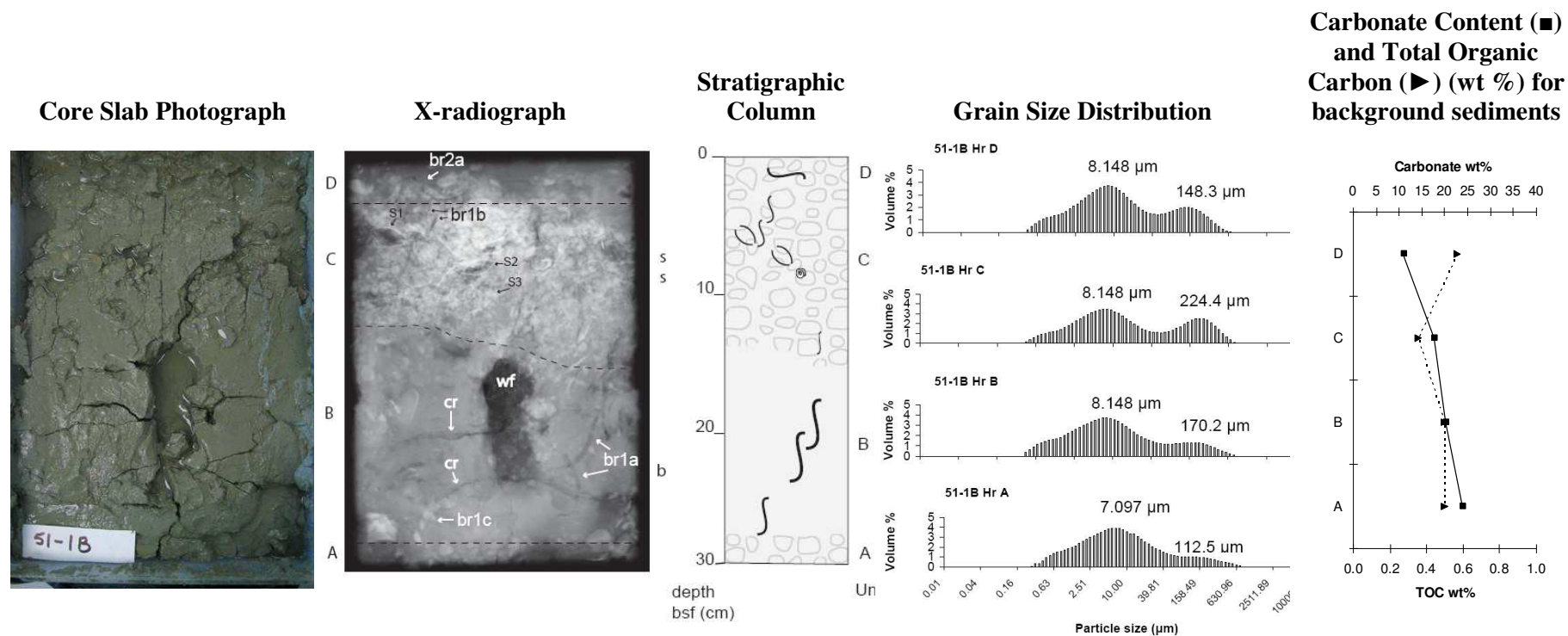cr=crack, bm=burrow mottling, sh=shell hash, S14 = cemented *Calyptogena* sp. and S16 = fragmented, cemented *Acharax clarificata* (refer to **Figure 16**, for shells).
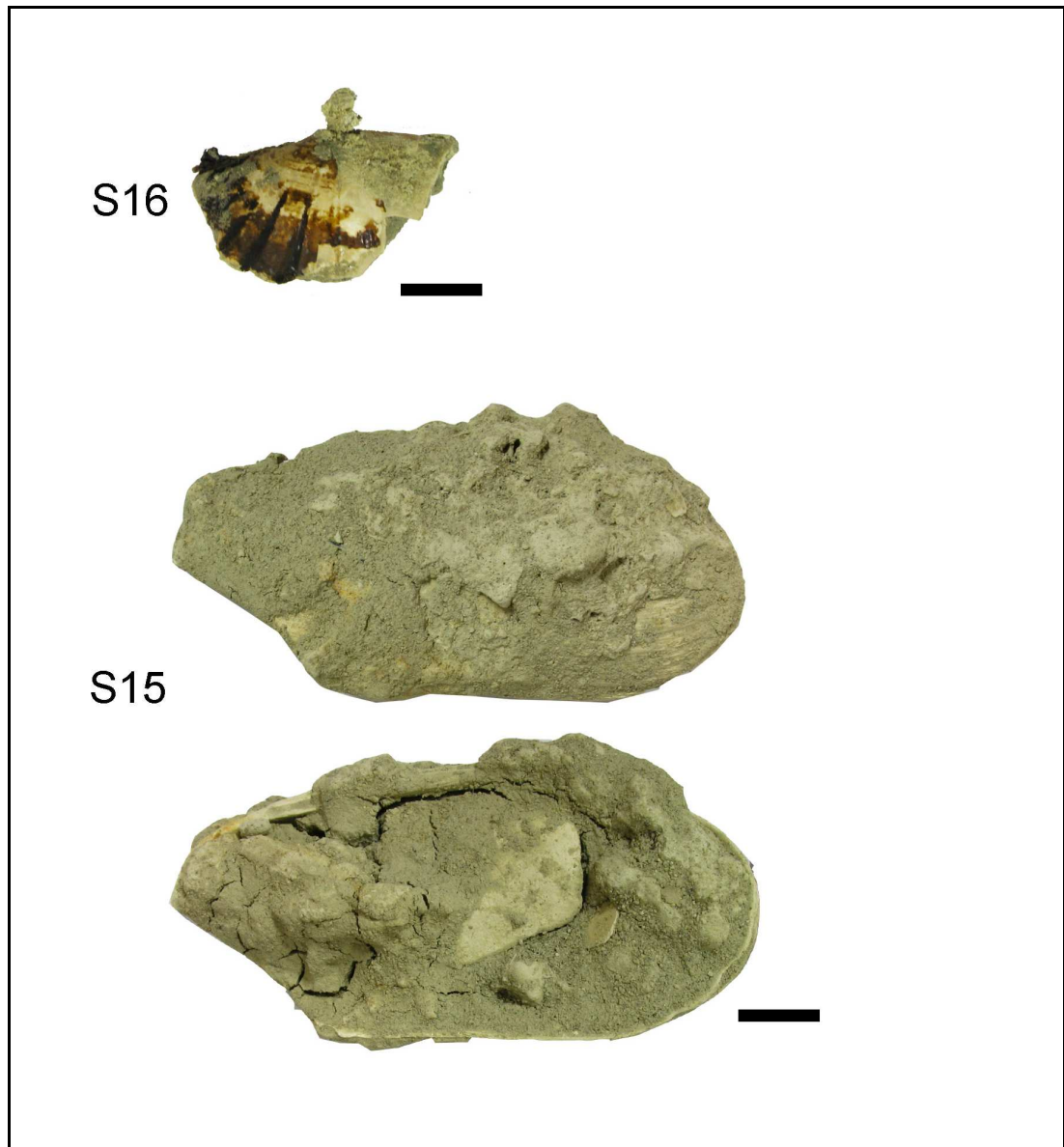
Figure 16. 51-5B shell specimens: S16 shell fragment of *Acharax clarificata*, S15 *Calyptogena* sp. exterior of right valve (top) and interior of left valve (bottom). All scale bars = 1 cm.

3.2 Station SO191-2/66, LM9 (1097 m bsl)

Figure 17 is a representative box core sample for Station 66. The top view of the box core shows the sediment surface covered with shell debris of *Calyptogena* sp. (Figure 17A). The side view of the box core shows the progressive change from sediments with shell debris to sediments coalesced with carbonate nodules deep within the sediment column (Figure 17B). Figure 17D shows some disarticulated, articulated and fragmented shells in various taphonomic characters states common in seep habitats with past active seepage (e.g. Callender et al. 1992).

3.2.1 *Station SO191-2/66, subsample 66-1B (Figure 18)*

Sediment descriptions

The box core sediment consisted of three horizons: A (13-24 cm bsf), B (6-13 cm bsf) and C (6-13 cm bsf), with non-planar bedding contacts between horizons. The grain size distribution for all horizons was bimodal, and very poorly sorted. Horizon A was coarse skewed and mesokurtic, and Horizons B and C were very fine skewed and platykurtic. Horizon A comprised grey, very fine sandy medium silt. The bottom right corner of this horizon contained some black, medium silty medium sand. Horizons B and C consisted of grey, medium silty medium sand.

Total organic carbon (TOC) and carbonate contents of sediments

There was no change in TOC with increasing depth within the sediment column. Horizon B had a high carbonate content compared with Horizons A and C, which due to extensive carbonate nodules therein.

Burrow feature descriptions

There was no evidence of bioturbation throughout the horizons or visible burrow features on the X-ray image. However, there were some empty sinuate chitinous

60

tubes attributed to ?*Lamellibrachia* sp. in the box core sample (Figure 17C). Some

polychaetes also were collected from this box core sample through sieving and sorting

on board RV SONNE, which were preserved in a buffered 10% formalin and later

stored at NIWA for taxonomic identification.

Carbonate descriptions

Horizon A contained some medium grey, small carbonate nodules and a few dark grey

ones dispersed throughout sand (~ 0.5 cm in diameter).   Horizon B had some medium

grey, small sandy carbonate nodules (≤ 1 cm), fine with some gritty. Horizon C

contained some medium grey, grainy, small carbonate nodules (~ 1 cm) with black

flecks (organic matter?) which were mixed in with shell debris.

Shell descriptions

Horizon C contained some shell hash that was a mixture of articulated and disarticulated

shells belonging to *Calyptogena* sp. and some empty gastropods (e.g. Figure 19, S17).

A cemented shell fragment was found at 7-9 cm bsf (Figure 19, S18). Horizon B

contained some shell fragments (6-14 cm bsf), gastropods (8-9 cm bsf) (e.g. Figure 19,

S20) and disarticulated and articulated *Calyptogena* shells (8-17 cm bsf) (e.g. Figure 19,

S29).

Figure 17. Station SO191-2/66 box core: A) top view, B) side view, C) oblique cut away showing siboglinid tubes and D) representative death assemblage of vesicomyid molluscs.
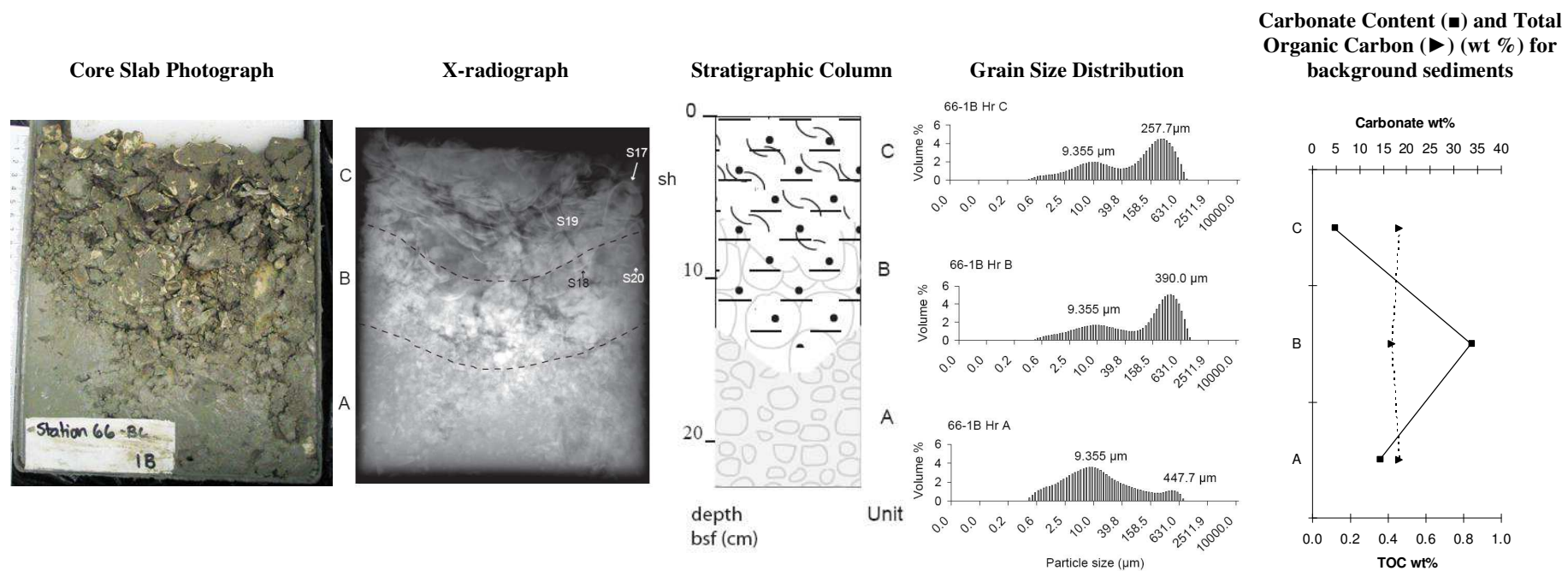
Figure 18. Core slab of the box core sub-sample 66-1B from Station SO191-2/66, 24 cm recovery. Key legend for X-radiograph: sh=shell hash, S17 to19 = *Calyptogena* sp., S20 = *Nassarius ephamillus.*
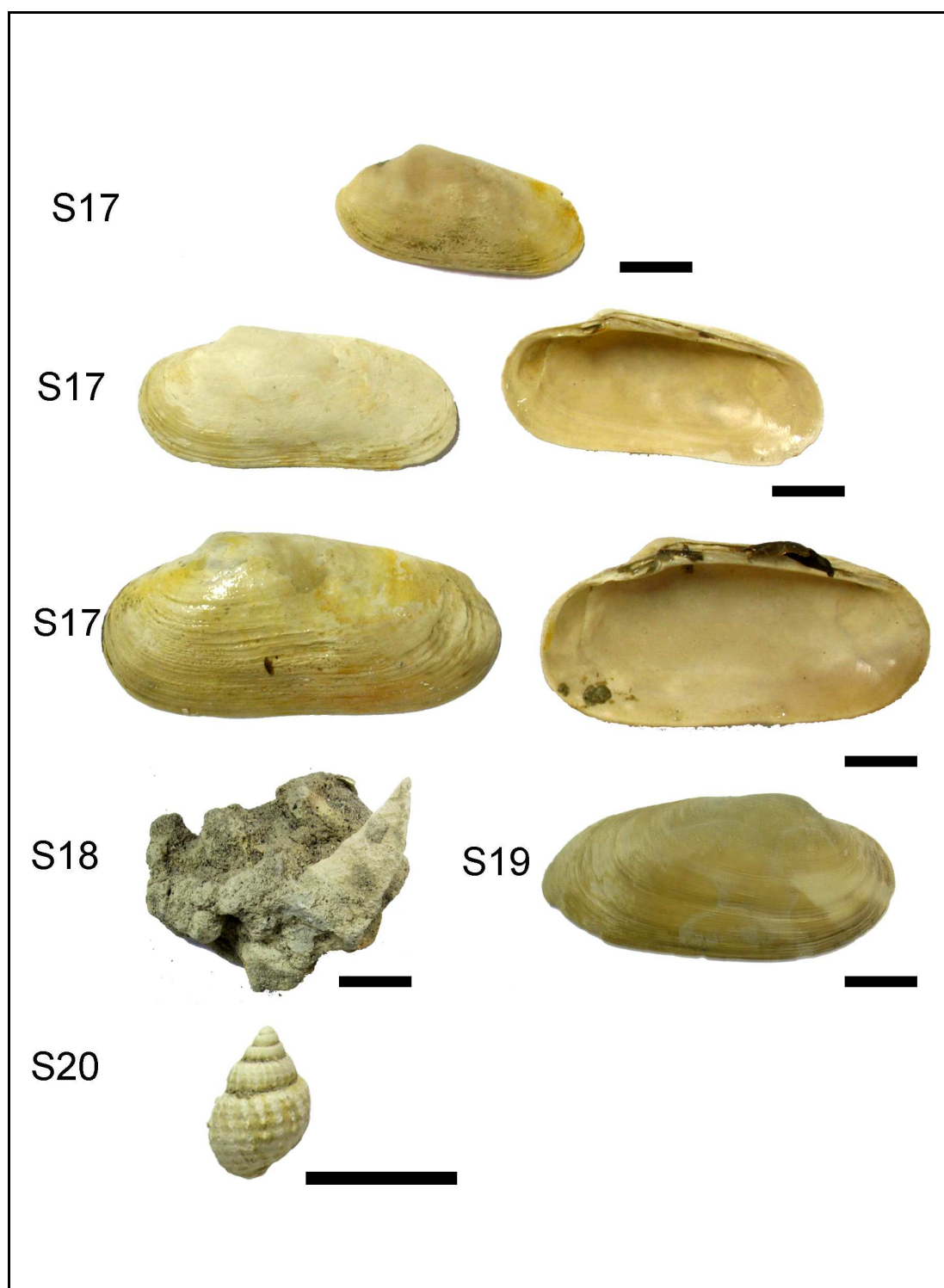
Figure 19. 66-1B shell specimens: S17 and S19 *Calyptogena* sp., S18 cemented shell fragment, S20 *Nassarius ephamillus*. All scale bars = 1 cm.

3.2.2 *Station SO191-2/66, subsample 66-2B (Figure 20)*

Sediment descriptions

The box core sediment consisted of three horizons: A (11-30 cm bsf, centre of the slab), B (8-30 cm bsf) and C 0-8 cm bsf). The grain size distribution for Horizon A was unimodal, very poorly sorted, symmetrical and mesokurtic; for Horizon B, bimodal, coarse skewed and mesokurtic; and for Horizon C, bimodal, very fine skewed and mesokurtic. Horizon A had very poorly sorted grey very fine sandy medium silt. Horizons B and C comprised very poorly sorted, grey, medium sandy medium silt.   The bedding contact between each horizon was non-planar due to differences in sediment texture and composition.

Burrow feature descriptions

The burrow structures are obscured throughout the X-ray image.

Carbonate descriptions

Horizon A had very few carbonate nodules. Horizon B had extensive solid nodular carbonates with irregular margins and Horizon C had some dispersed carbonate nodules.

Shell descriptions

Horizon C had shell hash with disarticulated shells (S21, A, Figures 20 and 21) attributed to *Calyptogena* sp. and a *Provanna* shell in Horizon B (Figure 21b). No shells were present in Horizon A.
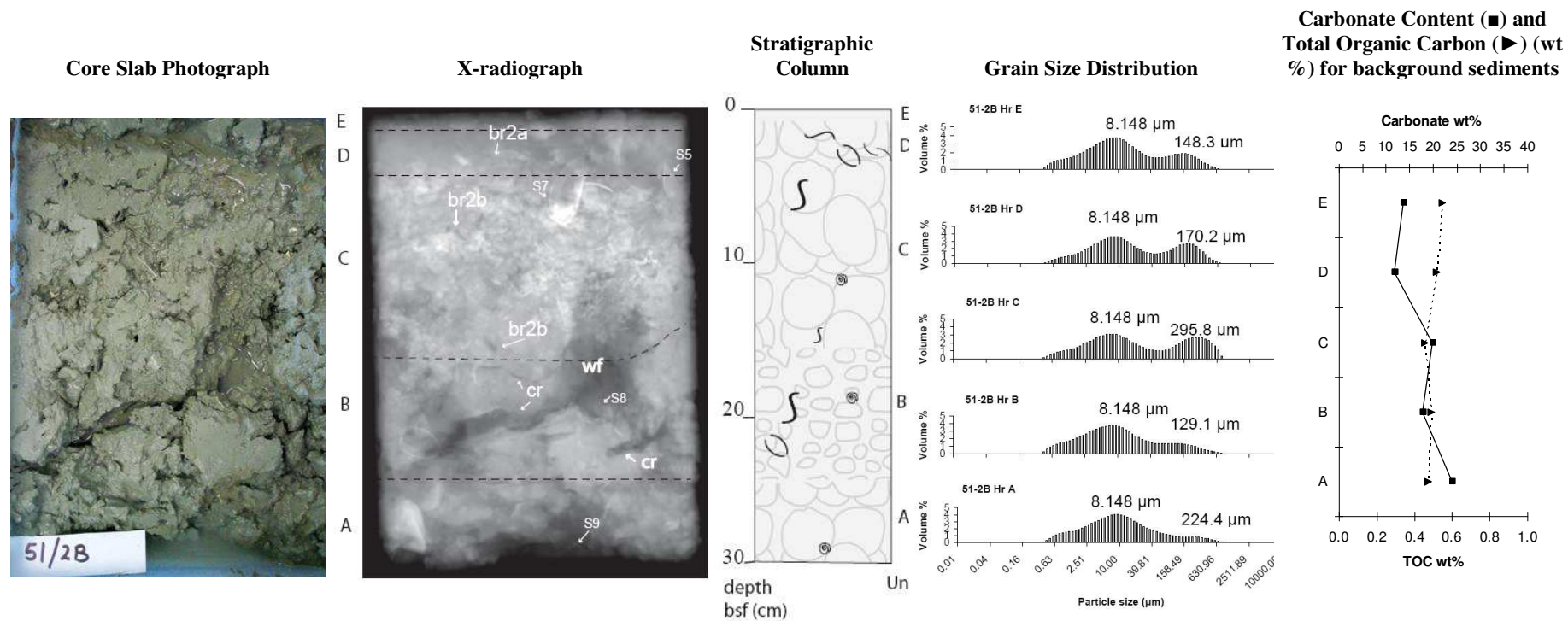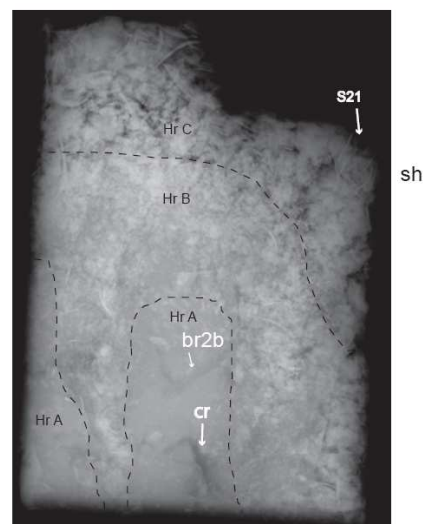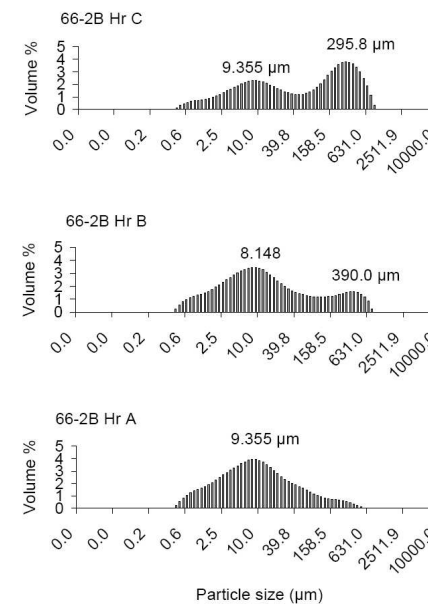
Figure 20. Core slab of the box core sub-sample 66-2B from Station SO191-2/66, 30 cm recovery. Key legend for X-radiograph: sh=shell hash, br2b = crawling trace, cr = crack, S21 = *Calyptogena* sp.
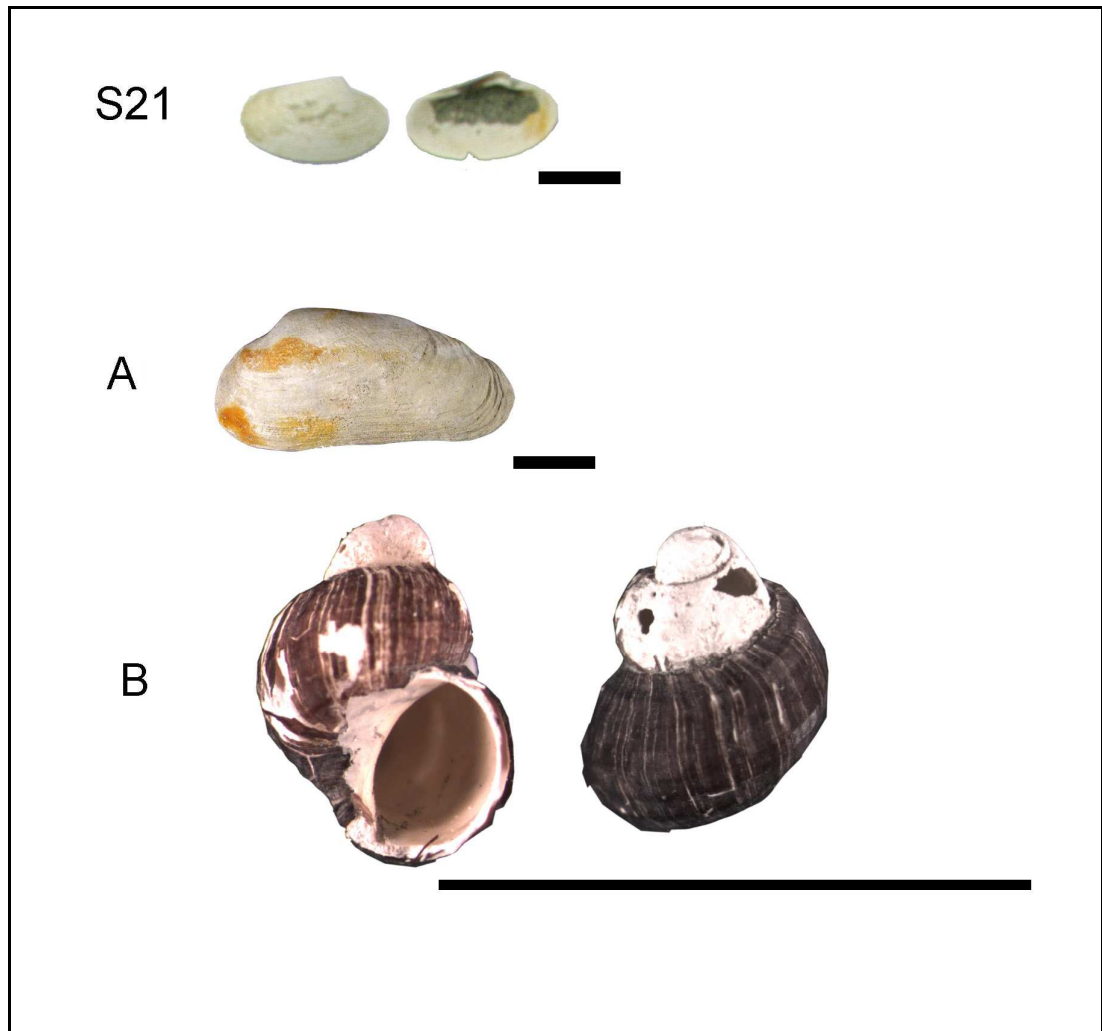
Figure 21. 66-2B shell specimens: S21 juvenile *Calyptogena* sp., A) exterior left valve of *Calyptogena* sp., B) *Provanna* sp. All scale bars = 1 cm.

3.3   Station SO191-2/96, south of LM9 (1096 m bsl)

The box core sample for this site contained no shell debris or carbonates which was different from other box core samples (Figure 22).   This shows some variations in the texture of seep sediments in the region.

3.3.1   *Station SO191-2/96, subsample 96-1B (Figure 23)*

Sediment descriptions

The box core sediment consisted of three horizons: A (14-30 cm bsf), B (2.5-14 cm bsf) and C (0-2.5 cm bsf). The bedding contact between each horizon was gradational and was defined by the differences in colour and texture of the sediment. The grain size distribution for Horizon A was bimodal, coarse skewed and mesokurtic; for Horizon B, bimodal, coarse skewed and platykurtic; and for Horizon C, bimodal, symmetrical and platykurtic. Horizon A constituted very poorly sorted, grey, very fine sandy fine silt. Horizon B comprised fine sandy medium silt with colour changes in depth, from greenish brown to greyish brown-green. Horizon C consisted of very poorly sorted, brownish, fine sandy medium silt with a strong odour of hydrogen sulfide.

Burrow feature descriptions

Horizon A had sparse bioturbation (BI = 1) containing an obliquely inclined, slightly j-shaped burrow 10 mm in diameter (br1e), which was identified as a dwelling trace. Horizon B had low bioturbation (BI = 1) with two dwelling traces (br1b – *Skolithos* and br1e) and one crawling trace of *Palaeophycus.* Horizon C was faintly burrow mottled (BI = 2) throughout (Figure 23,X-radiograph).

Carbonate descriptions

There were no carbonates in this box core sample.

Shell descriptions

There were no shells in this box core sample.
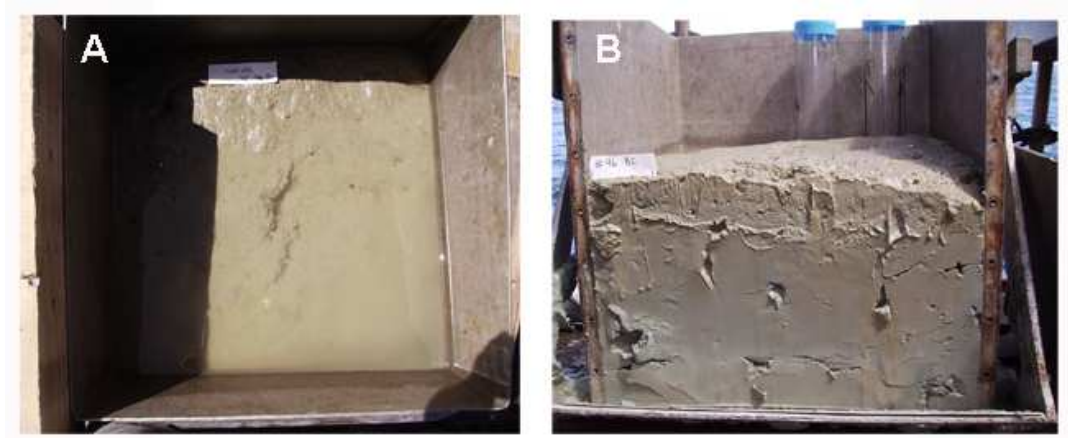
Figure 22. Station SO191-2/96 box core: (A) top view and (B) side view

| Core Slab Photograph | X-radiograph | Stratigraphic Column | Grain Size Distribution | Carbonate Content (■) and Total Organic Carbon (►) (wt %) for background sediments |

Figure 23. Core slab of the box core sub-sample 96-1B from Station SO191-2/96, 30 cm recovery. Key legend for X-radiograph: bm = burrow mottling, cr = crack, wf = water feature, br1b-e (dwelling), br2a (crawling) = burrow types, S22 = *Nassarius ephamillus.*

70

3.3.2 *Station SO191-2/96, subsample 96-2B (Figure 24)*

Sediment descriptions

The box core sediment consisted of three very poorly sorted horizons: A (9-30 cm bsf),

B (1-9 cm bsf) and C (0-1 cm bsf), with gradational bedding contacts between horizons

defined by the differences in the sediment colour and texture. The grain size

distribution for all horizons was bimodal, coarse skewed and mesokurtic for Horizon A,

platykurtic for Horizons B and C. Horizon A constituted grey, very fine sandy fine silt.

Horizon B comprised greyish brown, fine sandy fine silt. Horizon C consisted of olive-

brown, fine sandy medium silt.

Total organic carbon (TOC) and carbonate contents of sediments

There was no trend in TOC or carbonate content with increasing depth within the

sediment column. This reflected the lack of carbonate nodules in the core sample.

Burrow feature descriptions

There was some evidence of bioturbation (BI = 1) throughout all horizons. Horizon A

had a large water feature and a crawling trace of *Planolites.* Horizon B had four burrow

types. These were two dwelling traces, one obliquely inclined, slightly j-shaped and

8 mm in diameter (br1e), and an obliquely inclined, cylindrical structure identified as

Skolithos. Moreover, there was one crawling trace of *Planolites* (br2b) and one resting

trace (br3) which was occupied by a sea anemone, *Isoparactis farex* (Figure 25.

Carbonate descriptions

There were no carbonates in this box core sample.

Shell descriptions

There were no shells in this box core sample.
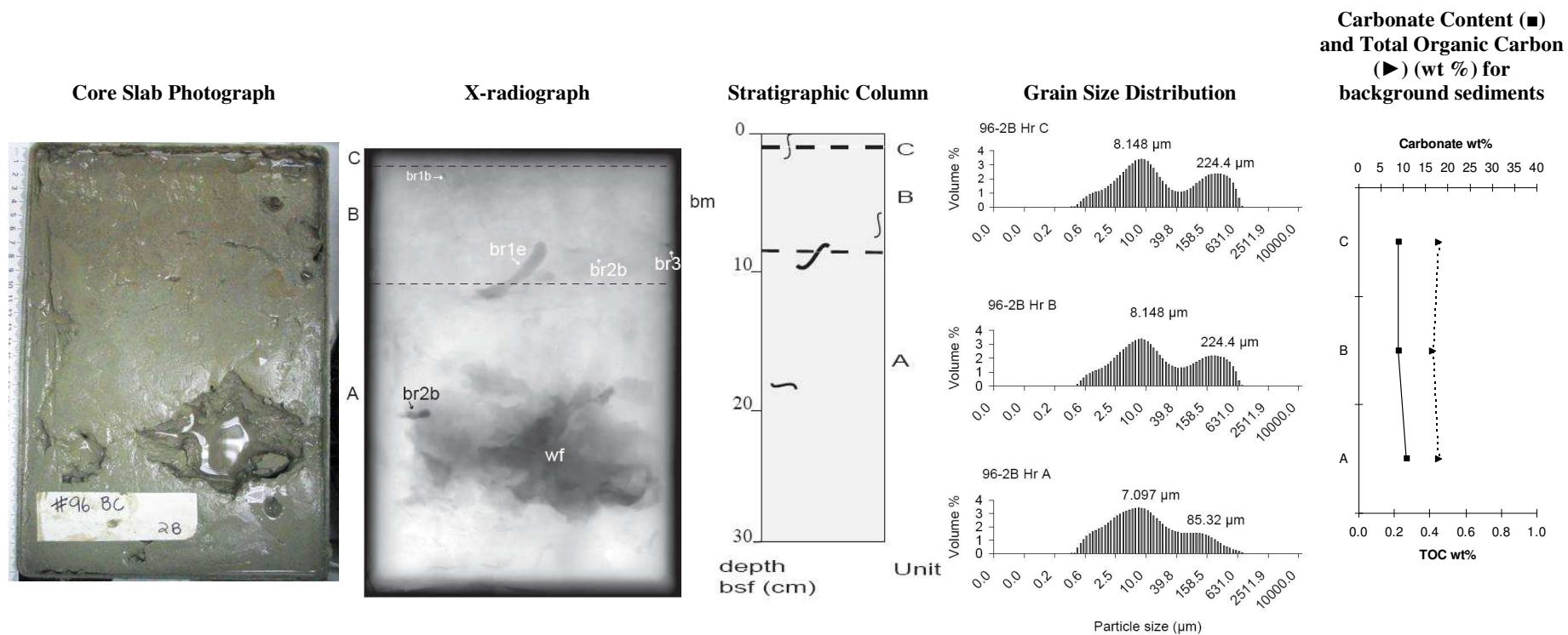
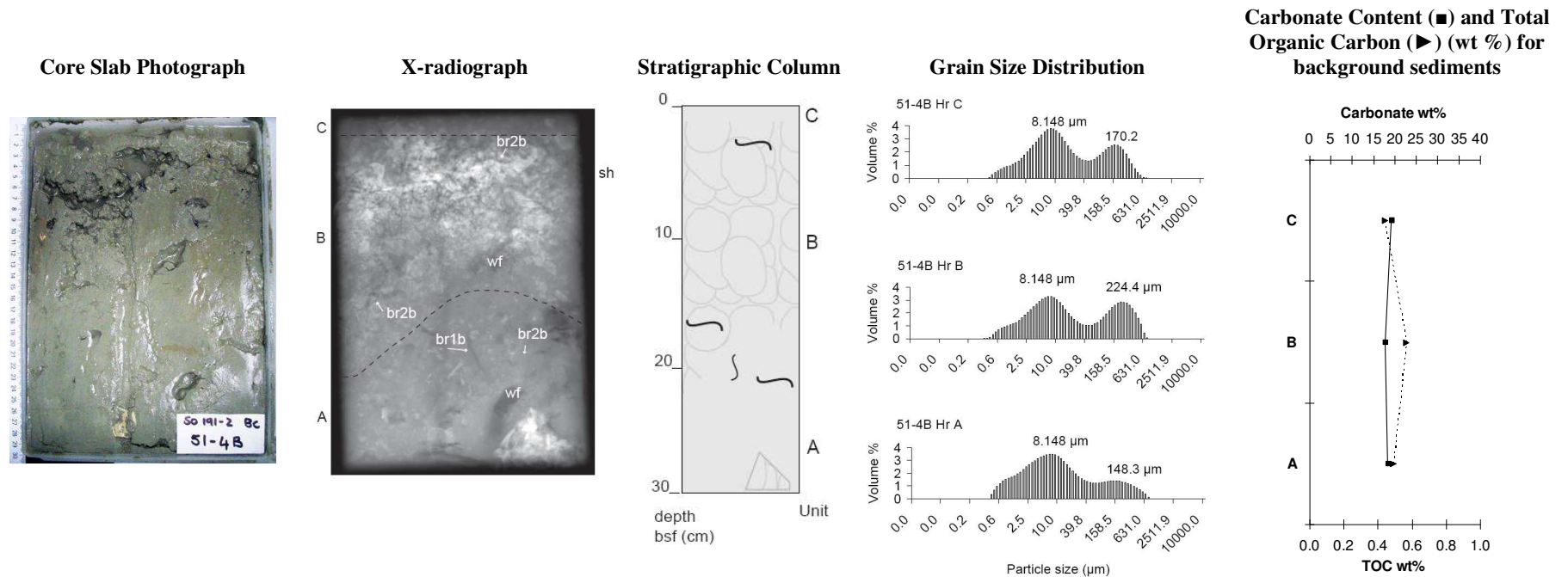**Figure 24.** Core slab of the box core sub-sample 96-2B from Station SO191-2/96, 30 cm recovery. Key legend for X-radiograph: bm = burrow mottling, wf = water feature, br1b,e (dwelling), br2b (crawling) br3 (resting) = burrow types.

Figure 25. *Isoparactis ferax* retrieved from box core subsample 96-2B, SO191-2, A) In situ; B) extracted specimen. Scale bars = 1 cm.

3.4 Station SO191-2/98, south of LM9 (1101 m bsl)

Figure 26 shows the top and side a representative box core sample and one live adult
Acharax clarificata that was retrieved from this core through sieving and sorting.

3.4.1 *Station SO191-2/98, subsample 98-1B (Figure 27)*

Sediment descriptions

The box core sediment consisted of three horizons: A (9-24 cm bsf), B (5-9cm bsf) and
C (0-5 cm bsf), with a non-planar bedding contact between Horizons A and B and
gradational contact between Horizons B and C. These bedding contacts were defined
by the differences in composition of sediments between each horizon. The grain size
distribution for Horizon A was bimodal, coarse skewed and platykurtic; for Horizon B,
unimodal, coarse skewed and mesokurtic; and for Horizon C, bimodal, symmetrical and
platykurtic. Horizons A and C comprised very poorly sorted, grey, medium sandy
medium silt. Horizon B constituted very poorly sorted, grey, very fine sandy fine silt.

Total organic carbon (TOC) and carbonate contents of sediments

There was a slight increase in TOC between the top horizon and middle horizon. In
contrast, the carbonate content was inversed. These differences are attributed to the
sediment texture. Overall, there was no trend in either TOC and carbonate content.

Burrow feature descriptions

Bioturbation activities were evident (BI = 1) throughout the horizons. There were two
types of burrow structures in this subsample, a dwelling trace (br1f) and a crawling
trace (br2c). The dwelling traces (br1f) in this core subsample were obliquely inclined
burrows (1 mm in diameter) occupied by tube dwelling polychaetes (?Chaetopteridae)
(Figure 28). The crawling trace was an U-shaped burrow, 3 mm in diameter which was
identified as cf. *Solemyatuba* and it was occupied by juvenile *Acharax clarificata*

(length of shells: 8 mm) (S23, Figures 27 and 29).

Carbonate descriptions

Extensive, solid, nodular carbonates were present throughout all horizons in the subsurface. However, Horizon B contained only carbonates while Horizons A and C contained carbonates mixed in with shell fragments.

Shell descriptions

Horizon C comprised shell hash with some disarticulated and fragmented *Calyptogena* shells and some well worn gastropods belonging to *Nassarius* sp. (S24, Figures 27 and 29). Horizon A had some shell fragments. A right valve of *Calyptogena* sp. (S25, Figures 27 and 29), retrieved from Horizon C, had some borings on its surface.

Figure 26. SO191-2/98 box core sample: A) top view with *Ophiomusium lymani* (arrow), B) side view and C) adult *Acharax clarificata* retrieved from the core through sieving.
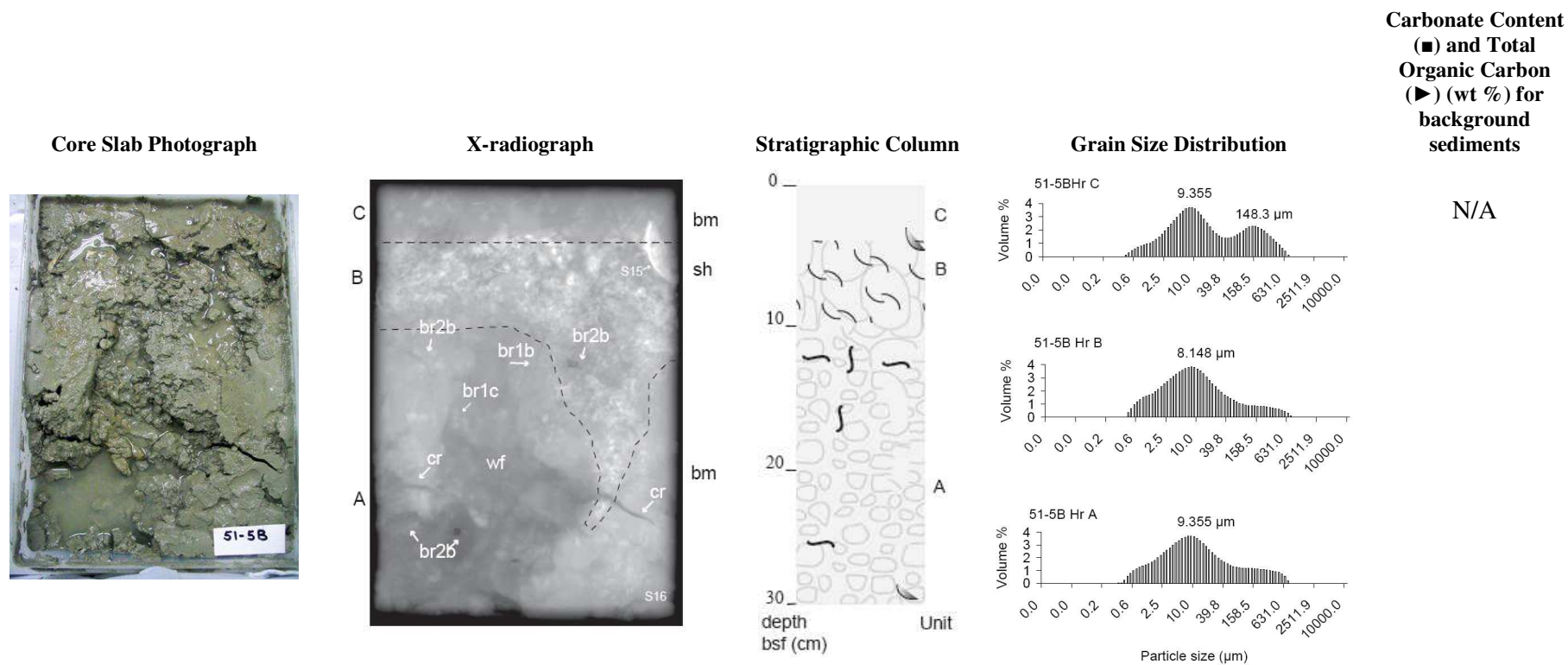
75
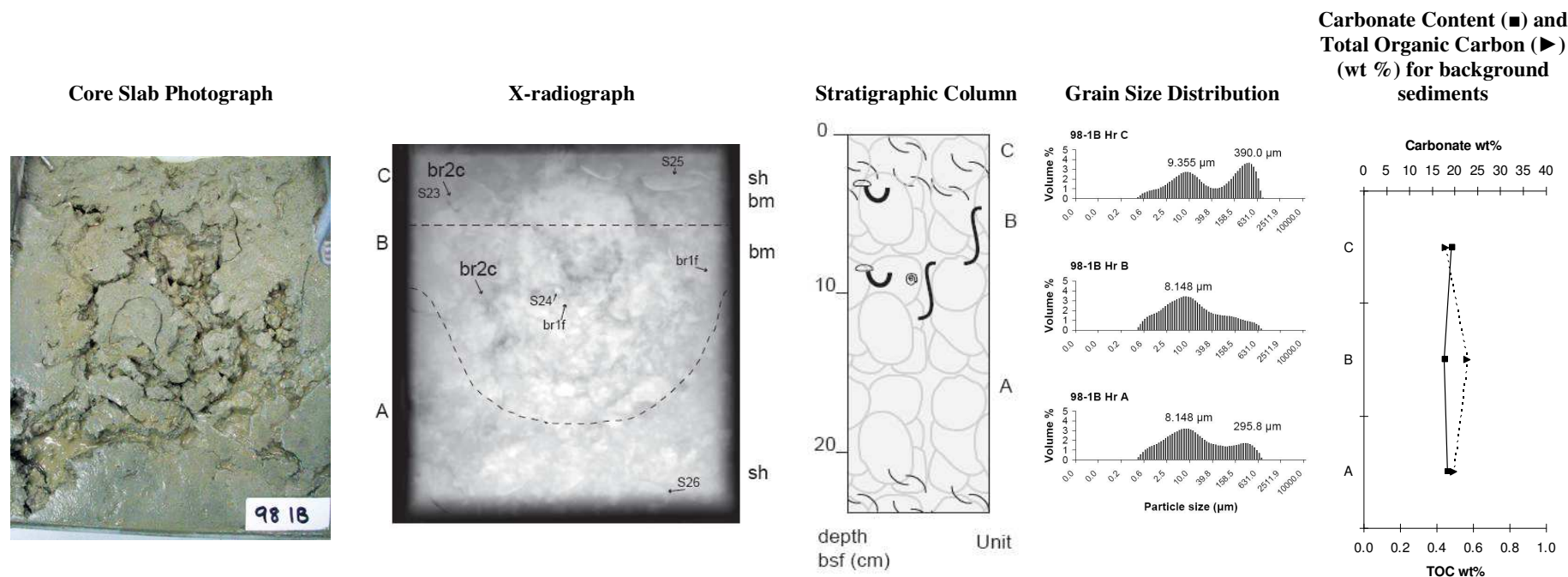
Figure 27. Core slab of the box core sub-sample 98-1B from Station SO191-2/98, 24 cm recovery. Key legend for X-radiograph: br1f (dwelling) 2c (crawling) = burrow types, bm=burrow mottling, sh=shell hash, S23 = juvenile Acharax clarificata, S24 = Nassarius ephamillus, S25 = Calyptogena sp. S26 shell fragment.
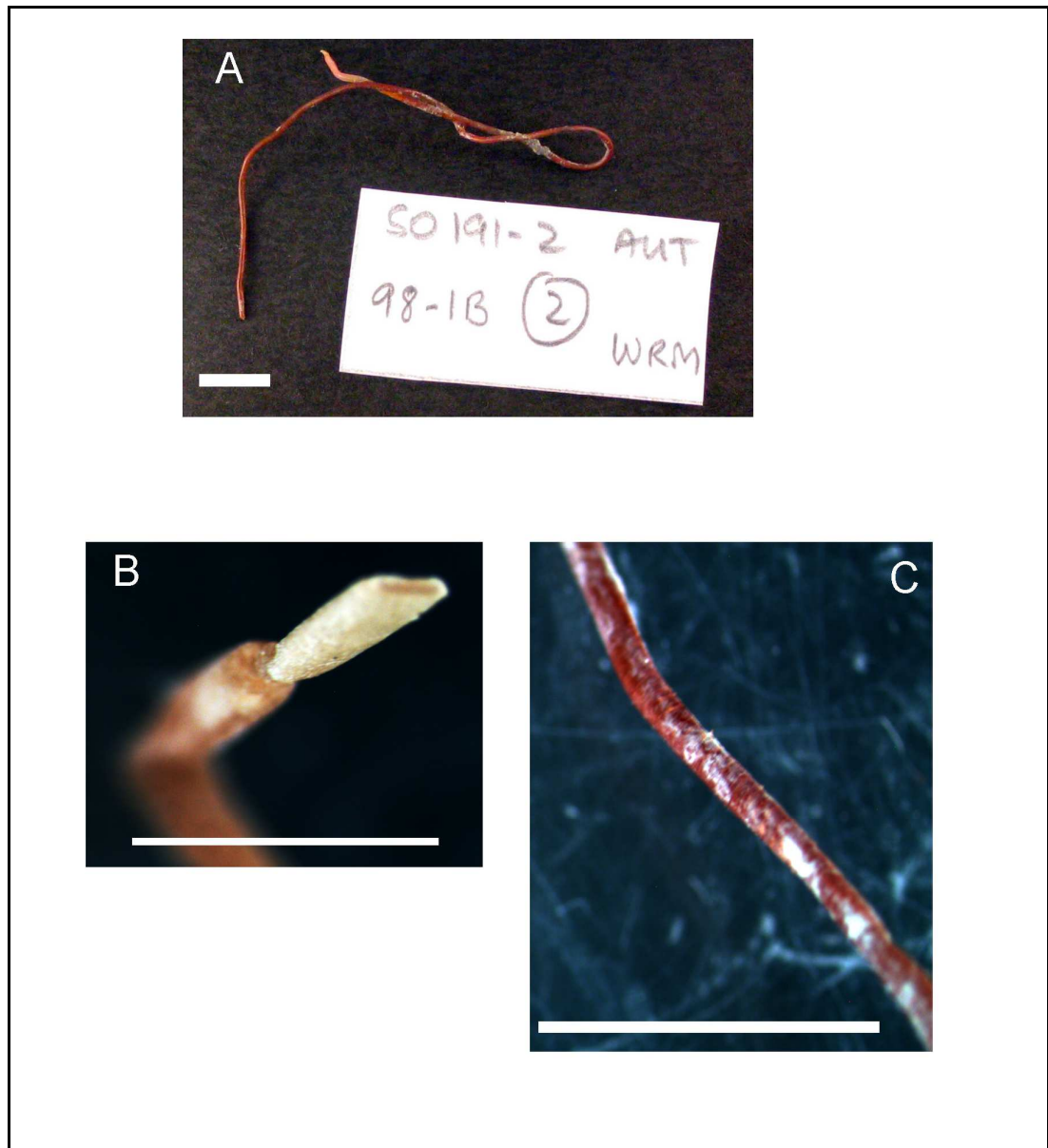
Figure 28. 98-1B: A) Live tube dwelling polychaete (?Chaetopteridae); B) close up of the mouthpart; and C) close up of the tube, 1 mm diameter. Scale bars = 1 cm.
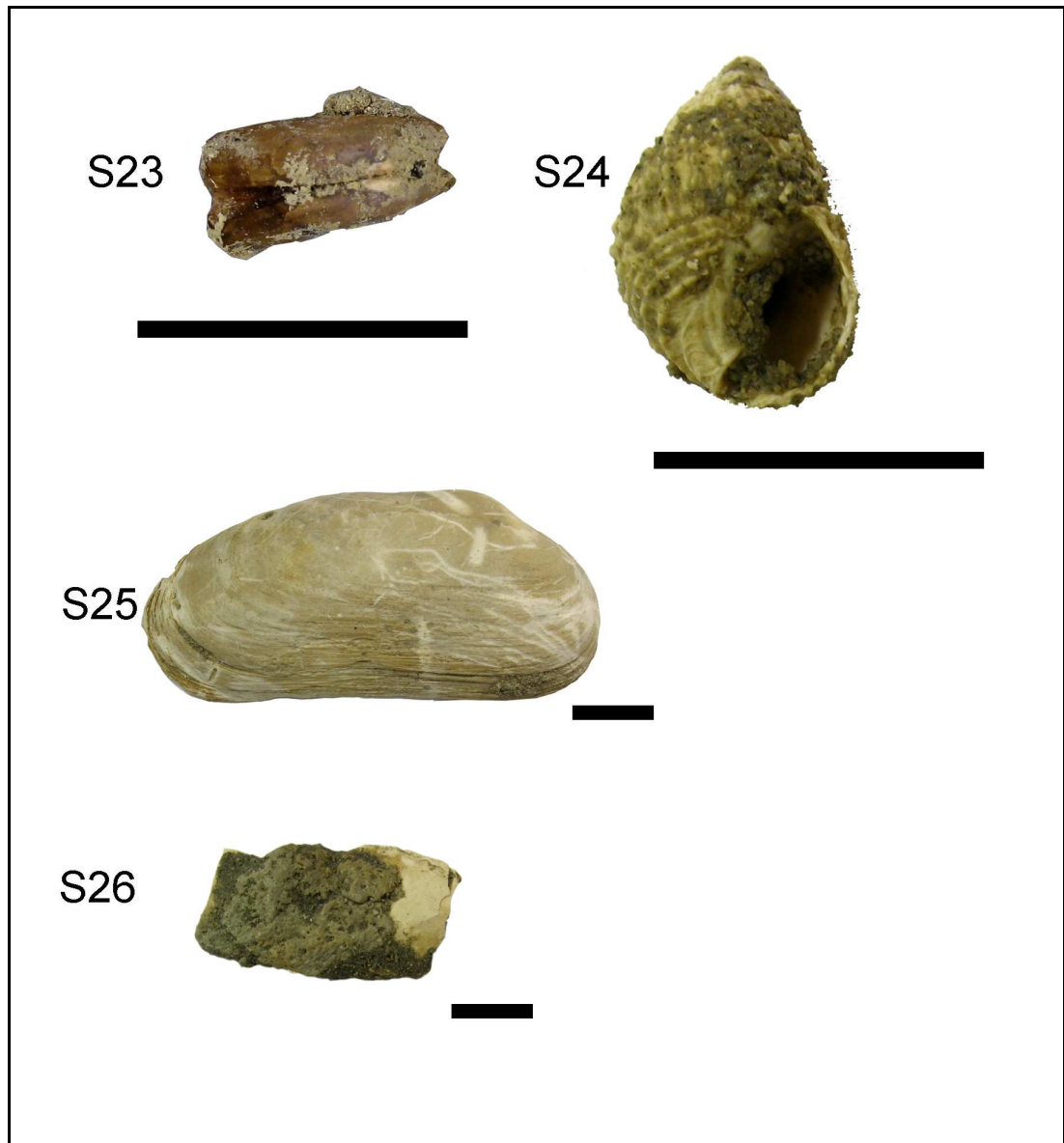
Figure 29. 98-1B shell specimens: S23 juvenile *Acharax clarificata* (dorsal view), S24 *Nassarius ephamillus*, S25 *Calyptogena* sp., S26. unidentified cemented shell fragment. Scale bars = 1 cm.

3.4.2 *SO191-2/98, subsample 98-2B (Figure 30)*

Sediment descriptions

The box core sediment consisted of two horizons: A (10-30 cm bsf) and B (0-10cm bsf) of poorly sorted, grey, medium sandy medium silt with undulating bedding contacts between them. The grain size distribution for these two horizons was bimodal, coarse skewed and platykurtic.

Total organic carbon (TOC) and carbonate contents of sediments

There was a slight increase in TOC but no change in carbonate content with increasing depth within the sediment column.

Burrow feature descriptions

Bioturbation activities (BI = 2) were evident in Horizon B and there were three ethologies in this horizon, comprising a dwelling trace (br1a) of *Skolithos,* some crawling traces of *Planolites* (br2b) and U-shaped burrow of cf. *Solemyatuba* (br2c). A juvenile cf. *Acharax clarificata* (8 mm in length) occupied a U-shaped burrow. No evidence of bioturbation activity in Horizon A (BI = 0) is shown on the X-ray image.

Carbonate descriptions

 Horizon A contained some medium grey, irregular to smooth, sandy carbonate nodules (~ 1 cm) mixed in with some disarticulated shells. Horizon B contained some medium grey, carbonate nodules dispersed throughout.

Shell descriptions

Both horizons contained some disarticulated cemented *Calyptogena* shells (S27-29, Figures 30 and 31).
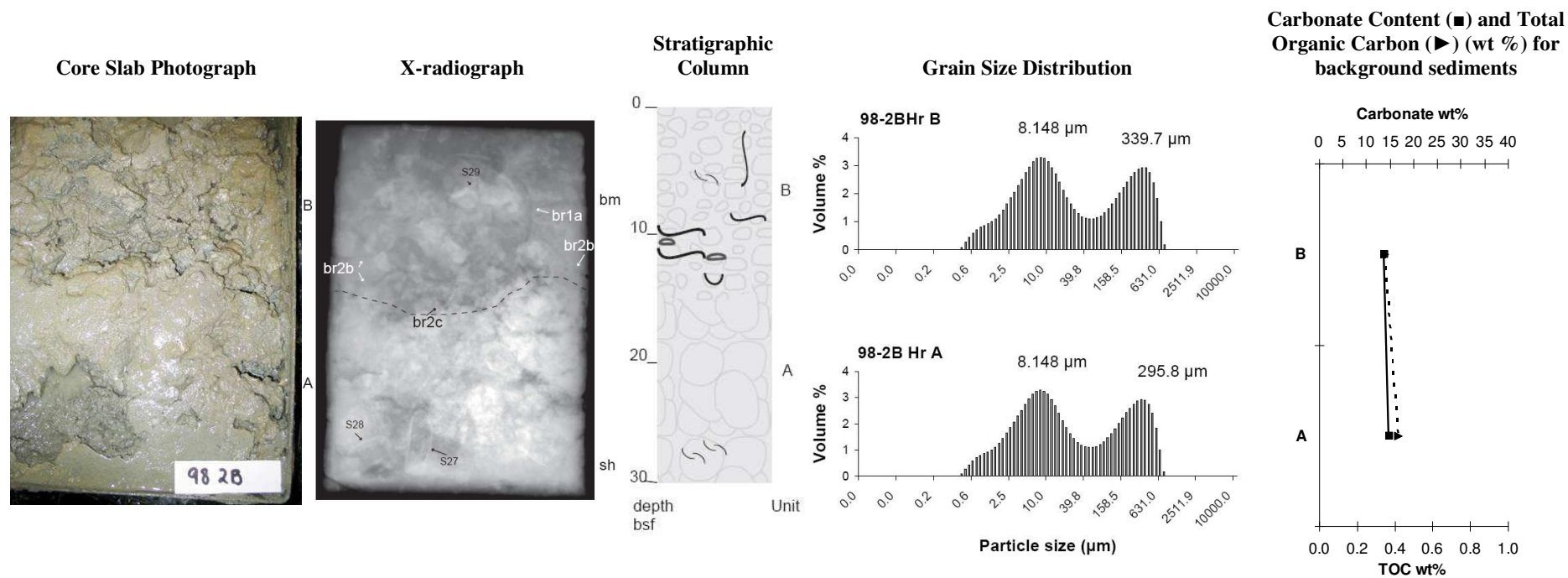
Figure 30. Core slab of the box core sub-sample 98-2B from Station SO191-2/98, 30 cm recovery. Key legend for X-radiograph: br1a (dweling), 2b-c (crawling) = burrow types, bm=burrow mottling, sh = shell hash, S27-29 = disarticulated, cemented *Calyptogena* sp**.**
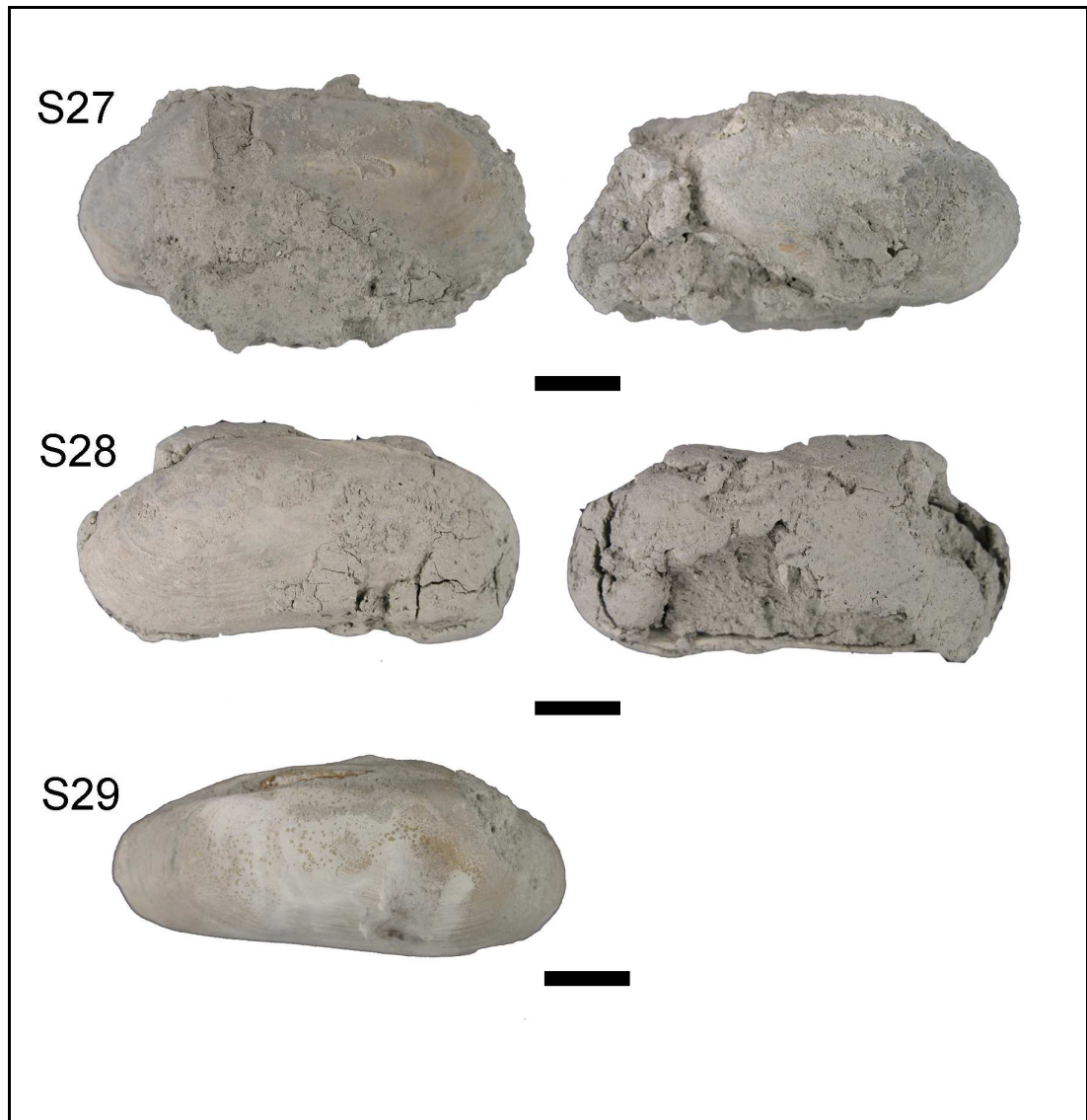
Figure 31. 98-2B shell specimens: *Calyptogena* sp: S27, S29 exterior left valve on the left and interior left valve on the right; S29 articulated cemented shell. Scale bars = 1 cm.

3.5 Station SO191-2/156, North Tower of Wairarapa (1072 m bsl)

3.5.1 *Station SO191-2/156, subsample 156 (Figure 32)*

Sediment descriptions

The multi-core sediment was divided into four horizons: A (4-9 cm bsf), B (2-4 cm bsf), C (0.5-2 cm bsf) and D (0-0.5 cm bsf), comprising poorly sorted medium silt. The bedding contact between each horizon was gradational and was defined by changes in sediment colour from olive brown to greyish brown to grey as the depth increased. The grain size distribution for Horizons A and B was unimodal, symmetrical and mesokurtic, and for Horizons C and D, unimodal, symmetrical and leptokurtic.

Burrow feature descriptions

There was no evidence of bioturbation (BI=0) in any of these horizons.

Carbonate descriptions

This core subsample had carbonate clasts throughout and their size and number decrease with increasing depth subsurface.

Shell descriptions

Only an empty, well worn gastropod belonging to family Naticidae (S30, Figures 32 and 33) was found in a parautochthonous position at 9 cm bsf.

Split Core Photograph	X-radiograph	Stratigraphic Column	Grain Size Distribution	Carbonate Content (■) and Total Organic Carbon (►) (wt %) for background sediments
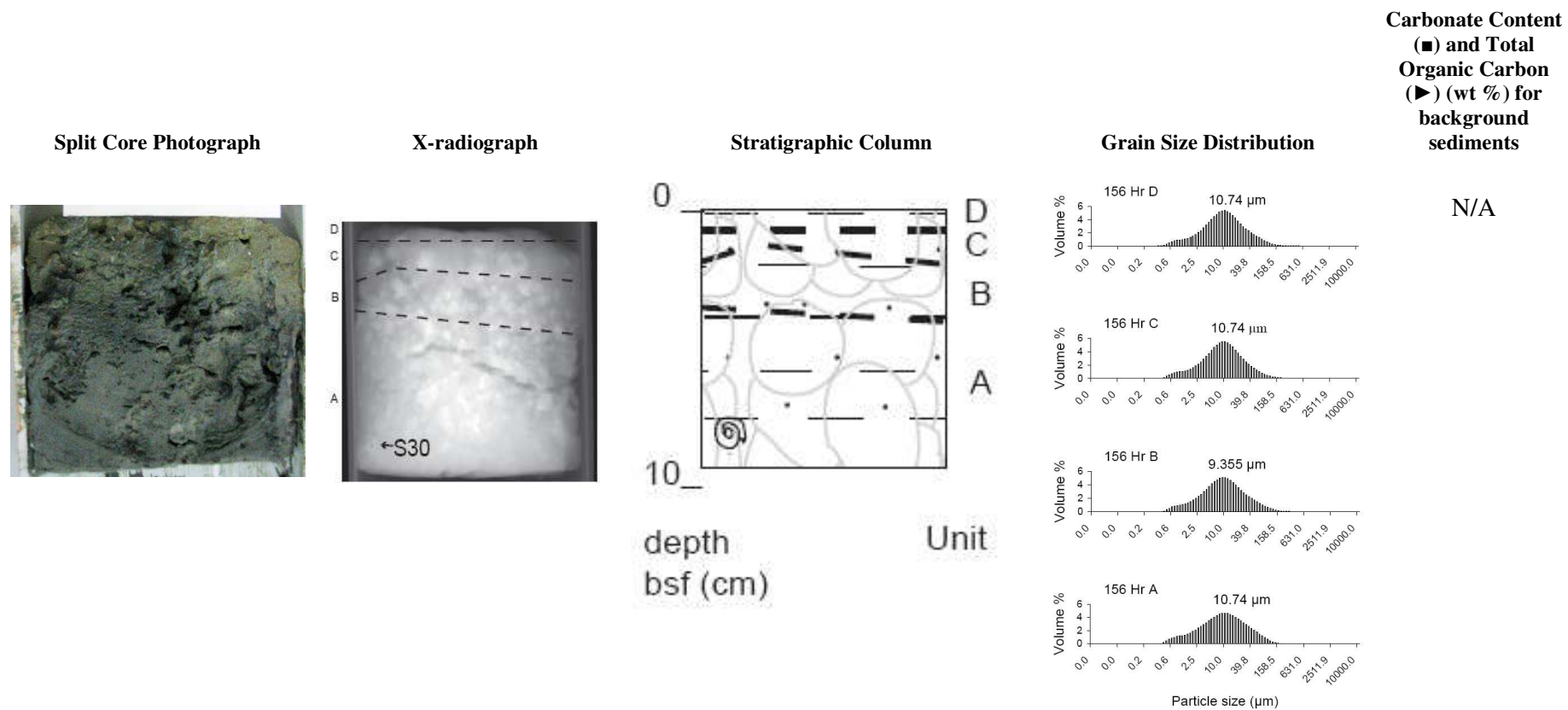
Figure 32. Core log of the multicore core sub-sample 156 from Station SO191-2/156, 9 cm recovery. Key legend for X-radiograph: S30 = Naticidae sp.

S30

Figure 33. 156 shell specimens: Naticidae sp.

3.6   Station SO191-2/158, North Tower of Wairarapa (1060 m bsl)

3.6.1   *Station SO191-2/158, subsample 158A (Figure 34)*

Sediment descriptions

The multi-core sediment consisted of two horizons: A (12-28 cm bsf) and B (0-12 cm bsf), with a gradational bedding contact between them, defined by differences in sediment composition. That is, Horizon A had some disarticulated shells mixed in with the sediment; whereas, Horizon B had very little shell debris. Both horizons constituted poorly sorted, grey, medium silt.

Total organic carbon (TOC) and carbonate contents of sediments

There was no trend in TOC or carbonate content; however, there was a large difference in the amount of TOC and carbonate content compared with other core samples. This core sample (158A) had the highest TOC by far (0.9%) and the lowest carbonate content (4.1%).

Burrow feature descriptions

There was evidence of bioturbation activity (BI=2) in Horizon A, with a strong vertical fabric of burrows (br1d) of 8 mm in diameter and length gre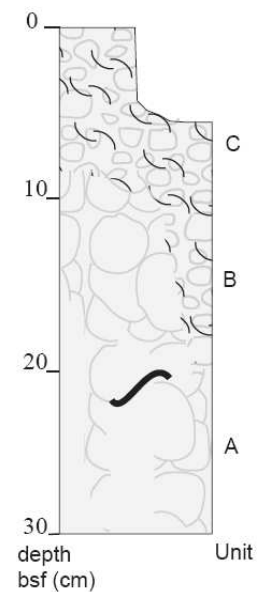ater than ≥ 30 mm.   These burrows are filled with black sulphide rich sediment and are shown in dark grey X-ray shade. Figure 35 shows a close up of one of these burrows with wall scratch-marks.   It is identified as cf. *Spongeliomorpha*.Horizon B had some moderately strong fabric of burrows (br1b) inferred as *Skolithos* (Figure 34, X-radiograph).

Carbonate descriptions

No carbonate nodules were present in this subsample.

Shell descriptions

Horizon A had sparse shell hash consisting of two, empty, small, well-worn gastropods (S32 and S33, Figure 34) belonging to *Nassarius ephamillus,* which was in a parautochthonous position at 14 cm and 17 cm bsf, respectively. Horizon B had one, empty, well-worn gastropod (*Nassarius ephamillus*, S31 Figures 34 and 36), which was in a parautochthonous position at 7 cm bsf. These shells were situated next to the burrow structure of *Spongeliomorpha.*
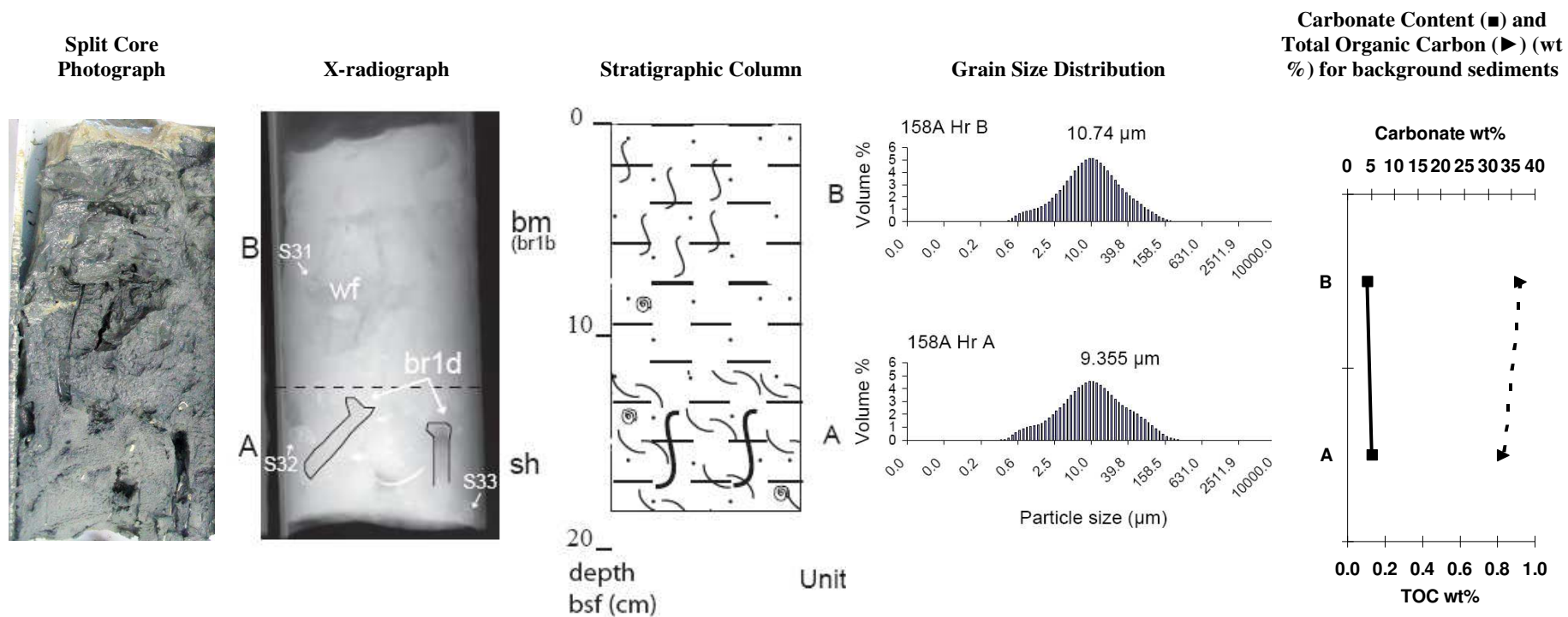
Figure 34. Core log of the multicore sub-sample 158A from Station SO191-2/158, 18 cm recovery. Key legend for X-radiograph: wf = water feature, br1b,d (dwelling) = burrow types, bm = burrow mottling, S31-33 = *Nassarius ephamillus* (refer to Figure 36 for shells)**.**
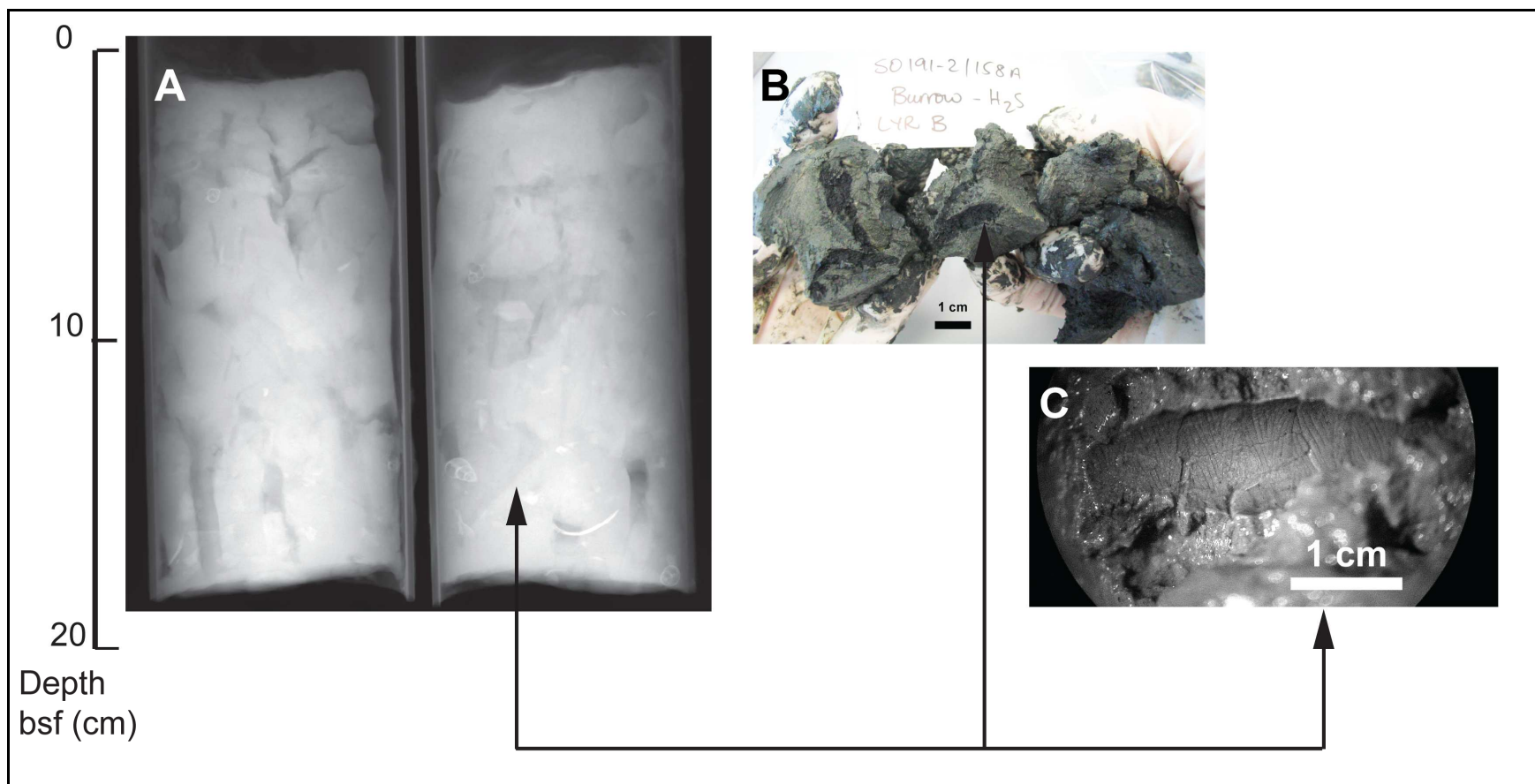
Figure 35. A) *Spongeliomorpha* fabric. B) Dissected burrow structure. C) Close up of wall scratch-marked.

Figure 36. 158A shell specimens: S31-33 *Nassarius ephamillus.* Scale bars = 1 cm.

3.6.2 *Station SO191-2/158, subsample 158B (Figure 37)*

Sediment descriptions

The multi-core sediment consisted of three horizons: A (15-23 cm bsf), B (7.5-15 cm bsf) and C (0-7 cm bsf) with undulating bedding contacts between them defined by sediment texture and colour. The grain size distribution for these horizons was unimodal, symmetrical and mesokurtic. Horizons A and B constituted poorly sorted, grey, medium silt. Horizon C comprised poorly sorted, grey, medium silt, except for the topmost 2 cm subsurface of Horizon C, which had muddy brown, weakly consolidated sediment with a soapy feel to it.

Burrow feature descriptions

There were bioturbation activities throughout all horizons with high bioturbation (B=4) in Horizon B and moderate bioturbation in Horizons A and C. Dwelling traces (br1b) of cf. *Skolithos* were evident in all horizons (Figure 37, X-radiograph and Figure 38) and a feeding-dwelling trace (br2a) of *Palaeophycus* was found in Horizon C.

Carbonate descriptions

Some carbonate nodules were in the lower part of Horizon A.

Shell descriptions

Horizon A had shell hash containing some unidentified shell fragments, one fragment of stony coral (*Flabellum* sp.), and some well-worn empty gastropods belonging to *Nassarius ephamillus* and *Friginatica* sp. (S34-37, Figure 39).

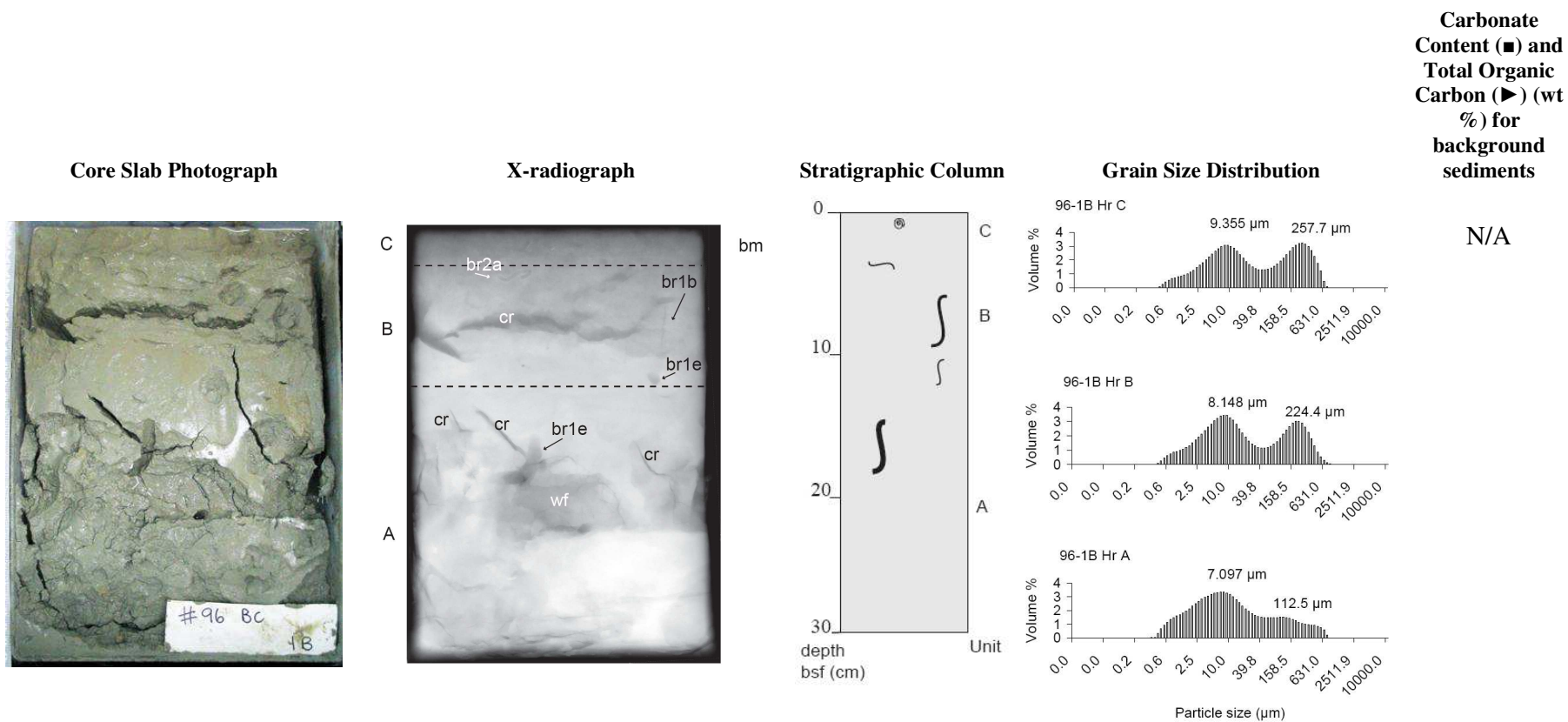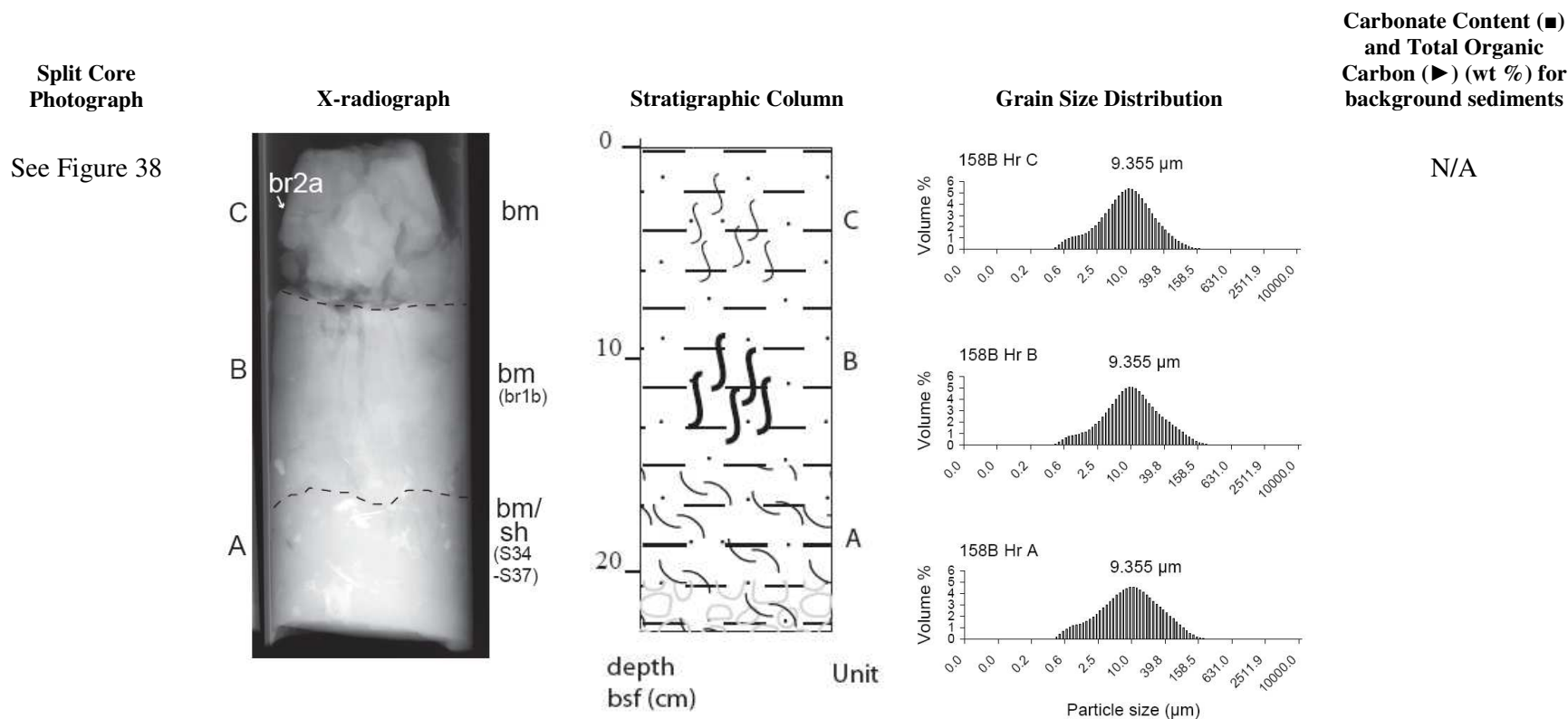**Figure 37.** Core log of the multicore sub-sample 158B from Station SO191-2/158, 23 cm recovery. Key legend for X-radiograph: bm=burrow mottling, br2a (crawling) br1b (dwelling) = dwelling traces, sh=shell hash, S34-S37 shell specimens.
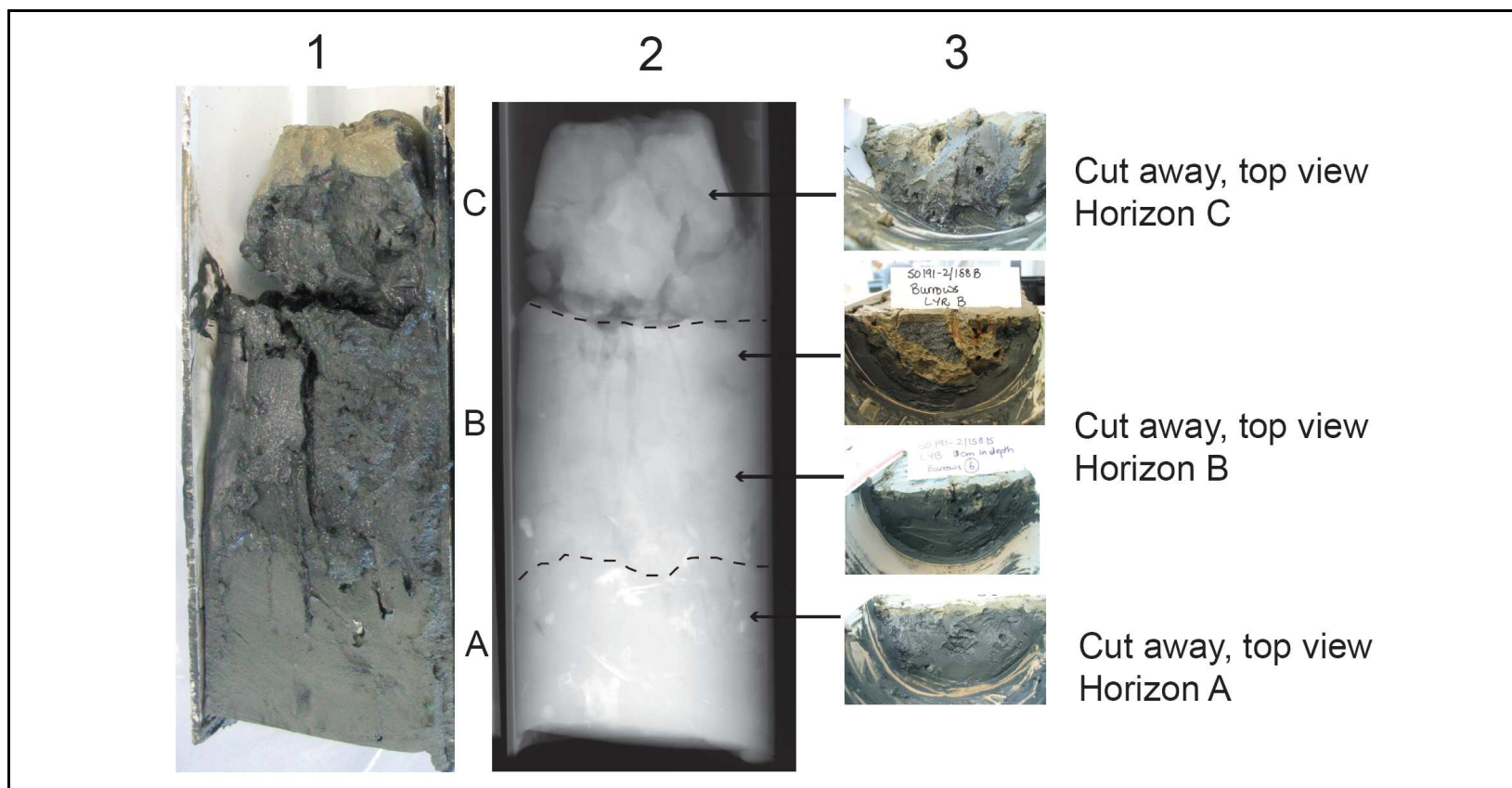
Figure 38. Cross-section of the multicore subsample 158B: 1) split core; 2) X-radiograph image of the split core; 3) and cross-section view of each horizon showing burrow structures.
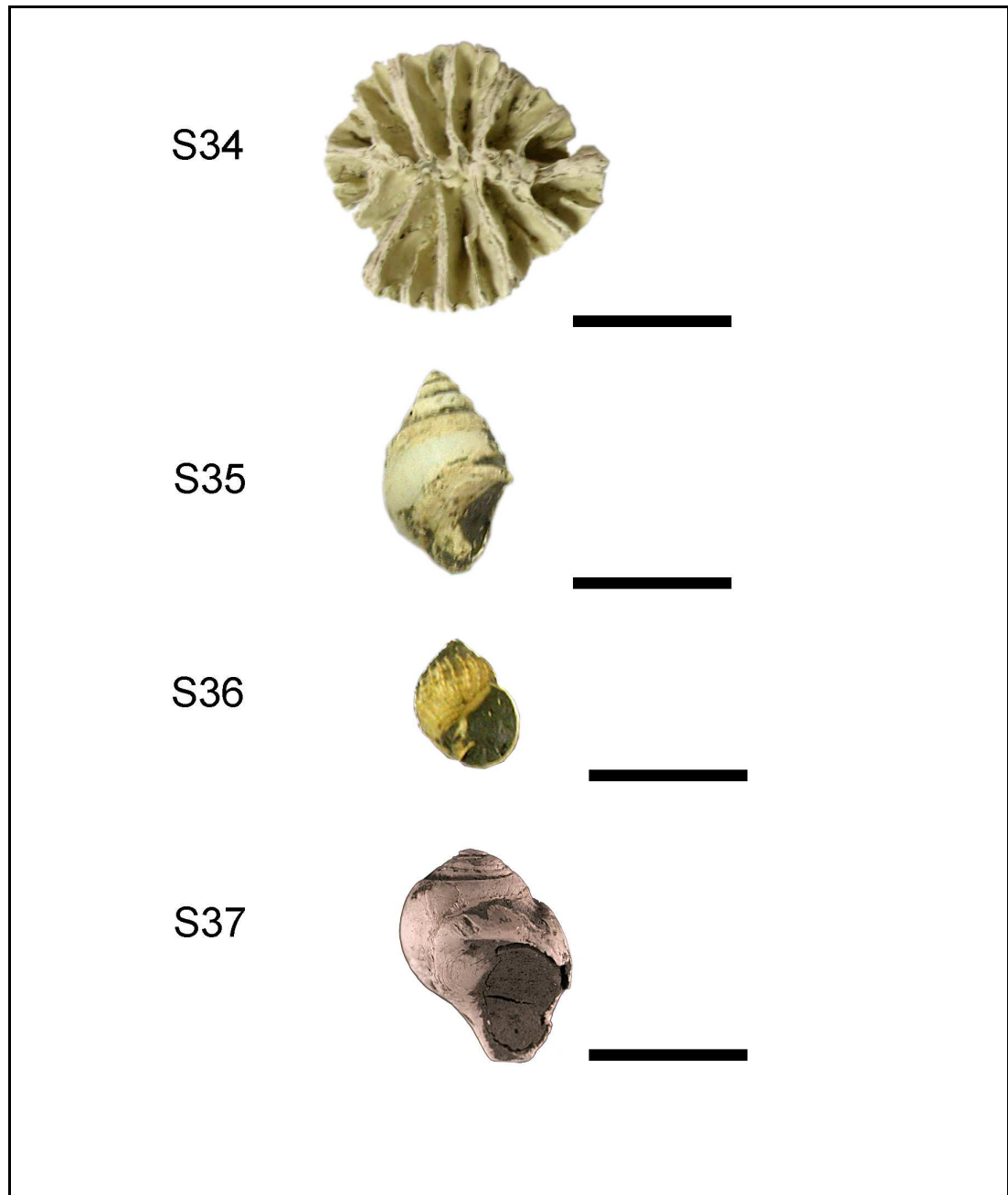
Figure 39. 158B shell specimens: S34 *Flabellum* sp., S35-S36 *Nassarius ephamillus*, S37 *Friginatica* sp. Scale bars = 1 cm.

3.7 Station SO191-2/173, Bear's Paw, LM9 (1106 m bsl)

3.7.1 *Station SO191-2/173, subsample 173 (Figure 40)*

Sediment descriptions

The multi-core sediment consisted of two horizons: A (7-15 cm bsf) and B (0-7 cm bsf) with gradational bedding contacts between them and it was defined by differences in sediment composition. Both horizons constituted very poorly, sorted, fine sandy medium silt. The grain size distribution for these was unimodal, coarse skewed and mesokurtic.

Total organic carbon (TOC) and carbonate contents of sediments

There was a slight decrease in TOC and increase in carbonate content with increasing depth within the sediment column. The increase in carbonate content in the lower horizon was due to the presence of carbonate nodules and shell debris.

Burrow feature descriptions

Horizon B had low bioturbation (BI=1) with two types of burrow structures, a dwelling trace (br1c), an obliquely inclinded segmented burrow filled with carbonate nodules, and a crawling trace (br2b) of *Planolites*. Horizon A had no bioturbation.

Carbonate descriptions

Horizon A had extensive nodular carbonates with irregular margins.

Shell descriptions

Horizon A had shell hash containing some disarticulated, fragmented and pitted *Calyptogena* sp.(e.g. S38 and S41, Figures 40 and 41). Empty articulated *Lucinoma galathea* was found in a parautochthonous position in this Horizon. A well worn gastropod belonging to *Nassarious ephamillus* (S40, Figures 40 and 41) was found in

Horizon B.
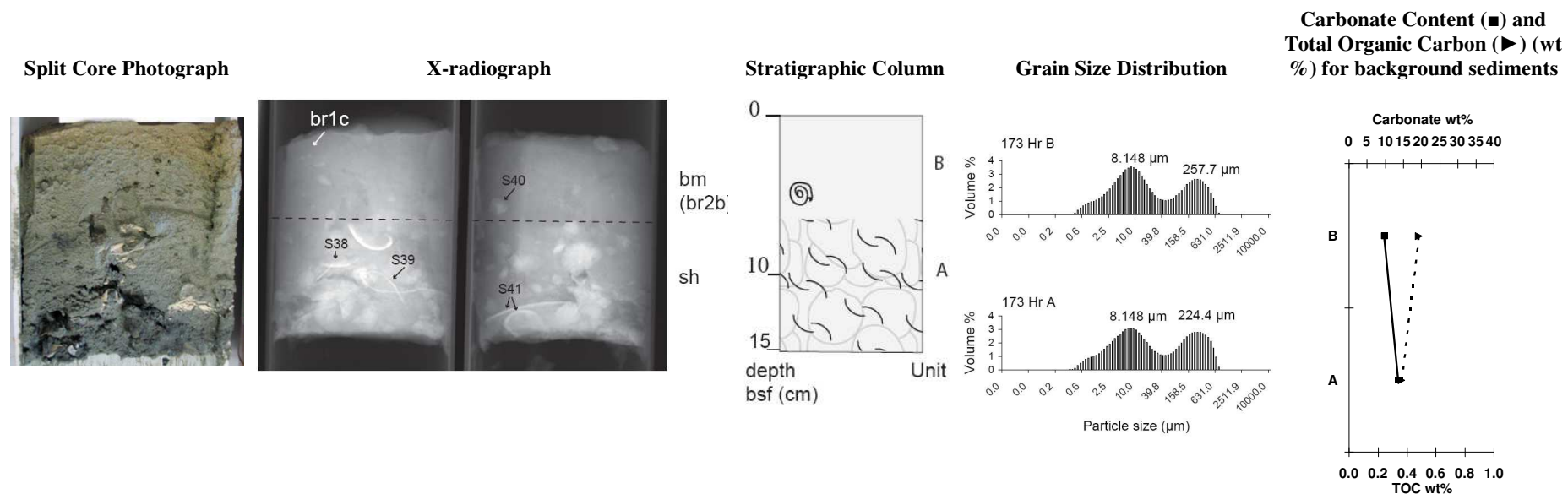
Figure 40. Core log of the multicore sub-sample 173 from Station SO191-3/173, 15 cm recovery. Key legend for X-radiograph: sh = shell hash, bm = burrow mottling, br2b (crawling), br1c (dwelling) = burrow types; S38, 41 *Calyptogena* sp. S39, *Nassarius ephamillus*, S39 *Lucinoma galathea*.
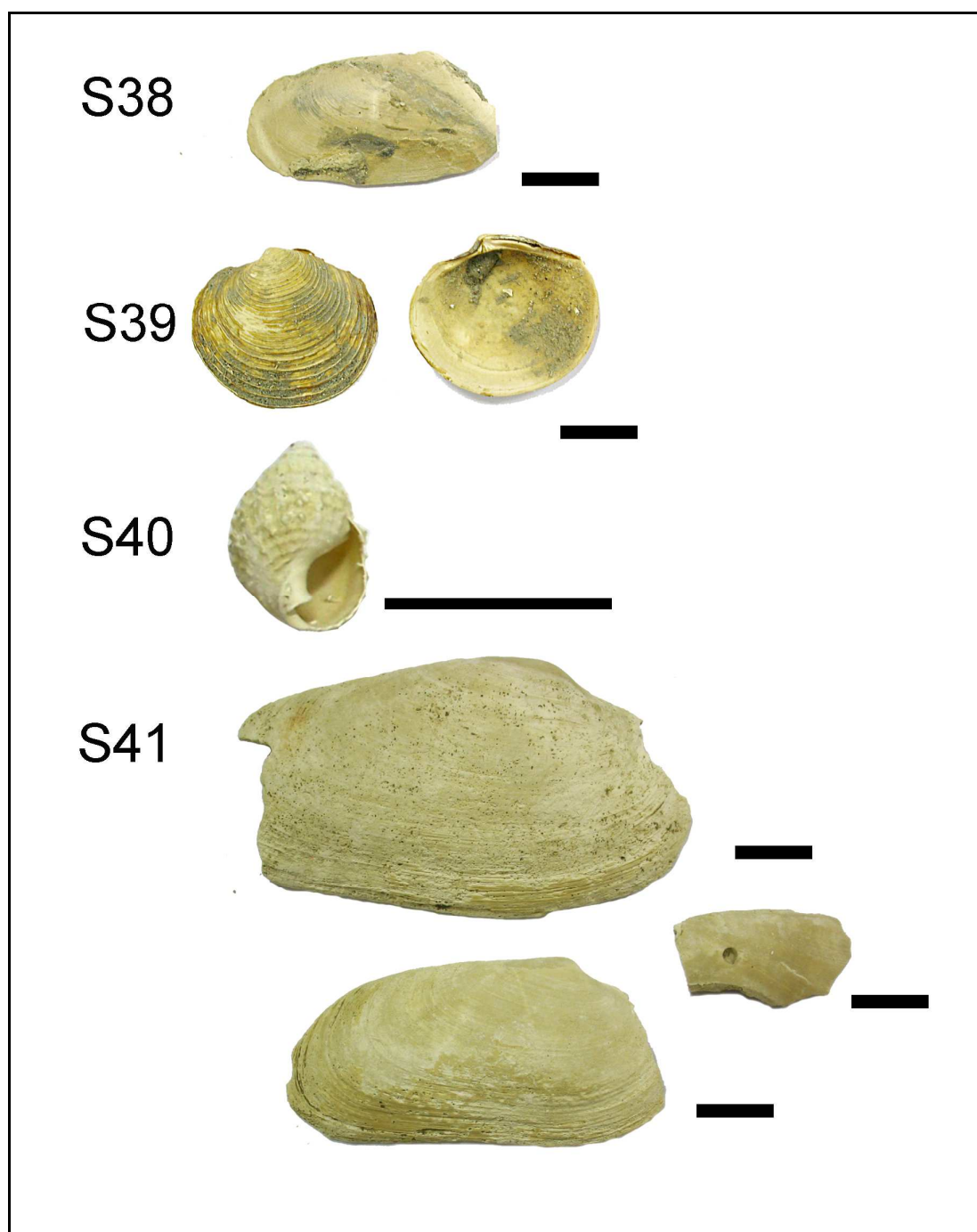
Figure 41. 173 shell specimens: S38 *Calyptogena* sp, S39 *Lucinoma galathea*, S40 *Nassarius ephamillus* (actual size on the left and 3x the actual size on the right), S41 *Calyptogena* sp. Scale bars = 1 cm.

3.8 Station SO191-3/232, Kaka (1172 m bsl)

3.8.1 *Station SO191-3/232, subsample 232-1A (Figure 42)*

Sediment descriptions

The multi-core sediment consisted of four very poorly sorted horizons: A, B, C and D, with gradational bedding contacts between these horizons defined by sediment texture and colour. The grain size distribution for all horizons was bimodal, coarse skewed, and mesokurtic for Horizons A and C, and platykurtic for Horizons B and D. Horizons A and B constituted very poorly sorted, grey, very fine sandy medium silt. Horizon C had very poorly sorted grey fine sandy medium silt. Horizon D comprised very poorly sorted, olive brown, medium sandy medium silt.

Burrow feature descriptions

There was no evidence of bioturbation (BI-0) in any of these horizons.

Carbonate descriptions

No carbonates were found in this core subsample.

Shell descriptions

There were some shell fragments in Horizon A.
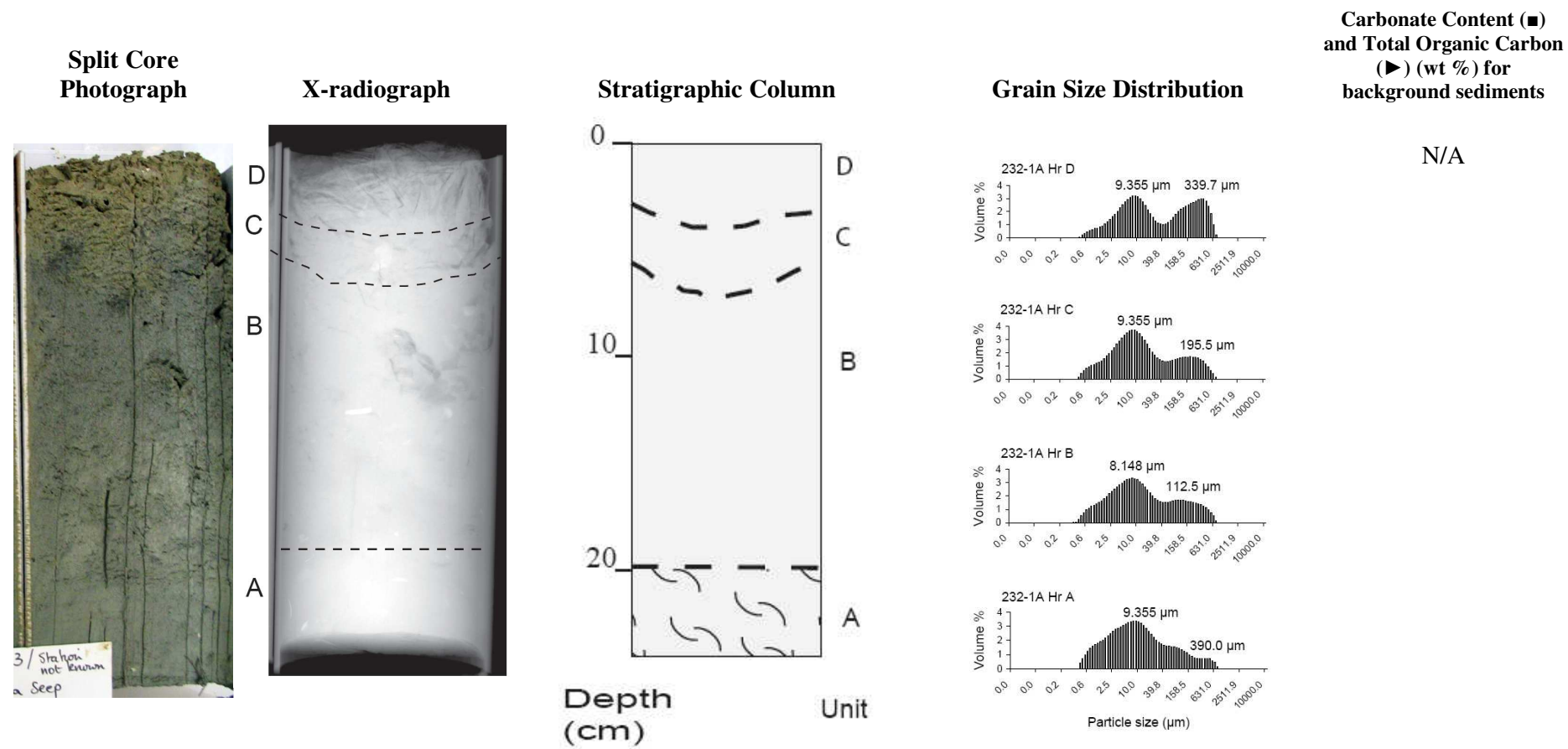
Figure 42. Core log of the multicore sub-sample 232 from Station SO191-3/232-1A, 25 cm recovery.

3.8.2 *Station SO191-3/232, subsample 232-1B (Figure 43)*

Sediment descriptions

The multi-core sediment consisted of three horizons: A (20-27 cm bsf) and B (4-20 cm bsf) and C (0-4 cm bsf) with gradational bedding contacts between them and defined by sediment texture and colour. The grain size distribution is unimodal, symmetrical and mesokurtic, for Horizons A and C, and unimodal, coarse skewed and mesokurtic for Horizon B. Horizon A comprised very poorly sorted, grey, very fine sandy medium silt. Horizon B constituted very poorly sorted, grey, very fine sandy medium silt. Horizon C consisted of poorly sorted, olive brown, fine silt.

Burrow feature descriptions

Horizon B had low bioturbation (BI=2) with some burrow mottling of dwelling traces (br2b) and probing traces (br4). These dwelling traces are identified as cf. *Planolites*, while radiating root-like traces beneath mollusc formed by mollucs' extensible foot (Figure 43, X-radiograph br4) are identified as cf. *Chondrites.*

Carbonate descriptions

No carbonates present in this core sample.

Shell descriptions

Only one live *Lucinoma galathea* was found in an autoautchnous position at 13 cm subsurface which was damaged by a multicorer (S42, Figures 43 and 44).
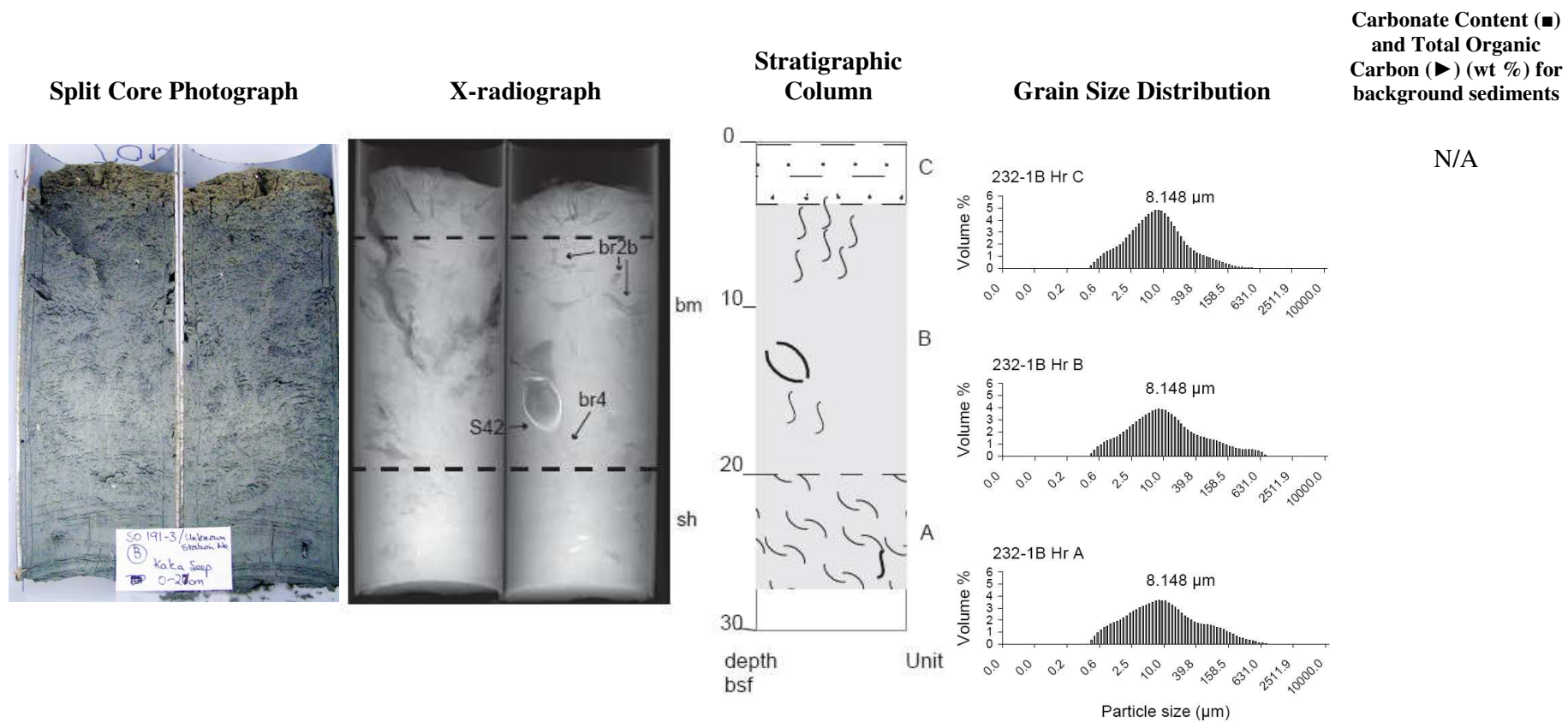
Figure 43. Core log of the multicore sub-sample 232 from Station SO191-3/232-1B, 27cm recovery. Key legend for X-radiograph: bm = borrow mottling, br2b (crawling), br4 (probing) = burrow types, S42 *Lucinoma galathea*.

Figure 44. Live adult *Lucinoma galathea* (S42) retrieved from split core 232-1B. Scale bar = 1 cm.

3.9   Station SO191-3/242, Kaka, raindrop site (1175 m bsl)

3.9.1   *Station SO191-3/242, subsample 242 (Figure 45)*

Sediment descriptions

The multi-core sediment consisted of three horizons: A (12-18 cm bsf), B (3-12 cm bsf) and C (0-3 cm bsf) with gradational bedding contacts between them defined by differences in colour and composition of sediment. All horizons comprised very poorly sorted, very fine sandy fine silt, and the colour of sediment for Horizons A and B was grey, and olive-brown for C.   The grain size distribution for all horizons was bimodal, course skewed and mesokurtic.

Burrow feature descriptions

Horizon B had low bioturbation (BI=1), comprising two dwelling traces, cf. *Planolites* (br2b) and cf. *Solemyatuba* (br2c). Juvenile *Acharax clarificata* (Figure 46) occupied a U-shaped burrow (br2c). No visible evidence of bioturbation in both Horizons A and C on the X-ray image.

Carbonate descriptions

No carbonates found in this core sample.

Shell descriptions

There was some shell fragments in Horizon A.

| Split Core Photograph | X-radiograph | Stratigraphic Column | Grain Size Distribution | Carbonate Content (■) and Total Organic Carbon (►) (wt %) for background sediments |

N/A
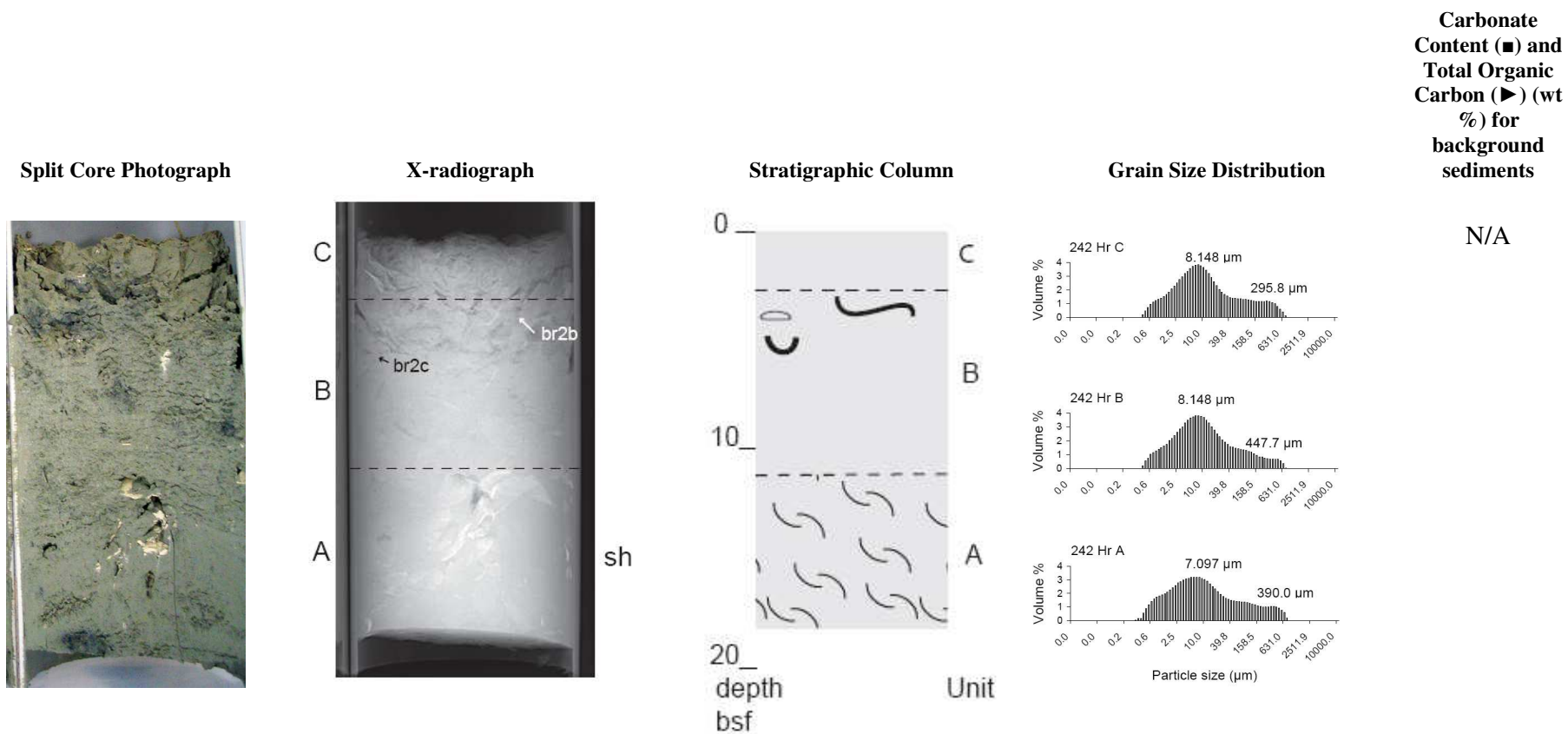
Figure 45. Core log of the multicore sub-sample 242 from Station SO191-3/242, 18cm recovery. Key legend for X-radiograph: br2b-c (crawling) burrow types. (refers to Plate 23 for detail of *Acharax clarificata* found in br2c)

Figure 46. Live juvenile *Acharax clarificata* (8 mm length) (S43) retrieved from the split core subsample 242.

3.9.2 *Station SO191-3/242, subsample 242B (Figure 47)*

Sediment descriptions

The multi-core sediment consisted of three very poorly sorted horizons: A (12-22 cm bsf), B (2-12 cm bsf) and C (0-2 cm bsf) with gradational bedding contacts between them defined by colour and composition of sediment. The grain size for all horizons was unimodal, except for Horizon C, which was polymodal, coarse skewed and mesokurtic. All horizons comprised very poorly sorted, grey, very fine sandy fine silt. In the top 2 cm of subsurface, the colour of sediment was olive-brown.

Burrow feature descriptions

Horizon B had low bioturbation (BI-1) containing crawling traces (?br2b).

Carbonate descriptions

No carbonates were found in this core sample.

Shell descriptions

Horizon A contained some shell fragments some of which these belonged to *Calyptogena* (S45, Figures 47 and 48). Disarticulated shells of *Lucinoma galathea* in a parautochthonous position was found at 20cm subsurface (S44, Figures 47 and 48).
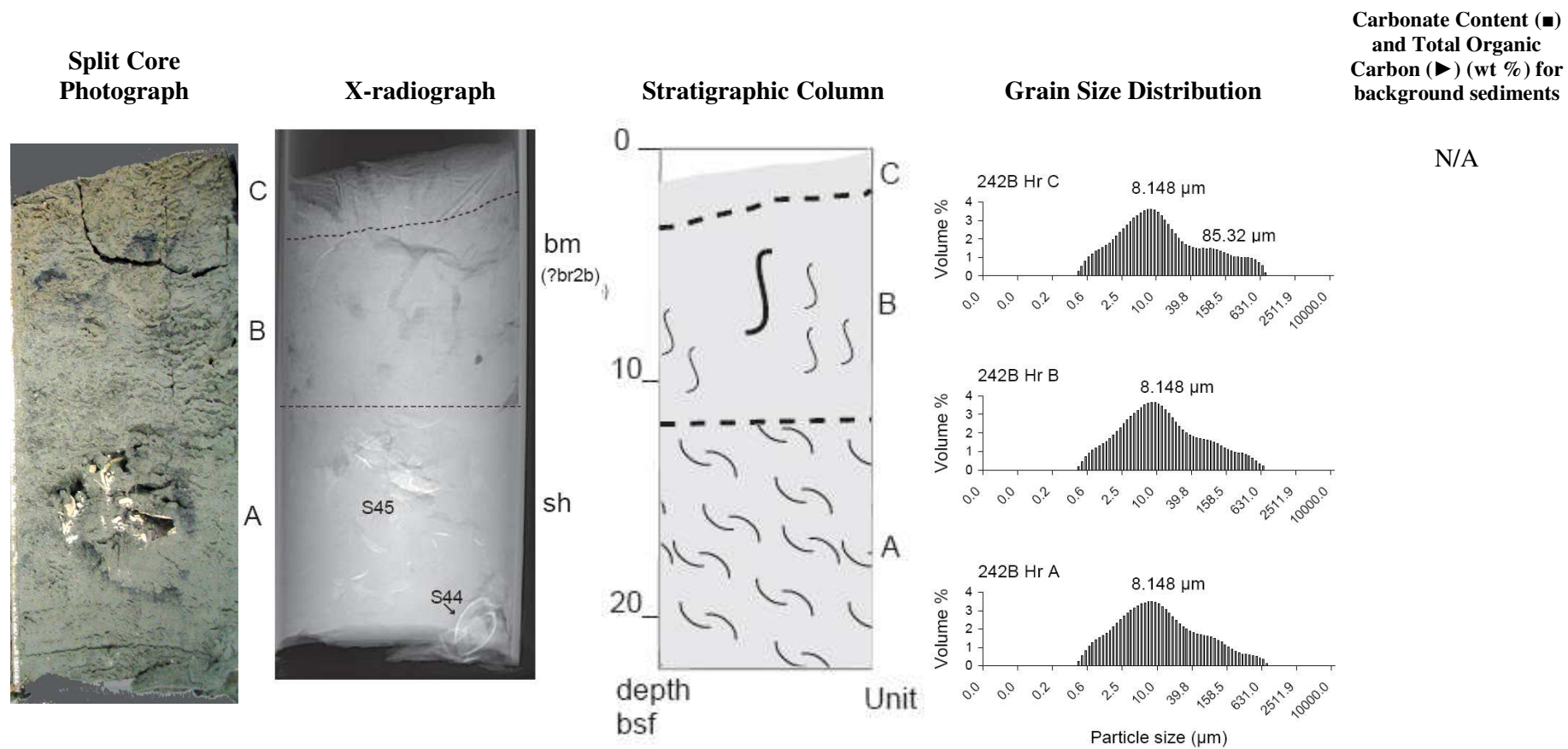
Figure 47. Core log of the multicore sub-sample 242 from Station SO191-3/242B, 22cm recovery. Key legend for X-radiograph: bm = burrow mottling, ?br2b crawling trace, sh = shell hash, S45 shell fragments, S44 *Lucinoma galathea.*

Figure 48. 242B shell specimens: disarticulated shells of *Lucinoma galathea* (top) and shell fragments of ?*Calptyogena* sp. (bottom). Scale bars = 1 cm.

3.10 Station SO191-3/261, Kaka, raindrop site (1171 m bsl)

3.10.1 *Station SO191-3/261, subsample 261 (Figure 49)*

Sediment descriptions

The multi-core sediment consisted of three horizons: A (0-0.5 cm bsf), B (0.5-4.5 cm bsf) and C (4.5-16 cm bsf) with gradational bedding contacts between them defined by sediment colour and texture. Horizon A constituted very poorly sorted, grey, very fine sandy fine silt. Horizons B and C comprised olive-brown, medium sandy medium silt. The grain size distribution for Horizon A was bimodal, coarse skewed and leptokurtic; for Horizon B, bimodal coarse skewed and platykurtic; and for Horizon C, bimodal, symmetrical and platykurtic.

Total organic carbon (TOC) and carbonate contents of sediments

There was a slight increase in TOC and decrease in carbonate content between the middle horizon and lower horizon which was reflected by the change in sediment texture.

Burrow feature descriptions

High bioturbation activity (BI=4) was evident throughout the core; however on the X-ray image, only Horizon B displayed a strong fabric of burrows that are characteristic of *Skolithos* (br1b Figure 49, X-radiograph). On the photographed core, there are some vertical shafts (8 mm in diameter) filled with black sulphide rich sediment in Horizon C, and a Y-shaped burrow (> 8 mm in diameter) in Horizon B which are not shown on the X-ray image. These are dwelling traces that are characteristic of *Solemyatuba* produced by solyemids (Figure 49, photograph).

Carbonate descriptions

No carbonates were present in this core sample.

Shell descriptions

No shells were present in this core sample.
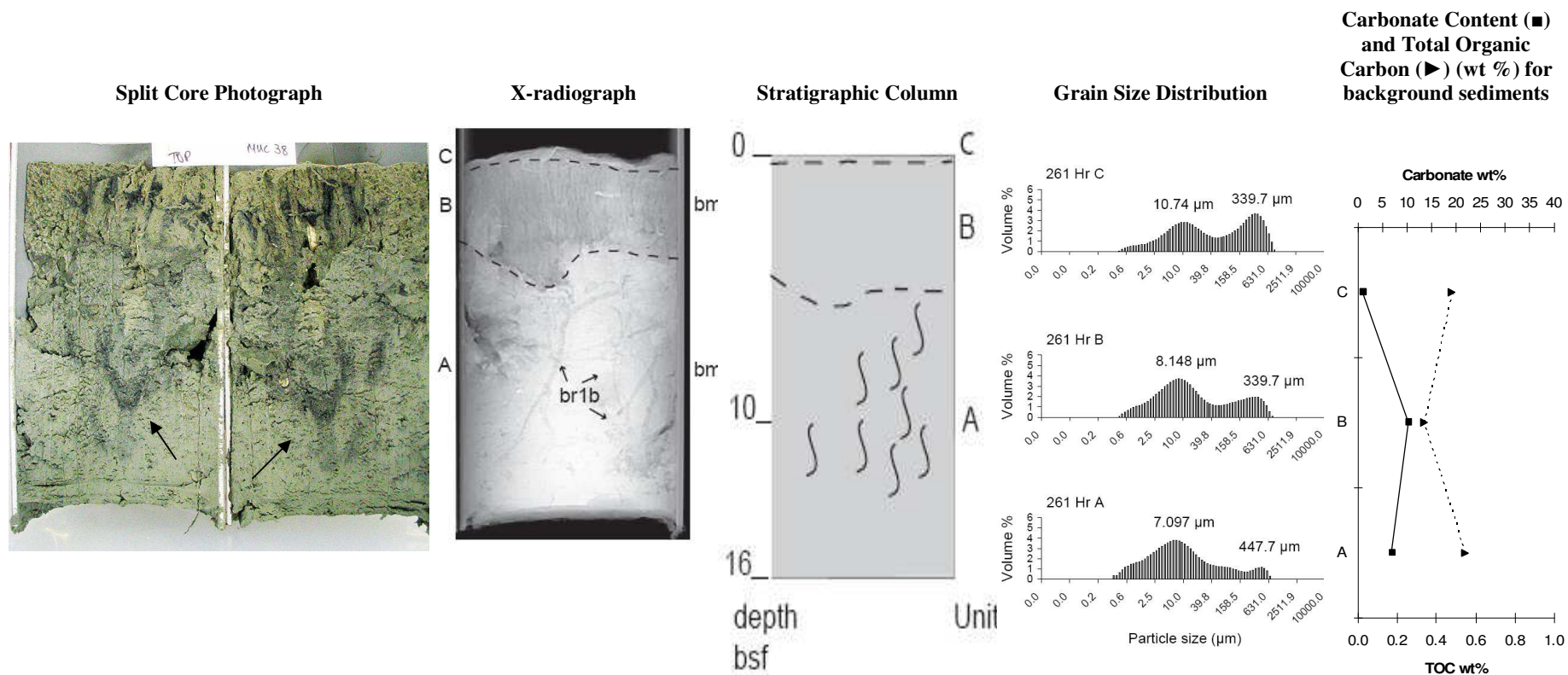
Figure 49. Core log of the multicore sub-sample 261 from Station SO191-3/261, 15cm recovery. Split core photograph with arrows pointed to *Solemyatuba.* Key legend for X-radiograph: br1b = dwelling traces.

3.11 Station SO191-3/262, Kaka, non seep reference site (1167 m bsl)

3.11.1 *Station SO191-3/262, subsample 262 (Figure 50)*

Sediment descriptions

The multi-core sediment consisted of two poorly sorted horizons: A (5-28 cm bsf) and B

(0-5 cm bsf) (σ_A = 1.890, σ_B = 1.738) with a gradational bedding contact between them

that was defined by the colour of the sediment. Horizon A comprised poorly sorted,

grey, medium silt; while Horizon B constituted poorly sorted, olive-brown, medium silt.

The grain size distribution for both horizons was unimodal, symmetrical, and

mesokurtic for Horizon A and leptokurtic for Horizon B.

Burrow feature descriptions

There was no evidence of burrows in this core sample.

Carbonate descriptions

No carbonates were present in this core sample.

Shell descriptions

No shells were present in this core sample.
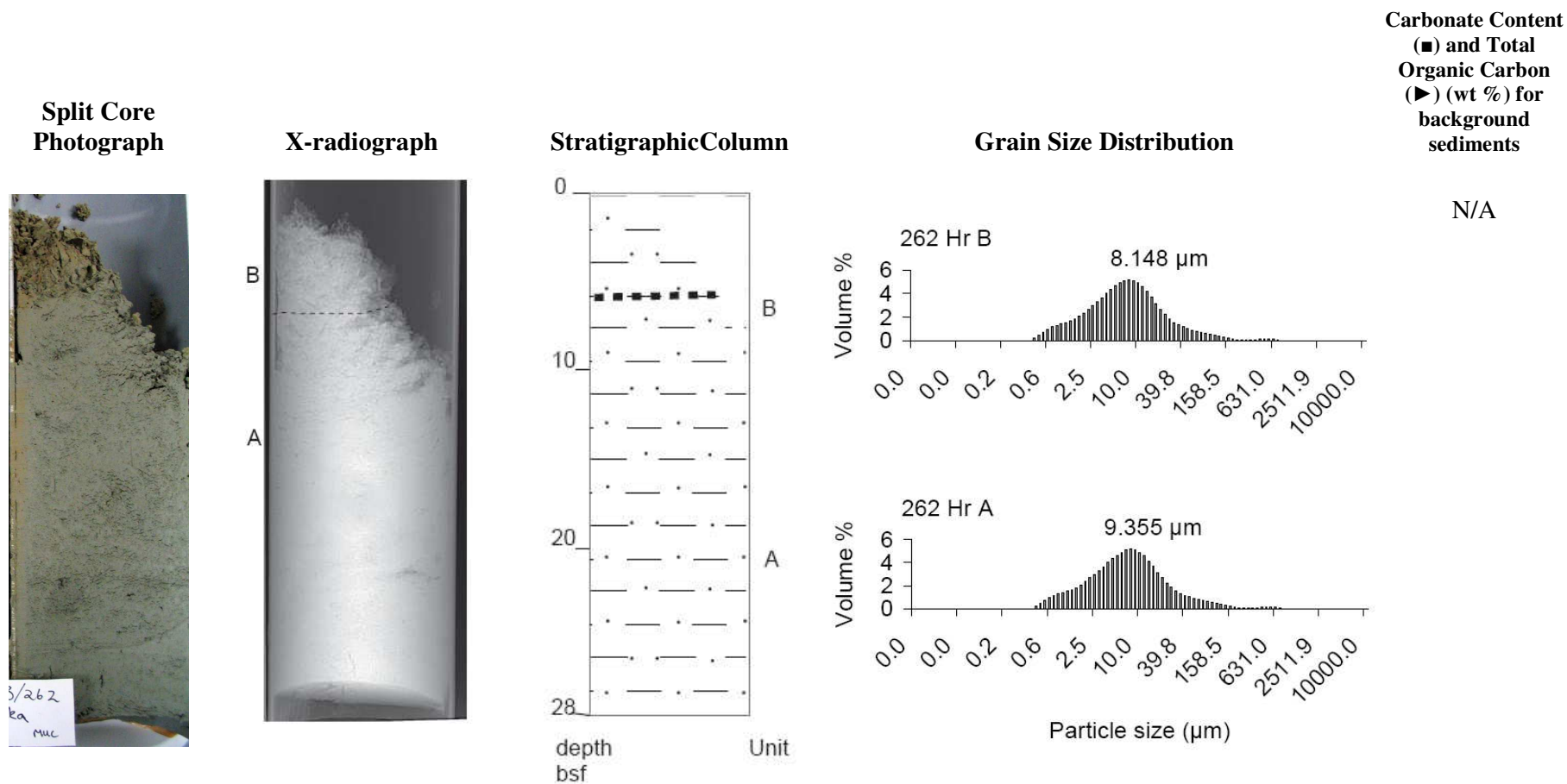
Figure 50. Core log of the multicore sub-sample 262 from Station SO191-3/262, 28cm recovery.

3.11.2 *Station SO191-3/262, subsample 262B (Figure 51)*

Sediment descriptions

The multi-core sediment consisted of three horizons: A (14-32 cm bsf), B (4-14 bsf) and C (0-4 cm bsf) with gradational bedding contacts between them defined by sediment colour. The grain size distribution for all horizons was unimodal, symmetrical and mesokurtic. All horizons have grey poorly sorted medium silt except in the first 4 cm of sediment subsurface which was olive-brown.

Burrow feature descriptions

There was no evidence of burrows in this core sample.

Carbonate descriptions

No carbonates were present in this core sample.

Shell descriptions

No shells were present in this core sample.
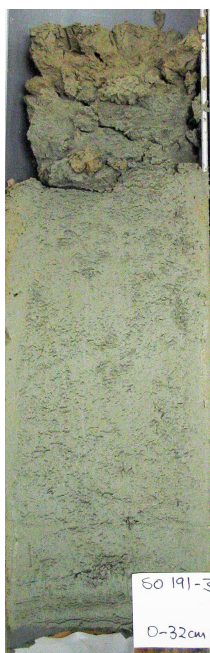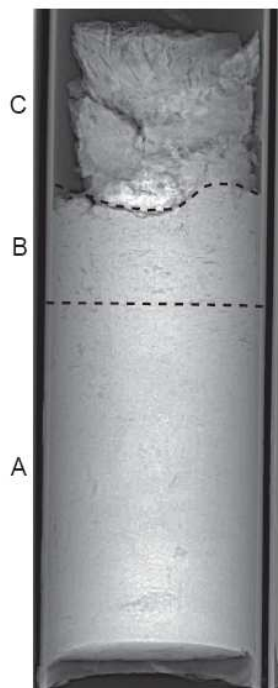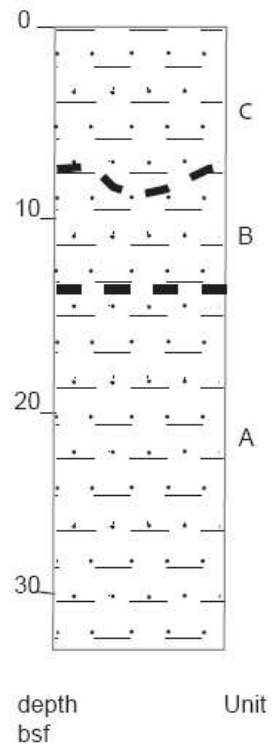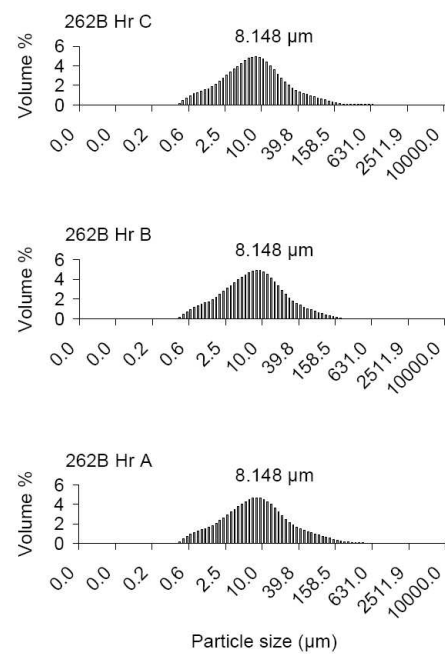
Figure 51. Core log of the multicore sub-sample 262B from Station SO191-3/262, 32cm recovery.

3.12 Station SO191-3/305, Wairarapa (1051 m bsl)

Sediment descriptions

Figure 52 shows a complete core log of the gravity core from Station SO191-3/305, which served as a reference, that is, non-seep site for X-ray purposes. It was divided into four sections: 1 (67-81 cm bsf), 2 (48-67 cm bsf), 3 (23-48 cm bsf) and 4 (0-23 cm bsf) for X-ray purposes. The gravity core sediment consisted of three horizons: A (39-81 cm bsf), B (28-39 cm bsf) and C (0-28 cm bsf) with poorly sorted, grey, medium silt. The grain size distribution for these horizons was unimodal, symmetrical and mesokurtic. The bedding contact between each horizon was gradational and defined by differences in facial appearance of the cross-sectioned stratigraphic log based on the X-ray image, and to some extent, the feel of the sediment texture. Horizon A, especially below 48 cm bsf, had a cross-laminated structure; while Horizon B had a slightly cross-laminated feature with some burrow structures. Horizon C had a thick layer of burrow mottled fabric and some large elite burrow structures. No organisms or shells were found or any evidence of methane hydrates in this gravity core sample.

Burrow feature descriptions

There was evidence of low to moderate bioturbation (BI = 2-3) throughout all horizons. Horizon A (Section 3) had one type of horizontal undulating burrow structure (br2b) with two different in diameters, 4mm and 8 mm, and these were identified as crawling traces of *Planolites*. There was another burrow structure in Horizon A (Section 2), 2mm in diameter, also identified as a crawling trace of *Planolites*. Horizon B had two types of horizontal undulating burrow structures. The small one, 2mm in diameter (br2a), was a dwelling-feeding trace identified as *Palaeophycus* and the larger ones, 8mm in diameter (br2b) were a crawling trace of *Planolites*. (br2a). Horizon C (Section 4) had a strong fabric of burrow mottling containing both vertical and slightly

116

obliquely inclined burrows (2 mm in diameter), which were inferred as dwelling traces of *Skolithos.* These burrows were filled with black sulphide-rich sediments and were delineated by a medium dark grey X-ray shade. Another burrow structure (br2a), 14 mm in diameter, in Horizon C was an undulating horizontal crawling trace of *Planolites* shown in white X-ray shade.

Carbonate descriptions

No carbonates were present in this core sample.

Shell descriptions

No shells were present in this core sample.

Figure 52. Core log of the gravity core from Station SO191-3/305, 81cm recovery.

3.13 Total organic carbon

The values of TOC for Omakere Ridge was ranged between 0.24 and 0.57 % wt and for Wairarapa, between 0.72 and 0.92 % wt. The gradient of TOC values changed very little with increasing depth within the sediment columns for both regions (Appendix 3).
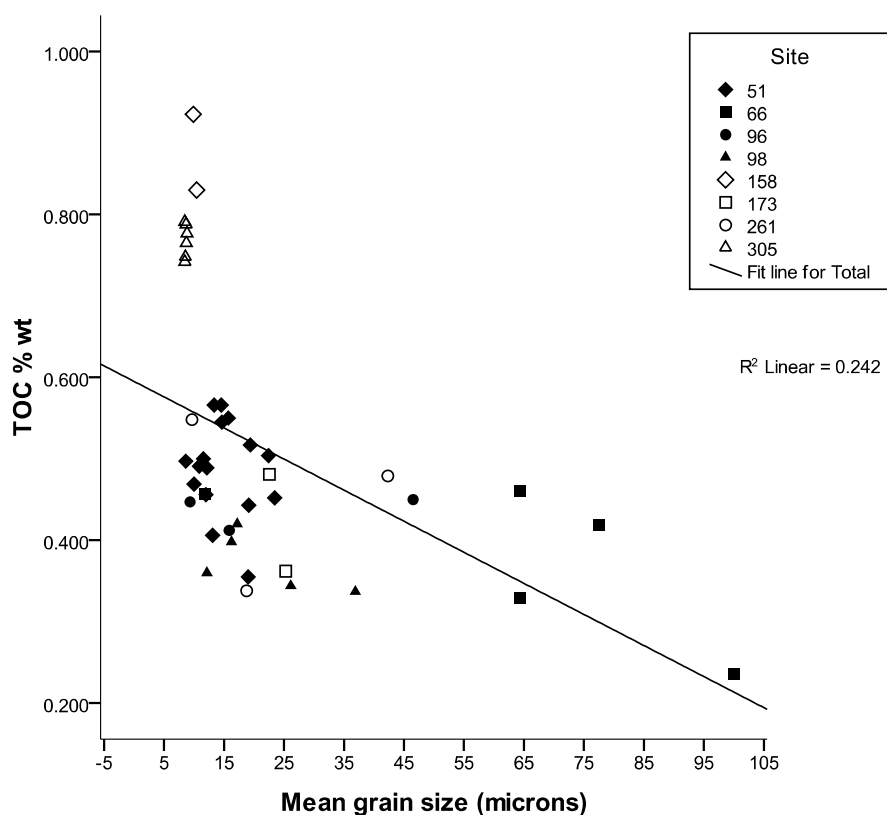
Figure 53. Correlation between grain size and total organic carbon for siliciclastic sediments of the selected sites.

There was a weak negative linear relationship (r = -0.492, p-value = 0.001) between mean grain size and total organic carbon but some outliers evident (Figure 53). This correlation plot had three subgroups: Group 1: Site # 66 (Omakere), Group 2: Site # 51, 96, 98, 173 and 261 (Omakere); and group 3: Site # 158 and 305 (Wairarapa). The coefficient of determination was $r^2 = 0.242$, therefore 24.2% of the variation in total organic carbon can be explained by the differences in mean grain size. Group 3 had

119

the highest total organic content with a finer grain size fraction (very fine silt) compared with Groups 1 and 2. Group 1 had an outlier with the lowest total organic carbon and coarser grain size fraction (very fine sand).
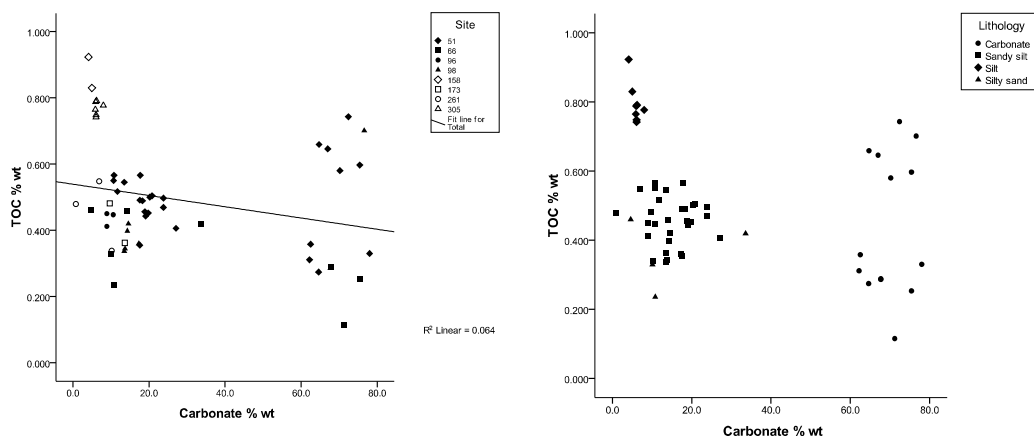
Figure 54. Correlation between carbonate content and total organic content for all sites (left graph) and for the lithology evident at those sites (right graph).

There was a very correlation (r = -0.252, p-value = 0.06) between carbonate content and total organic carbon content (Figure 54). These correlation plots had three subgroups that characterised the habitat type: Habitat 1 had sandy silt with high carbonate content and a wide range of TOC content; Habitat 2 had sandy silt with low carbonate content and medium TOC content; and Habitat 3 had silt with low carbonate content and high TOC content. Habitat 1 included Sites 51, 66 and 98 (LM9 of Omakere Ridge). Habitat 2 included Sites 96 (LM9), 173 (Bear's Paw) and 261 (Kaka) – all of these were of Omakere Ridge. Habitat 3 included Sites 158 and 305 (Wairarapa). Site 66 had dominant silty sand and minor sandy silt and low TOC (0.24-0.46% wt) and a wide range of carbonate content (4.6-75.4% wt).

120

3.14 Stable isotopes of carbonate and carbonate mineralogy

Only three sites (SO191-2/51, 66 and 98) that contained bands of nodular carbonates were used for the analysis of stable carbon and oxygen isotopes and mineral content of carbonates. Stable isotopes and mineralogy of representative sediment samples were included for most sites.
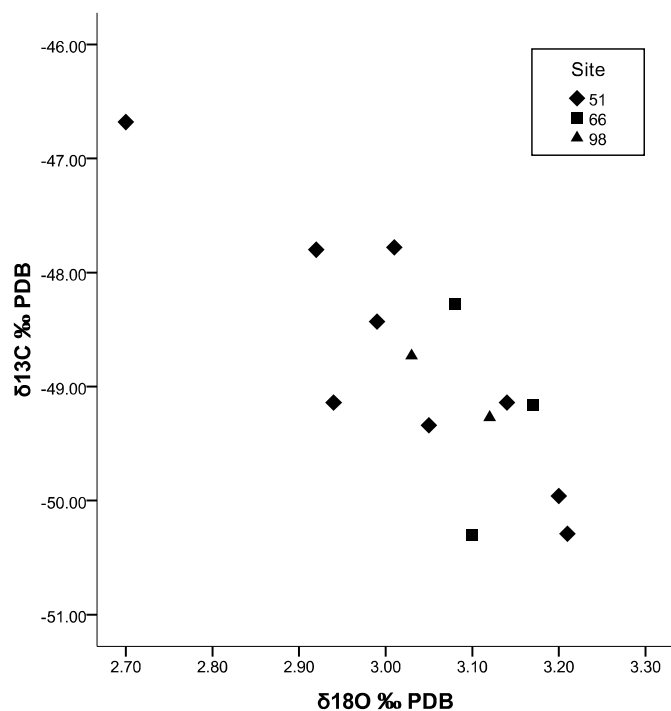
Figure 55. Carbon and oxygen isotope values of carbonates from selected sites containing bands of carbonate nodules in box cores

There was a strong negative linear relationship (r = -0.83) between stable carbon isotope and stable oxygen isotope. Note the carbonates constituted a combination of mineral content between aragonites (major constituent), Mg-calcite and quartz (minor constituent) (Appendix 3). Site #51 had a wider range of mineral content, with values ranging between -46.68 to -50.29 δC^{13} ‰ PDB and 2.7 to 3.21 δO^{18} ‰ PDB, compared with Site #66 (-48.73 to -49.27 δC^{13} ‰ PDB; 3.03 to 3.12 δO^{18} ‰ PDB and Site

121

#98 (-48.28 to -50.30 δC^{13} ‰ PDB; 3.08 to 3.17 δO^{18} ‰ PDB). Further, these

carbonates exhibited negative δC^{13} values which indicated their carbon was derived

from anaerobic oxidation of methane.
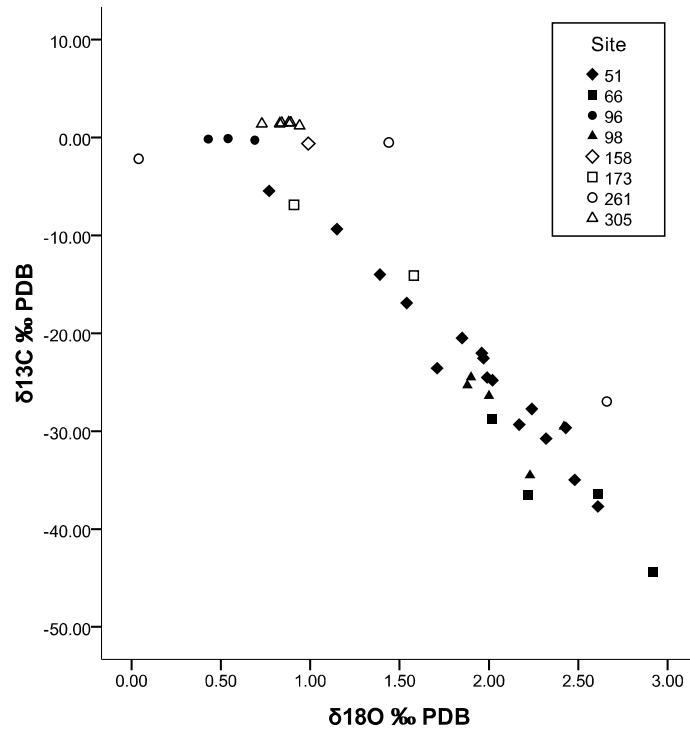
Figure 56. Stable isotopic composition of background sediments.

There was a strong negative linear relationship (r = -0.942) between the stable oxygen

isotope and the stable carbon isotope values with a wide range of δ^{13}C values of the

background sediment samples, having positive values up to +1.51 ‰ and negative

values down to -44.4 ‰ (Figure 56). Site #305 had the strongest positive δ^{13}C values;

while Site #66 had an extremely negative δ13C value coupled with the highest δ^{18}O

value. Site #51 had the widest range of δ^{13}C values. Site #98 had moderately negative

^{13}C values. Carbon and oxygen isotopic composition of sediments with values for

seawater derived carbon was between +8 and -7 δ^{13}C ‰ PDB. Sites #96, 158, 261 and

305 fell into this category. However, there was an outlier for Site #261 with a δ^{13}C value of -26.97 and δ^{18}O value of 2.66 which can not be explained.

A second group with carbonate δ^{13}C values between -15 and -25 ‰ PDB for sedimentary organic diagenesis (Campbell 2006) included Site #51. A third group with carbonate δ^{13}C values for oil fractions (-20 to -35 ‰ PDB) included Site #98. The carbon sources for sediments of Sites #173 fall in between the two groups, seawater and sedimentary organic diagenesis derived carbon. Carbon sources of sediment samples for Site #66 were likely thermogenic methane, or mixing between seawater and biogenic methane (-40 to -50 δ^{13}C ‰ PDB). Quartz was the major constituent for all sediments sampled; while mixtures of feldspars (plagioclase and potassium), low-and high-magnesian calcite, and aragonite were minor constituents (Appendix 3). Results from a mineralogic analysis of the sediments sampled showed that these sediments were siliciclastic. In addition, these sediments contained ≤ 30% carbonate content inferring hemipelagic terrigenous mud deposits (Appendix 3).

3.15 Benthic invertebrate assemblages

Table 8 and Appendix 4 lists all the species, both living and dead, found at each site. There was a general with respect to number of species between sites. Site 51 had the highest number of species. In contrast, two non-seep reference sites, 262 and 305 had no macrofaunal species. In addition, all sites marked with superscript 1 were box core benthic samplings which contained higher number of species compared with the ones marked with superscript 2. These differences were probably due to the sampling size and the type of sampling gear used.

There were no live polychaetes in any of the multicore or gravity core samples, unlike the box core samples. This variation is attributed to the different sampling methods. Live polychaetes were randomly collected from all box core samples through sieving and sorting, and then preserved in a buffered solution containing10% formalin on board RV SONNE. The multicore and gravity core samples were stored in the cooler on the ship until the end of leg 3 and subsequently were sieved and sorted for organisms at AUT laboratory. By that time, polychaetes from the multicore and gravity core samples would have disintegrated, and hence there were no live specimens, apart from two ?terebellids (158A and 261) and one unidentified tubeworm (98-1B). In addition, all tubes collected through sieving and sorting from these core samples belonged to the class Polychaeta, and their taxon was indeterminate. The live specimens (Polychaeta and Sipunculidea) listed in Table 8 were identified by experts at NIWA.

For molluscs, the order of the most to the least occurrence of species was: *Calyptogena* sp. (6), *Nassarius ephamillus* (6), *Lucinoma galathea* (4), *Falsinulatia* sp. (4), *Acharax clarificata* (3), *Provanna* sp. (3), *Friginatica* sp. (2) and *Ennucula strangeiformis* (1) and *Vesicomya* sp. (1). The classes of Bivalvia, Gastropoda and Polychaeta were the

most common. In contrast, the classes of Actinaria, Hydrozoa, Malacostraca and Ophiuroidea were the least common and the species under these families were vagrants or opportunists.

Table 8. Presence/absence data for regional distribution of benthic invertebrates sampled ([1]box core, [2]multicore, [3]gravity core, □ = live, ■ = dead; *symbionts-containing species)

Class	Order	Family	Genus	Species	Omakere Ridge									Wairarapa		
					51[1]	66[1]	96[1]	98[1]	173[2]	232[2]	242[2]	261[2]	262[2]	156[2]	158[2]	305[3]
Anthozoa	Actiniaria	Bathyphellidae	*Isoparactis*	*farex*				□								
Anthozoa	Actiniaria	Unidentified			□											
Bivalvia	Nuculoidea	Nuculidae	*Ennucula*	*strangeiformis*	□											
Bivalvia	Solemyoida	Solemyidae*	*Acharax*	*clarificata*	□■				□		□■					
Bivalvia	Veneroida	Lucinidae*	*Lucinoma*	*galathea*	□■				■	□	■					
Bivalvia	Veneroida	Vesicomyidae*	*Calyptogena*		□■	■		■	■	■					■	
Bivalvia	Veneroida	Vesicomyidae*	*Vesicomya*		■											
Gastropoda	Caenogastropoda	Provannidae	*Provanna*		■	■	■									
Gastropoda	Neogastropoda	Drilliidae	*Splendrilla*		■											
Gastropoda	Neogastropoda	Nassariidae	*Nassarius*	*ephamillus*	□■	■	■	■	■						■	
Gastropoda	Neotaenioglassa	Naticidae	*Falsinulatia*		■	□								■	□■	
Gastropoda	Neotaenioglassa	Naticidae	*Friginatica*		■										■	
Gastropoda	Neotaenioglassa	Naticidae	Unidentified											■		
Gastropoda	Patelliform				■											
Hydrozoa	Leptothecata	Lafoeidae	*Acryptolaria*	*gracilis*		□										
Malacostraca	Decapoda	Paguridae			□											
Ophiuroidea	Ophiurida	Ophiuridae	*Ophiomusium*	*lymani*					□							
Polychaeta	Phyllodocida	Nephtyidae			□											
Polychaeta	Phyllodocida	Sigalionidae			□		□									
Polychaeta	Sabellida	Siboglinidae*							□		■					
Polychaeta	Scolecida	Capitellidae				□										
Polychaeta	Scolecida	Maldanidae	*Asychis*	*asychis-B*				□								
Polychaeta	Scolecida	Maldanidae	*Nicomache*	*nichmache-B aff. ohtai*		□										
Polychaeta	Spionida	Chaetopteridae							□							
Polychaeta	Terebellida	Flabelligeridae							□							
Polychaeta	Unidentified					□			□							
Polychaeta	Unidentified		black tube		■						■	■	■			
Polychaeta	Scolecida	?Capitellidae	red and white stripes tube						■	■					■	
Polychaeta	Unidentified		brown sinuous chitinous tube						■							
Polychaeta	Unidentified		red chitinous tube						□■		■		■			
Polychaeta	?Terebellida		disintegrated									□			□	
Polychaeta	Unidentified		soft grey mucus lined with crystal fragments		■	■			■							
Polychaeta	Unidentified		firm tube lined with crystal fragments		■				■							
Sipunculidea	Unidentified				□											
			No. of species:		19	9	8	9	6	4	4	3	0	2	6	0

3.15.1 *Summary of results for benthic invertebrate assemblages*

Omakere Ridge

Station SO191-2/51

The death assemblage of molluscs comprised *Lucinoma, Calyptogena, Vesicomya, Nassarius, Falsilunatia, Friginatica* and *Provanna*. These were either articulated or disarticulated and were predominantly in parautochthonous positions apart from one specimen of *Calyptogena* at 4 cm bsf (Horizon C, 51-2B), which was cemented in an autochthnous position. There were some shell fragments with high dissolution and pitting. The life benthic invertebrate assemblages included *Acharax, Lucinoma, Calyptogena, Ennucula, Nassarius*, sea anemone, pagurid, sipunculid, and polychaetes.

Station SO191-2/66

Shell hash at Site contained some articulated and disarticulated *Calyptogena* and gastropods (*Nassarius* and *Provanna*), and cemented shell fragments. *Provanna* and polychaetes were predominant while *Falsinulatia* was minor and these form a living assemblage at this site.

Station SO191-2/96

Polychaetes and a sea anemone form a living assemblage and gastropods (*Provanna* and *Nassarius*) form a death assemblage of this site.

Station SO191-2/98

A shell hash contained some disarticulated, fragmented and cemented shells of *Calyptogena* and some empty shells of *Nassarius*. *Acharax, Ophiomusium* (ophiurid) and polychaetes form a living assemblage at this site.

Station SO191-2/173

Extensive carbonate nodules were mixed in with shell hash containing disarticulated fragmented shells of Calyptogena and one empty parautochthonous articulated *Lucinoma* and *Nassarius*. These carbonates were overlain with bioturbated sandy silt containing *Planolites* ichnofabrics. No living organisms were found in this core sample.

Station SO191-3/232

Live adult *Lucinoma* was found in this core.

Station SO191-3/242

Some shell fragments of *Calyptogena,* a living juvenile *Acharax*, and one disarticulated shells of *Lucinoma* form an assemblage at this site.

Station SO191-3/261

The sediments of SO191-3/261 (Kaka, rain drop site) contained some unidentified worms.

Station SO191-3/262

No benthic invertebrates were present.

Wairapapa
Station SO191-2/156

No organisms were found in these sediments, except for one empty shell of *Falsinulatia.*

Station SO191-2/158

Death assemblages of gastropods occurred, predominantly *Nassarius* and some *Friginatica*. *Falsinulatia* and terebellids form an association at this site.

Station SO191-3/305

No organisms were found in this core sample.

In summary, chemosymbiotic bivalves (*Calyptogena, Lucinoma* and *Acharax*), non-symbiont polychaetes, grazing gastropods (*Provanna*) and carnivorous shell-drilling gastropods form an association for Type 1 habitat. Stratified layers comprising shell hash of *Calyptogena* and *Nassarious* overlain with sandy silt containing live *Lucinoma,* juvenile *Acharax* and polychaetes form benthic assemblages for Type 2 habitat. Assemblages of carnivorous gastropods and polychaetes form an association for Type 3 habitat.

3.15.2 *Representative epifauna of Rock Garden (SO191-3/224)*

Figure 57 shows some selected rocks teemed with epibenthic invertebrates, which were found exposed on the seafloor. These rocks were collected by video guided grab. Bryozoa appears to be the dominant taxa (Figures 58 and 59). The majority of organisms observed were sedentary species. *Psolus* sp. (Figure 61B) and *Leptochiton* sp. (Figure 61D were the only two mobile organisms found on the rock. Figure 60 is representative of benthic foraminifera discovered.
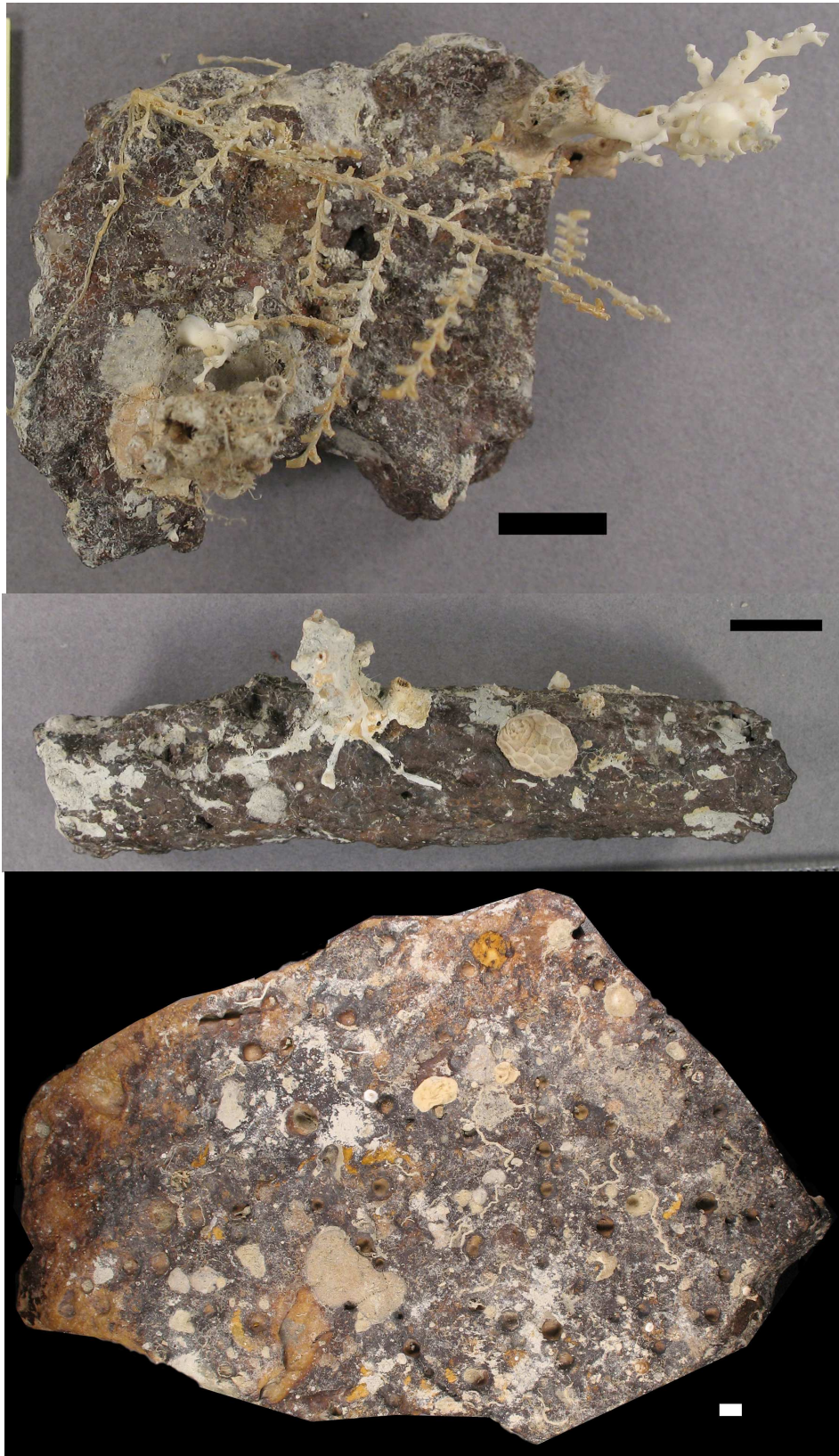
Figure 57. SO191-3/224. Selected carbonates rocks with representative epifauna. Scale bars = 1 cm.
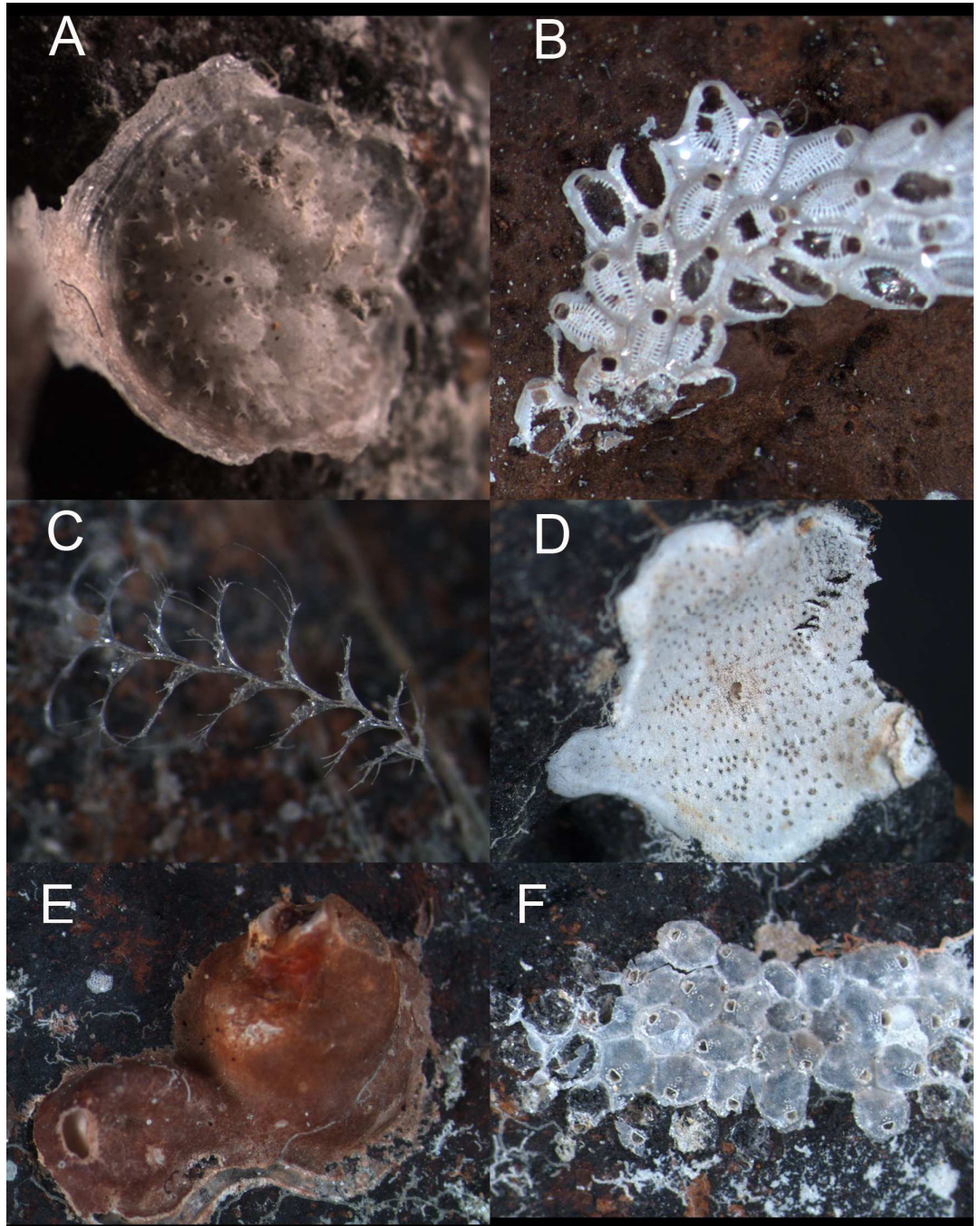
Figure 58. Bryozoa: A) *Disporella sacculus* (~ 5 mm diameter); B) *Figularia pelmatifera*; C) *Cornucopina* sp.; D) unidentified, probably not a bryozoan; E) *Macropora filifera*; and F) *Fenestrulina* n. sp. Individual zooid, < 1mm length.
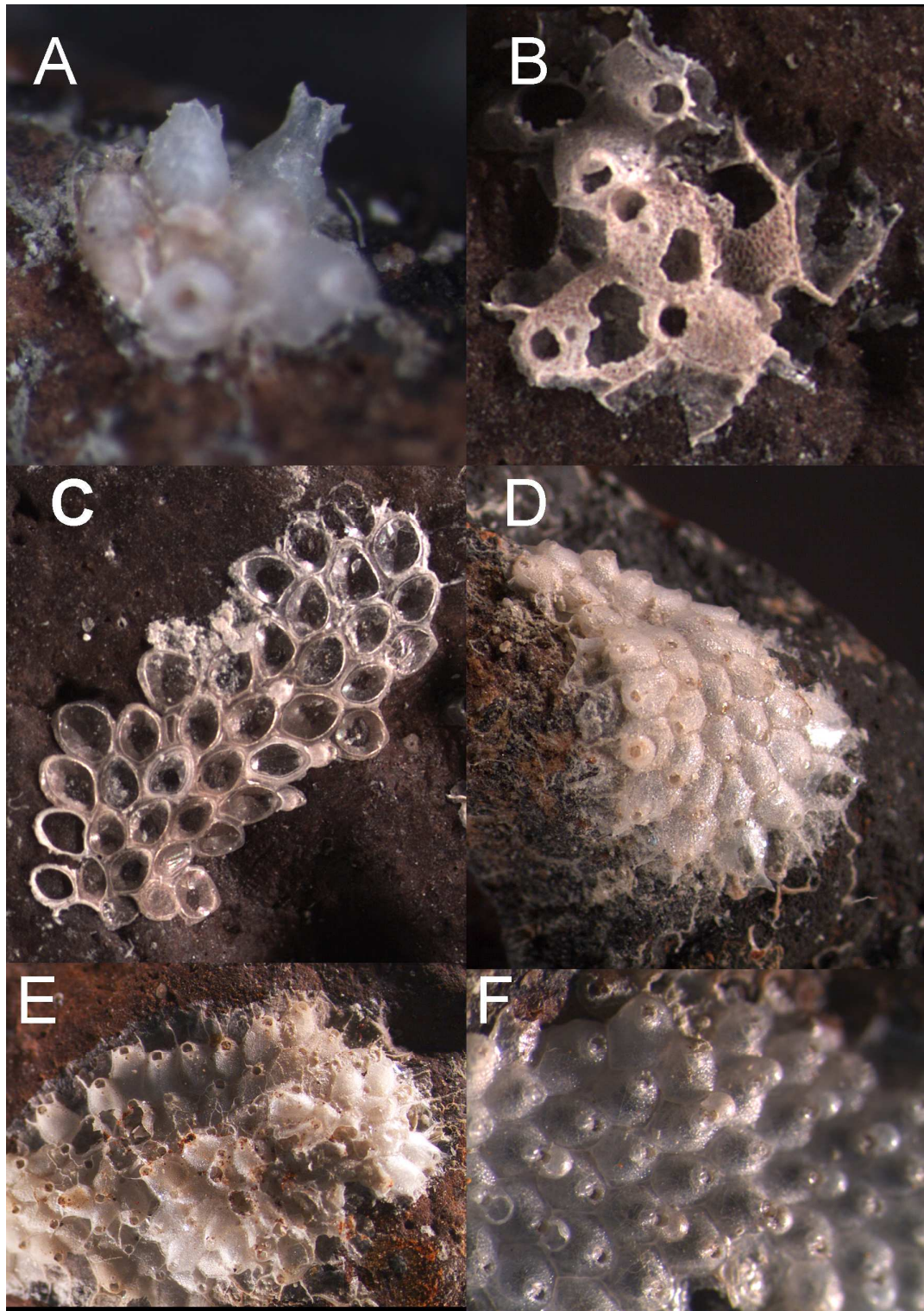
Figure 59. Bryozoa: A) ?*Lagenipora* sp.; B) ?*Bitectipora* sp.; C) *Ellisina* n. sp.; D) *?Parkermavella* sp.; E) ?*Fenestrulina* sp., and F) ?*Parkermavella* sp. Individual zooid, < 1mm length.
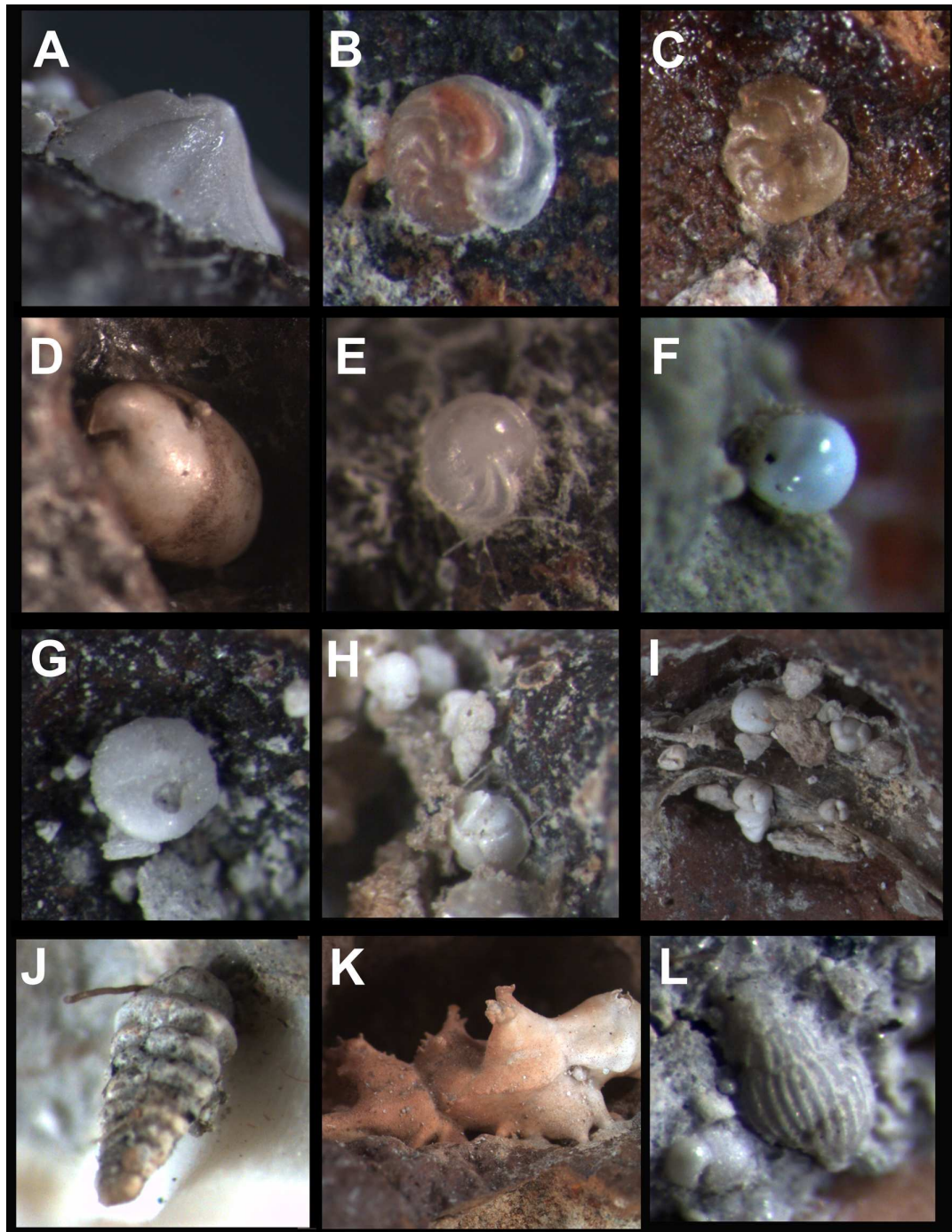
Figure 60. Foraminifera. A) *Carpentaria monticularis*; B-C) *Cibicides wuellerstorfi*; D) unidentified; E) *Discorbinella bertheloti*; F) ?*Pyrgo*; G) unidentified; H) *Uvigerina peregrina* (centre) and *Cibicides* sp. (bottom); I) *Globorotalia inflate* (top), *Neogloboquadrina dutertrei* (right)*;* aggulinate? (bottom); J) *Bolivina variabilis*; K) *Carpenteria monticularis* or sacculate foraminifera; and L) *Uvigerina mediterranea*. The width of all forams were approximately < 150 μm.
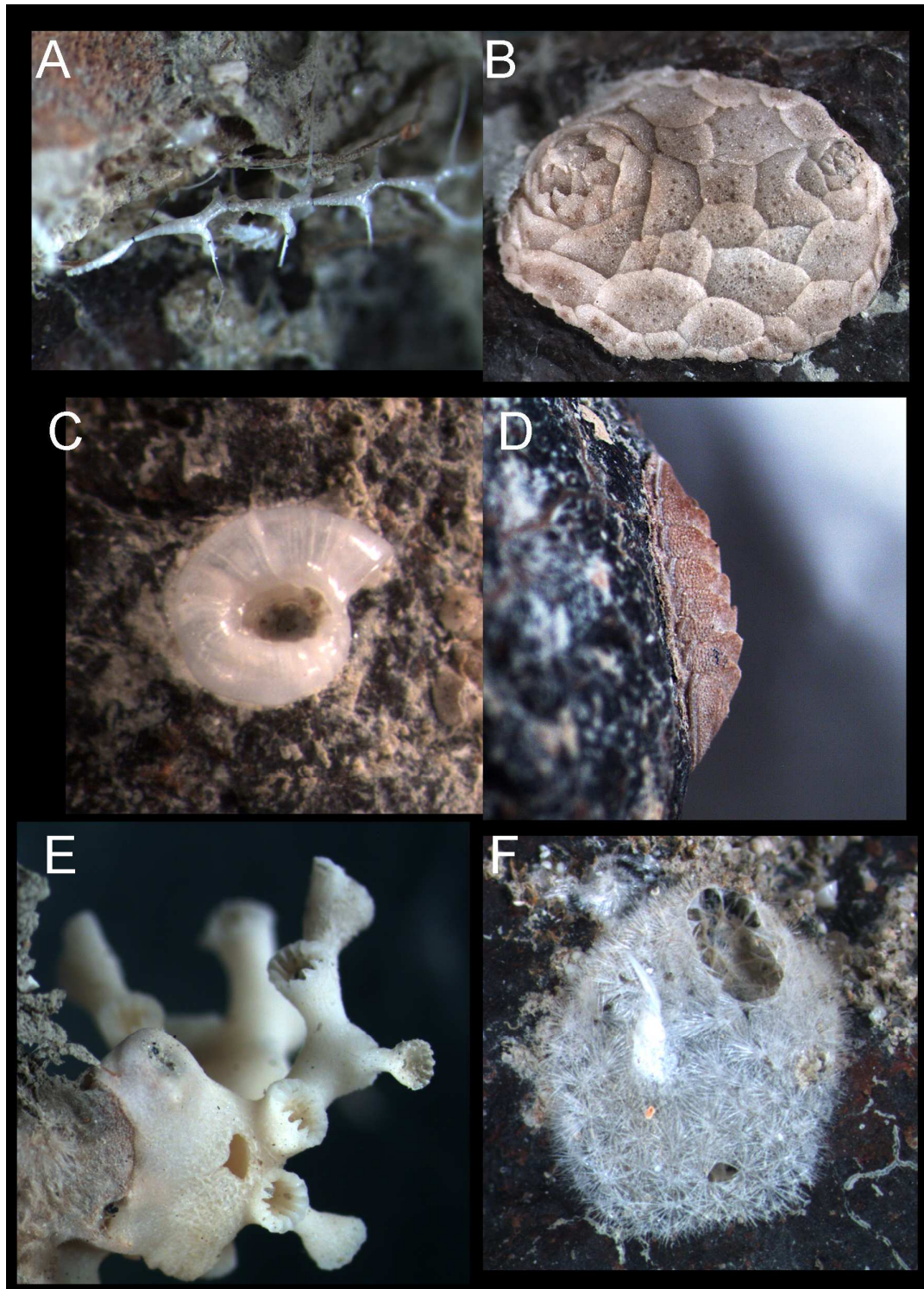
Figure 61. Representative epifauna: A) bamboo coral, Gorgonacea; B) holothurian, *Psolus* sp. (8 mm length); C) tube of Spirorbinae (Polychaeta) (~1 mm length); D) chiton, *Leptochiton* sp. (~5 mm length); E) hydrozoan, Stylasteridae and F) sponge?
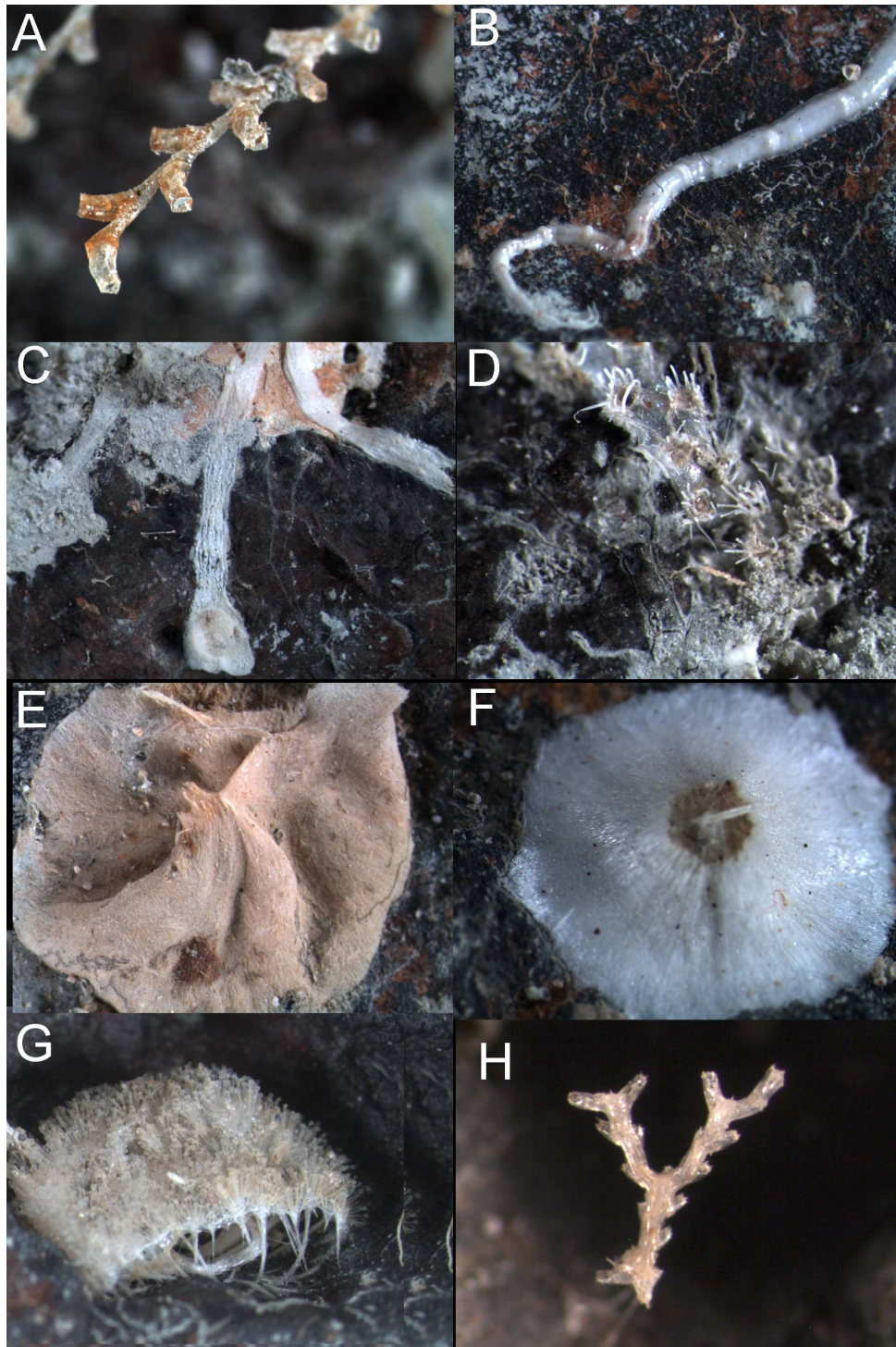
Figure 62. Representative epifauna: A) *Symplectoscyphus* (Hydrozoa), B) unidentified, C) unidentified, D) *Chaperia* n. sp., E) Porifera 5 mm length and F) unidentified, 3 mm diameter, G) Porifera, H) Leptothecata (Hydrozoa)

4 DISCUSSION

Results of this study revealed three distinctive groups of seep habitats and associated benthic invertebrate assemblages, reflecting temporal and spatial variability of methane seepage activity. These groups can be roughly classified according to their distance from seep outlets, whether presently active or relict. Habitat 1 includes Sites 51, 66, 98 at LM9 of Omakere Ridge, which signify areas that have been active in the past but are presently waning or inactive. Habitat 2 includes Sites 96 and 173 of Omakere Ridge and 261 of Kaka, which are all generally located on the periphery of active seeps. Habitat 3 includes Sites 158 and 305 of Wairarapa, which are non-seep related sites. There was no analysis for TOC content, carbonate content, mineralogy and stable isotopic composition carried out for the remaining sites, which included 232, 242 and 261 of Kaka, and 156 of Wairarapa, due to financial constraints.

Initially this discussion focuses on each component that contributes to the distinct characteristics of seep habitats, starting with the sedimentologic aspects, followed by ichnologic assemblages and benthic invertebrate assemblages (Figure 63). Next, the ecologic interpretation of the seep habitats is briefly discussed. Subsequently, comparisons are made between the findings of this study and Northern Hemisphere modern seep counterparts. Lastly, the limitations of this study and the effectiveness of the use of X-ray radiography for the examination of burrow structures in seep habitats are considered.
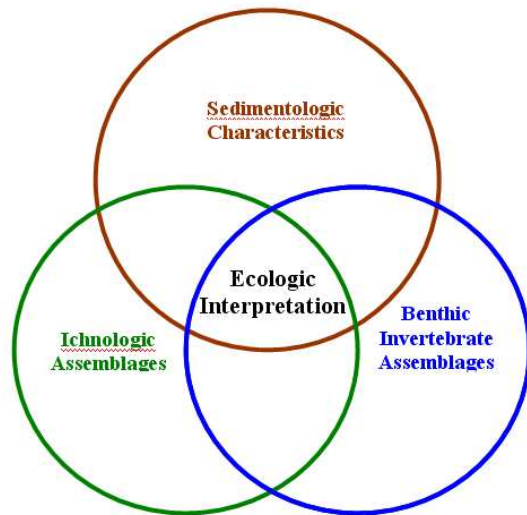
Figure 63. Chart diagram of the discussion layout

4.1   Sedimentologic characteristics

4.1.1   *Origins of background sediments*

The silt portion of the hemipelagic terrigenous mud deposits at the Omakere Ridge had

quartz as the dominant mineral species, while the clay fraction ($\leq$ 19%) comprised

smectite and illite as dominant mineral species with common kaolinite and minor

chlorite (CS Nelson, pers. com.). These mineral components originated in the Tertiary

mudstones of the East Coast Basin (CS Nelson, pers. com.). Analytical results for

mineralogy of the clay fraction in the marine sediments of the Wairarapa region were

not obtained in this study; therefore their origins were indeterminate. However, based

on past studies on the mineralogy of the silt fraction for Wairarapa region, quartz was

the dominant mineral species together with a mixture of illicite, chlorite and

montmorillorite in various concentrations, and these also derived from Tertiary

mudstones (Carter 1975).

4.1.2 *Organic carbon content for siliciclastic sediments*

Differences were revealed in the values of TOC for the siliciclastic sediments between regions, 0.24-0.57 wt % for Omakere Ridge and 0.72-0.92 wt % for Wairarapa. However, the gradient of TOC values changes very little with increasing depth within the sediment columns for both regions. The TOC values for the hemipelagic sediments on continental margins (outer shelf and slope settings) in most parts of the world are between 0.3 and 1 % (Rullkotter 2006), and the results of this study also fall within this range. Regarding the profile of TOC within sediment columns, for normal marine sediments TOC generally decreases as the depth increases, and this is attributed to microbial assimilation of nutrients from organic matter during early diagenesis (Rullkotter 2006). However, this was not the case in this study, where TOC levels are seen to remain fairly constant throughout all levels. One possible reasons for this variation in results may include bioturbation, in which benthic invertebrates bring organic matter deep within the sediment from the surface by their burrowing activities (Bauer et al. 1988). There was evidence of bioturbation of various degrees in all the sites studied which could explain the approximate constant values of TOC throughout the sediment depths. Oother potential factors that control TOC content within sediments involve the organic matter type (terrigenous or marine-derived) and sedimentation rate in relation to proximity to land (Canfield 1994; Aller and Blair 2004). A high sedimentation rate promotes rapid burial of organic matter, thus increasing its preservation and thus TOC remains constant through the sediment depths. Furthermore, terrigenous organic matter tends to be more resistant to degradation compared with marine-derived organic matter (Canfield 1994). The proportion of terrigenous organic matter incorporated into the sediments decreases seaward, while marine-derived organic matter increases. In this study, Sites 158A and 305 of

Wairarapa region, which are closer to land had the highest TOC values compared with selected sites of Omakere Ridge region that are farther away from the land in line with expectations. As for the sediments containing methane derived authigenic carbonate nodules, especially for LM9 (Omakere Ridge, Sites 51, 66 and 98), the TOC values were low compared with that of Wairarapa's. Bauer et al. (1988) suggested that TOC for seep sediments tend to be higher than the surrounding sediments due to active hydrocarbon seepage which enhances the organic matter content. However, this is not the case for LM9 and therefore these findings are not consistent with Bauer et al.'s (1988) concept of TOC in relation to seep sediments. Another possible factor may be a relationship between TOC and grain size.

4.1.3 *Relationship between TOC and grain size*

It is generally known that TOC increases as the sediments become finer grained, which can be explained by increased surface areas for adsorption (e.g. Keil et al. 1994). In addition to grain size, other parameters affecting the total organic carbon content include the level of local primary productivity, oxygen concentrations in the bottom water and in the surficial sediments, and porosity (Tyson 1995). For the active continental margins, water depth, terrestrial organic matter inputs, mean grain size, the percentage of silt and clay fractions and siliciclastic sediment accumulation rates are strongly interrelated with respect to TOC (Tyson 1995). Moreover, water depth and mean grain size are negatively correlated with TOC, while the rest are positively correlated. The Wairarapa region (Sites #158A and 305) had finer grained sediments with high TOC. In contrast, Omakere Ridge region had slightly coarser grained sediments with low TOC. These differences may be explained by their relative proximity to the land. The Wairarapa region lies in the direction of D'Urville Current from Cook Strait, but is also influenced by the Southland Current running north

along the east coast of South Island (Chiswell 2000). These two currents mix together thus bringing nutrients to the area. Moreover, the Wairarapa region is in close proximity to the land (~30 km) where organic nutrients are derived from the land, ocean currents and high sedimentation rates. These factors lead to the preservation of organic matter. On the other hand, the Omakere Ridge region is further offshore (~100 km), hence exhibiting a low TOC. Furthermore, the level of dissolved oxygen in the bottom water may be one of the controlling factors on the preservation of organic matter in sediments. Low concentration of dissolved oxygen in the bottom water corresponds to high TOC in the sediments (Hyland et al. 1991). These factors, coupled with finer grained sediments, likely enhanced the preservation of organic matter. Moreover, these factors also would have influenced the abundance and diversity of benthic invertebrates, and the diversity of organism traces. These matters are further discussed in Section 4.2. TOC values in relation to the carbonate contents of the studied sediments were negatively correlated, the latter of which are also influenced by the saturation state of seawater overlying the sediments or that of pore waters within the sediments. The relationship between sediment TOC and carbonate contents are discussed further below.

4.1.4 *Carbonate content*

The results of this study revealed a wide range of carbonate contents (0.8 to 78.0 % wt). The carbonate content of siliciclastic sediments for Wairarapa (Sites 158A and 305) were low compared with those of Omakere Ridge sites. In particular, LM9 of Omakere Ridge contained very poorly sorted, carbonate-rich sandy silt, with high carbonate owing to excess bicarbonate ions in the pore waters. The production of bicarbonate ions in the pore waters near the sediment-water interface, or within the sediments, was derived from the chemical reaction between methane and sulphide by microbial activities involving anaerobic oxidation of methane (AOM) by a

consortium of methanotrophic archaea and sulphate-reducing bacteria (Treude et al. 2003; Luff et al. 2004). Consequently, the excess bicarbonate ions react with mineral species to form carbonates. Mineral species include aragonite and magnesium calcite, which are derived from hard parts of marine benthic invertebrates such as molluscs, foraminifers, corals, bryozoans and sponges as well as AOM (Seibold and Berger 1993). The prerequisites for the precipitation of methane-derived authigenic carbonates are oxygenated pore water, temperature and available mineral species as well as methane supply and rate of microbial activity involving AOM (Judd and Hovland 2007).

Bioirrigation is carried out by burrowing benthic invertebrates that pump seawater through their burrows from the overlying sediments into the sediments and seawater is then mixed in with the pore waters in the surrounding sediments by diffusion. Moreover, thickness of bands of the carbonates within the sediment column is determined by bioirrigation intensity, bioturbation intensity, porosity of sediments, fluid flow velocity, AOM rates and the saturation state of pore waters with respect to calcium carbonate (Luff et al. 2004). For instance, at the base of a carbonate band, the pore waters are undersaturated with respect to carbonate (e.g. aragonite); therefore the precipitation of carbonate does not occur at that level. *Calyptogena* sp. may play an important role in bioirrigation at these sites, assisting in the formation of carbonate deep within the sediment column (Luff et al. 2004). Their role in this matter is further discussed in 4.4.3.

The formation of carbonate appears to be inversely proportional to porosity and fluid flow velocity. Sediments that are very poorly sorted have low porosity and low fluid flow velocity, thus promoting carbonate formation. The fluid flow velocity is the speed

at which the fluid containing solutes is transported from deep within the sediment column to the sediment-water interface. For example, when there is a restriction on fluid flow, bicarbonate ions released from the chemical reaction in the AOM zone are diffused into the surrounding sediments resulting in the cementation of sediments, by carbonate precipitates (Luff et al. 2004).

All box core samples of this study that contained bands of carbonate nodules were overprinted with low densities of burrows (e.g. BI=1, which means that the porosity of these sediments were low. By contrast, high bioturbation (e.g. BI=5) may create and maintain high porosity of the sediments, thus, inhibiting the precipitation of carbonates (Luff et al. 2004). This is due to the bicarbonate ions being lost to the bottom water overlying the sediments. The level of bioturbation may depend on the degree of uniformity (sorting) and sediment type as well as food availability (organic matter).

The carbonate content was low (< 8% wt $CaCO_3$) for the Wairarapa sites, which were typified by poorly sorted, silt. The accumulation of carbonate in the sediments also is controlled by the saturation state with respect to calcium carbonate in sea water overlying the sediments (Morse 2005). Since the sediments of the Wairarapa sites contained high total organic carbon compared with those of Omakere sites, the sea water overlying the sediments must be undersaturated with respect to calcium carbonate. In particular, this relationship may be attributed to sea water (or pore waters) being saturated with dissolved carbon dioxide from the oxidation of organic matter, which causes the dissolution of calcium carbonate; hence low content of carbonate in these sediments.   Furthermore, based on the isotopic composition of the siliciclastic sediments for Wairarapa, their carbon sources were derived from seawater, which indicates that these sites are not seep related.   Site 158A was situated on the edge of the

North Tower active seep containing clusters of carbonate blocks and scattered carbonate fragments. Site #305 was further away from the active seep. Moreover, these two sites and Site #156 were in the vicinity of trawl marks, which can be seen in the images produced by the side scan sonar (Klaucke et al. in press). It is unclear whether trawler activity may have affected these results.

4.1.5 *Stable isotopes and mineralogy of carbonate nodules*

Globally, seep-related, methane-derived authigenic carbonates (MDACs) have a wide range of $\delta^{13}C$ values between - 60 to -10 ‰ PDB (Judd and Hovland 2007), and the $\delta^{13}C$ values of the sampled carbonates from sites 51, 66 and 98 of Omakere Ridge were within that range. MDACs have various mineral contents, which include aragonite, high magnesian-calcite (HMC), and low magnesian-calcite (LMC) (e.g. Greinert et al. 2001; Gieskes et al. 2005; Muralidhar et al. 2006). These minerals co-exist in marine environments (Burton 1993), and variation in carbonate content is due to pore water conditions at the time of precipitation of available mineral species. Aragonite originates from AOM, the skeletal component of molluscs and annelid worms, and magnesian-calcite from forams, sponges, and decapods (Seibold and Berger 1993) and gas hydrate decomposition (Bohrmann et al. 1998). The mineral content of the sampled carbonates included all these aforementioned mineral species in various concentrations but aragonite was the dominant species. This suggests high alkalinity which is brought about by anaerobic oxidation of methane and high sulphate concentrations in the pore waters (Greinert et al. 2001).

Sites 51, 66 and 98 of Omakere Ridge (LM9) contained bands of extensive carbonate nodules overlain with shell hash comprising predominantly *Calyptogena* shells in various taphonomic states. The formation of carbonates may have been enhanced by

143

bioirrigation activity by *Calyptogena*. These clams oxygenate the surrounding sediments by pumping with their inhalant siphons (Wallman et al. 1997). Siphons pump bottom water containing sulphate into the mantle cavity and release it into the surrounding sediments when the foot extends out from within the shell. The mixing of sulphate-rich bottom water with methane-rich pore fluids provides a medium for AOM by a consortium of methanotrophic archaea and sulphate-reducing bacteria (Treude et al. 2005). The end result is the precipitation of aragonite-dominated carbonates near the sediment surface.

High Mg-calcite and/or low Mg-calcite were minor constituents of the carbonate nodules sampled and also present in background sediments from Site 51. The precipitation of carbonate containing Mg-calcite may be the result of destabilisation of the gas hydrates, which releases ^{18}O-enriched water (heavier δ^{18}O values) to mix with the pore waters of the sulphate reducing zone where AOM takes place (Bohrmann et al. 1998; Greinert et al. 2001). Low sulphate concentration and low alkalinity in pore waters favour the precipitation of Mg-calcite dominated carbonates (Greinert et al. 2001). In the study areas gas hydrates have been reported based on seismic reflection profiling (Jones et al. in press). This may explain the precipitation of Mg-calcite, especially for Site 51. Indeed, the concentration of methane in the water column above Omakere Ridge was high (up to ~155 nM for LM9) indicating active seepage (Faure et al. in press). The presence of shell hash coupled with the scarcity of living molluscs at LM9 sites, 51, 66 and 98 indicates that these sites were, in the past, teeming with chemosynthesis based benthic invertebrate communities fuelled by active methane seepage. However, the seepage is now either waning, inactive or being diverted. This is consistent with recent findings concerning seepage activity for LM9 (Jones et al.

2008).

4.2 Ichnologic assemblages

Overall in this study, dwelling traces and crawling traces were relatively common, while dwelling-feeding, resting and 'probing' traces were few. Some creators of these traces were unknown and for this reason, ichnogenus names were given for these traces which appear to be identical to the known trace fossils. *Skolithos* and *Planolites* were the main ichnogenera, with minor *Palaeophycus, Solemyatuba, Spongeliomorpha*, and *Bergaueria* also present. One other trace identified as a probing trace in this study was a chemosymbiont structure produced by a lucinid, which presently has no known ichnogenus. However, Seilacher (2007) ascribed it to ichnogenus *Chondrites* because of its feeding and ethological traits. This 'probing' trace is further discussed Section 4.2.7. Sediment sampled from the Kaka non-seep reference site (262) contained no burrow structures.

Traces produced by benthic invertebrates reflect their adaptation to environmental conditions, such as substrate type, water energy, food supply, water depth, salinity, oxygen concentrations and sedimentation/depositional rates (Ekdale 1988; Gaillard 1991; Wetzel 1991; Pemberton et al. 2001; Uchman 2007). Furthermore, oxygen concentration is one of the main determinant factors contributing to the type of ichnofabric preserved (Ekdale 1988). Where oxygen is not a limiting factor, there is generally a high diversity of traces and ethologies, which includes dwelling (domichnia), crawling (repichnia), resting (cubichnia) and grazing (pascichnia). Oxygen-poor environmental conditions are associated with low diversity of ethological traces and are dominated by feeding (fodinichnia*)* traces produced by opportunistic organisms colonising new or disturbed habitats. Oxygen-depleted environmental

conditions are associated with sediments containing no traces. The average bottom water oxygen concentration for the Wairarapa region was 195.6 ± 1.3 to 196.6 ± 0.9 micromolar (4.38 ± 0.03 to 4.4 ± 0.02 mL per litre), and for the Rock Garden was 216.6 ± 2.7 micromolar (4.8 ± 0.06 mL per litre) (Sommer in press). Based on these measurements, oxygen is not a limiting factor.

The autecology of traces present are discussed with respect to each ichnogenus present: *Skolithos*, *Planolites, Palaeophycus, Solemyatuba, Spongeliomorpha, Bergaueria* and *Chondrites.* Subsquently, the ichnological assemblages of the study sites are compared with the classification of ichnofacies based on substrate type, environmental conditions and the types of traces using Seilacher's concept of recurring ichnofacies classification (MacEachern et al. 2007).

4.2.1 *Skolithos*

The ichnogenus *Skolithos* is characterised by thin vertical or obliquely inclined cylindrical shaped dwelling burrows, either unlined or lined with dark organic mud or agglutinated sand and are found in a wide range of environmental conditions from the shallow sea to the deep sea (Pemberton et al. 1992). Benthic invertebrates that produce *Skolithos* are generally suspension feeders or passive carnivores, and they use substrate as an anchoring medium. The polychaetes, tube-building worms, are possible trace makers of *Skolithos* (Pemberton, 1992). There were many varieties of tubes found in this study and most sites that contained tubes, either empty or live had *Skolithos* fabrics. Others that had some burrow mottling of *Skolithos*, such as Sites 305 and 158A, but contained no live tube-building worms or tubes can be explained by the rapid degradation of tubes following the death of an organism.

4.2.2 *Planolites*

The ichnogenus *Planolites* is characterised by a horizontal, undulating cylindrical shaped, unlined burrow structure that has a fill composed of faecal pellets, and these structures represent a grazing trace of the deposit feeder (Bromley 1996). Mobile deposit feeding polychaetes or other worm-like invertebrates are trace makers of *Planolites* (Bromley 1996). The peanut worm belonging to the class Sipunculidea, is a mobile, cosmopolitan deposit feeder that burrows in sands and silts, and forms unlined burrow structures resembling a crawling trace (Edmonds 2000). Therefore, it is possible that the peanut worm retrieved from box core sample #51 is a trace maker of *Planolites*. Moreover, *Planolites* are cosmopolitan and can be found in both low energy and high energy marine environments, and are commonly associated with *Skolithos* and *Palaeophycus* (MacEachern et al. 2007).

4.2.3 *Palaeophycus*

The ichnogenus *Palaeophycus* is a horizontal, undulating cylindrical shaped, wall lined burrow that has a fill composed of sediments similar to its surroundings. It represents the dwelling trace of a suspension or detritus feeder (Bromley 1996). In addition, it is commonly associated with *Planolites* and *Skolithos* in a variety of environmental conditions, both in marine and brackish water (Pemberton et al. 2001). The bamboo worm is a sedentary deposit feeding polychaete (Morton and Miller 1968), and is a possible trace maker of *Palaeophycus* (Pemberton et al. 2001). Some bamboo worms were found in box core samples #66 and #96, *Nicomache nicomache-B aff. ohtai* and *Asychis asychis-B,* respectively, and it is possible that these species created some *Palaeophycus* traces.

4.2.4 *Solemyatuba*

The ichnogenus *Solemyatuba* is characterised by an elliptical U-shaped burrow constructed by solemyids and usually occurs in dysoxic environments, such as in suboxic sediments bordering the anoxic zone (Seilacher 2007). In addition, *Solemyatuba* facies are regular features of the marine environment where active methane seepage occurs, both present (as evidence in this study) and past (e.g. Quinault Strata, Campbell et al. 2006). The bivalve genera *Solemya* (Frey 1968) and *Acharax* (this study) are creators of *Solemyatuba*. They use a piston-like foot to create that type of burrow. Unlike other burrowing bivalves that use a U-shaped burrow as ventilation for inhalant and exhalant siphons, solemyids use the U-shaped burrow as a dwelling structure, by which they move freely about. Furthermore, solemyids also form a Y-shaped burrow, with a U-shaped structure for dwelling and a shaft below it that deepens into the sediment column to act as a suphide well. Dissolved sulphide is pumped in from below by an extensible foot, where it is transported to endosymbiotic sulfur-oxidising bacteria living in the host's gills. Solemyids are thus chemosymbiotic and otherwise gutless. There was evidence of these structures in three core samples, one with a U-shaped burrow containing live juvenile *Acharax* in box core sample #98 and multicore sample #242, and the other with a relict Y-shaped burrow in multicore sample #261. The presence of *Solemyatuba* indicates oxygen-poor environmental conditions. However, this is not the case in this study because oxygen was not a limiting factor, although, in-situ sediment may have been dsyoxic at the time when the trace was made.

4.2.5 *Spongeliomorpha*

The ichnogenus *Spongeliomorpha* Sapota, 1887, emend. Calzada, 1981 is characterised by inverse T-shaped branches with vertical chambers connected to the horizontal branch (D'Alessandro and Bromley 1995). The lining of the chambers are covered with

grooves in a criss-cross design. *Spongeliomorpha* facies commonly occur in the firmgrounds both in shallow marine and deep-sea settings (Gibert and Robles 2005 and references therein). Firmgounds are defined as "stiff but unlithified substrates," which includes dewatered muds, and carbonate sediments (Savrda 2007). The deposit-feeding thalassinid crustaceans may be the creators of these burrow structures (Goldring et al. 2007). In addition, these burrow structures may also be representative of crustaceans with different functioning modes such as trapping, gardening, breeding and suspension feeding (D'Alessandro and Bromley 1995 and references therein). Gardening refers to the cultivation of microbes feeding on organic matter within the chambers with seawater circulating through them. These provide food for the occupant. One of the multicore subsamples in this study (Site 158A) had a distinctive *Spongeliomorpha* fabric, which represents both dwelling trace and gardening activities. These sediments contained high organic carbon content (0.83-0.92 % wt) with carbon isotopic value of the carbonate fraction of -0.63 δ^{13}C ‰ PDB. High organic carbon content may be attributed to large inputs of terrigenous organic matter or microbial production, and the heavier δ^{13}C value indicates a seawater carbon source, which may indicate bioirrigation activity. The trace makers (graphoglyptids) of *Spongeliomorpha* are long-lived, late succession colonisers that are adapted to nutrient poor environments in quiescent settings (Uchman 2007). Therefore, they adopt a gardening strategy and cultivate microbes for food. *Vulcanocalliax,* an undescribed species of thalanassid shrimp, sampled from a Rock Garden from the previous cruise TAN0616 (Baco-Taylor et al. in press) could possibly be a trace maker of *Spongeliomorpha.* This inference was based on a recently described species, *Vulcanocalliax arutyunovi,* that was found associated with a chemosynthetic benthic community in the periphery of a mud volcano in the Gulf of Cadiz, southwest of Spain (Dworschak and Cunha 2007).

4.2.6 *Bergaueria*

The carnivorous sea anemones are trace makers of *Bergaueria* (Pemberton et al. 2001). In this study, *Isoparactis ferax* was identified as responsible for the resting trace observed, which constitutes an isolated find. *Isoparactis ferax* are commonly found attached to boulders or cobble buried in anoxic black sediment in nearshore settings (Morton and Miller 1968), and are also present in the deep sea (S. O'Shea, pers.com.). Moreover, *Bergaueria* is commonly associated with the *Skolithos* Ichnofacies (MacEachern et al. 2007).

4.2.7 *Chondrites*

Chondrites is a root-like branching tunnel system, that is, a fucoid-shaped pattern formed by benthic invertebrates involved in strip mining for sulphide (Seilacher 2007). They can be found in anoxic sediments in quiescent settings such as the deep sea. These structures are probing traces created by benthic invertebrates hosting bacterial chemosymbionts. Bivalves such as thyasirids and lucinids are examples of strip miners (Seilacher 2007). However, these bivalves are not classified as trace makers of *Chondrites* because initially this trace was associated with deposit-feeding activity (Bromley 1996). Nonetheless, Seilacher (2007) has proposed that these probing traces are not, in fact, characteristic of burrow structures created by deposit feeders that ingest sediments as they plough through the sediments, excreting faecal pellets behind them. Thyasirids and lucinids probe sediments below them, searching for dissolved sulphide using a chemosensory foot that serves as an inhalant to pump in sulphide for endosymbiotic sulphur-oxidising bacteria housed in their gills (Dando et al. 1994; Dufour and Felbeck 2003; Seilacher 2007). This mining strategy forms a tunnel system below the bivalves and subsequently, these tunnels are backfilled. In this study a live adult *Lucinoma galathea* was found in one of the core samples (#232, Kaka) with a

tunnel system below it, which can be seen vaguely in the X-ray image (Figure 43). The presence of these 'probing' traces indicates low-oxygen environmental conditions (Seilacher 2007).

4.2.8 *Classification of Ichnofacies*

Based on the Seilacher's classification of ichnofacies, two ichnofacies were recognised in this study, comprising *Skolithos* and *Cruziana*. The trace assemblages identified in this study were representative of one or more of these ichnofacies, which reflected the variability of the environmental conditions of the seep sites. Each ichnofacies is briefly described herein in terms of the relationship between ethology and environmental conditions.

4.2.9 *Skolithos Ichnofacies*

The *Skolithos* ichnofacies typically develops in well-sorted sediments subjected to moderately high wave action or current energy in a wide range of depositional environments. These are characterised by low diversity suites of burrow structures, with predominantly dwelling traces and minor crawling traces (MacEachern et al. 2007 Pemberton, 2001 #14). Moreover, the sediments of *Skolithos* ichnofacies vary from sparsely to intensely bioturbated and well-sorted sand, to slightly muddy (Savrda 2007). In addition, the degree of bioturbation depends on favourable conditions for colonisation as well as food availability. The *Skolithos* ichnofacies is characterised by primarily deep burrowing suspension feeders or passive carnivores (Pemberton et al. 1992). Three ichnogenera from this study are commonly associated with the *Skolithos* ichnofacies: *Skolithos, Bergaueria* and *Palaeophycus.*

4.2.10 *Cruziana Ichnofacies*

The *Cruziana* ichnofacies is developed in moderately to intensely bioturbated, well-sorted silts and sands, or poorly sorted muds with shell layers, subjected to moderate energy levels in nearshore or low energy levels in deeper and quieter water of continental shelves (MacEachern et al. 2007). In addition, the *Cruziana* ichnofacies is characterised by a mixture of ethologies comprising dwelling, feeding and grazing traces, and these are generally linked with relatively high organic carbon content. Horizontal burrows are common while vertical or inclined burrows are minor constituents of the *Cruziana* ichnofacies. The feeding guilds of benthic invertebrates that create these structures are deposit feeders, suspension feeders, mobile carnivores and scavengers. The ichnogenera *Skolithos* and *Planolites* are some of the ichnogenera that are commonly associated with *Cruziana* ichnofacies, and in this study, these two ichnogenera appear to have a strong association. The other two ichnogenera identified in this study included *Spongeliomorpha* and *Solemyatuba* that may also be associated with both the *Skolithos* and *Cruziana* ichnofacies. There appears to be no information on designating a 'probing' trace to any ichnofacies, perhaps because of poor preservation in unconsolidated sediments.

4.2.11 *Neoichnology of cold seeps*

In this study, there was evidence of an overall trend in the type of ethologies developed in relation to the sediment characteristics. The Habitat 1 group had dominant crawling-feeding traces and minor dwelling traces. The Habitat 3 group had dominant dwelling traces with minor crawling-feeding traces. The Habitat 2 group was between the two end-members. Overall, the seep habitats exhibited suites of traces that encompassed two aforementioned ichnofacies, *Skolithos* and *Cruziana*. However, overall abundance and diversity of the traces was low compared with other deep-sea sediments studied

152

elsewhere (western equatorial Pacific, Ekdale and Berger 1978; e.g. eastern equatorial Pacific, Berger et al. 1979). Based on studies of the deep-sea lebenspurren in the Venezuela Basin, Caribbean Sea (Young et al. 1985), the trace types are correlated with the organic matter content. Low organic matter input promotes high mobile deposit feeding activity, while high organic matter input promotes high sedentary deposit feeding activity. In that study, pelagic sediments containing low organic carbon content had a high density of mobile deposit feeding activity, while turbidites with high organic carbon content had a high density of sedentary deposit feeding activity. Hemipelagic sediments were in between these two end-members.   In the Hikurangi Margin study, the habitat 3 group with sediments of high organic carbon content also had strong ichnofabrics of the *Skolithos* facies, near the sediment surface. In contrast, the Habitat 1 and 2 groups contained low to medium organic carbon content and had a mixture of ethologicies, which is analagous to that of the Venezuela Basin for hemipelagic sediments. In this sense, these results are consistent with Young's (1985) concept of organic matter content in relation to functional feeding traces.

Concerning the degree of bioturbation and the number of ethological tiers within the sediment columns, there were variations of these two parameters among sites studied. Overall, the degree of bioturbation was low, which corresponded with low abundance of traces. Wetzel (1991) proposed that TOC correlates with degree of bioturbation within sediments, providing that the depositional rate and oxygen are not limiting factors. Moreover, the extension of bioturbated horizons, the penetration depth of burrows and the number of distinct ethological tiers within the sediment columns are controlled by food availability, oxygen level, sedimentation rate, grain size and substrate consistency and all these are interrelated (Wetzel 1991). A tier is defined as "a distinct depth interval containing co-occurring traces which intersect each other" (Wetzel 1991).

153

The Habitat 3 groups, which have homogeneous silty sediments with high TOC have

one tier comprising *Skolithos* facies, except for Site 305, which had two types of traces

comprising *Skolithos* near the sediment surface and *Planolites* at ≥ 5 cm below sea

floor. Changes in ethologies may reflect the difference in the type of benthic organisms

inhabiting the site in response to change in the conditions at the time of depositional

environments. For the Hikurangi Margin, the sedimentation rate is approximately

29 cm per a thousand year. At that rate, it would take at least 170 years to lay a deposit

of 5 cm thick. Habitats 1 and 2 had coarser-grained sediments with low TOC and

mixtures of ethological patterns but there were no distinctive tiers due to lack of

apparent cross-cutting relationship between traces in these sediment profiles. Moreover,

poor preservation of traces were due to sediment disturbance by the interaction between

benthic invertebrates and sediment characters, which differs from non-seep reference

sites. Habitat 3 had predominant *Skolithos*, which signifies a high sedimentation rate. In

contrast, the sedimentation rate for Habitats 1 and 2 may be lower than that of Habitat 3

because of their relative proximity to land. Overall, the abundance and distribution of

traces for Habitats 1 and 2 were low compared with other studies on deep-sea

lebenspurren (e.g. Young et al. 1985; Aller and Aller 1986), which indicates seep

sediments may be inhospitable for most benthic invertebrates, especially for those that

are intolerant of sulphidic conditions.

4.3   Benthic invertebrate assemblages

Some of the benthic invertebrates that inhabit seep environments are known to host

bacterial endosymbionts in their tissues, and these are endemic to cold seep habitats;

while other non symbiont-containing species are opportunists that are known to colonise

these habitats but are not strictly endemic to them (Sibuet and Olu 1998). In this study,

symbiont-containing species include all bivalves (*Acharax, Calyptogena and*

Lucinoma) and siboglinids. Non-symbiont species include most gastropods, brittle-stars, sea anemones and polychaetes. These bivalves were common in both Habitats 1 and 2 but rare in Habitat 3, which is indicative of their requirements for sulphide/methane supply to support their bacterial endosymbionts, which in turn supply nutrients to the hosts. The gastropods, including *Nassarius, Falsinulatia* and *Friginatica* are predators/scavengers; while *Provanna*, which are assumed endemic to seep environments, are grazers. The predatory/scavenging gastropods were present in habitats 1 and 3 while *Provanna* were restricted to Habitat 1. Polychaetes were present in all habitats, which indicated that food availability is not a limiting factor. However, there were no live benthic invertebrates found in the sampled reference sites, 262 of Kaka and 305 of Wairarapa. The biology of selected benthic invertebrates is examined in the following section.

4.4 Biology of the selected seep benthic invertebrates

4.4.1 *Lucinoma galathea*

Lucinoma sp. are known to be associated with both palaeoseeps (e.g. North East Pacfic, Campbell 1992; and others, see Campbell and Bottjer 1995 and references herein) and modern seeps (e.g. Gulf of Mexico; Carney 1994) worldwide. In New Zealand, a fossilised *Lucinoma galathea* of Pliocene age was first discovered embedded in fine-grained sandstone of Shakespeare Cliff in Wanganui in 1924, and the first living species was retrieved from Milford Sound at 268 m bsl by dredging during the Galathea expedition to New Zealand waters in 1951-2 (Marwick 1953). In addition, fossilised *Lucinoma* was found in the volcaniclastic sandstone of Lower Miocene (~ 17 Ma) exposed in the cliffs between Muriwai and Tirikohua Point on the west coast of North Island, which was uplifted from bathyal depth (Hayward 1976). Furthermore, in the present day, *Lucinoma galathea* is widely distributed in New Zealand deep waters,

155

including include the Chatham Rise, Chatham Islands and off eastern Otago (Powell 1979). There appears to be no data on *L. galathea* obtained from modern seeps around New Zealand in any of the published literature. However, in this study, a living *L. galathea* was collected from the Kaka site at 13 cm bsf in poorly sorted sandy silt with no carbonates at 1172 m bsf. Moreover, a death assemblage of articulated *L. galathea* with disarticulated shells of *Calyptogena* sp. was associated with bands of carbonates at LM9 site. These findings are probably the first evidence of *Lucinoma* associated with seeps in the New Zealand region.

L. galathea has a special feeding strategy that involves exploiting dissolved sulphide from the surrounding sediments using an extensible chemosensory foot. First, it uses its foot to construct a mucus-lined, semi-permeable inhalant tube to the sediment surface for oxygenation (Dando et al. 1994). Then, it probes sediments beneath it for dissolved sulphide using its chemosensory foot, where dissolved sulphide is taken up and transported to symbiotic sulphur-oxidising bacteria housed in its gills (Dando et al. 1994; Dufour and Felbeck 2003; Seilacher 2007). The foot of *Lucinoma* sp. can extend five times the shell length (Dufour and Felbeck 2003). Moreover, *Lucinoma* sp. are deep burrowers (15-20 cm) and they are able to penetrate beneath their shells into the sediment column to extract dissolved sulphide (Dando et al. 1986). In this study, two empty articulated *L. galathea* in life position were found next to a large cavity within the sediment column at ~22 cm bsf (Site #51, LM9). At this depth, the sediment was very poorly sorted sandy silt with low TOC and some dispersed carbonate nodules. The cavity in the box core sample was probably created by the impact of the gear on the seafloor. The empty shells next to that cavity cannot be explained other than perhaps by coincidence. *Lucinoma,* like *Acharax* (Sahling et al. 2002), prefer sediments with a low level of sulphide concentrations and may be colonisers of seep habitats during early

seepage, to become subsequently enveloped by the precipitation of carbonates. Their demise may be due to either a shortage of dissolved sulphide or their pathway being blocked by formation of carbonate concretions.

4.4.2 *Acharax clarificata*

In this study, live *Acharax* were observed in two types of habitats: Habitat 1 (sandy silt containing extensive carbonate nodules and shell debris of *Calyptogena* shells) and Habitat 2 (sandy silt underlain by shell hash comprising corroded shell fragments). The existence of only scattered carbonate nodules and shell debris at LM9 indicated that methane seepage must be either waning or no longer active, and this may contribute to a low concentration of sulphide in these sediments. These findings are consistent with other sites elsewhere in the world. *Acharax* species are known to be associated with chemosynthesis-based communities in low sulphidic sediments, and they can be found on the edge of vesicomyid clam fields close to the hydrate deposits (Sahling et al. 2002), in the vicinity of hydrothermal vents (Lau Basin near the Fiji Islands; Beninger and Le Pennec 1997), in cold seeps (e.g. Peruvian continental margin; Olu et al. 1996), and in the deep-water (Dell 1995). In addition, *Acharax* species also have been observed in the palaeoseeps with *Calyptogena* and *Lucinoma* species (e.g. Quinault Formation, Washington; Campbell et al. 2006). In this study the New Zealand species *Acharax clarificata* may be one of the representatives of the southwest Pacific Ocean cold seep communities.

4.4.3 *Calyptogena*

There was no life assemblages of *Calyptogena* found in any of the sites sampled. However, one live *Calyptogena* was found in box core sample #51 (LM9) through sieving and sorting on board RV SONNE SO191 leg 2 that was probably a wanderer in

search of sulphide. Since *Calyptogena* are known to be quite mobile and have chemosensory abilities, they are able to travel some distance in search of sulphide. There was evidence of past life assemblages of *Calyptogena* in all box core samples assigned to the Habitat 1 group. Some articulated and disarticulated *Calyptogena* shells were found entombed within bands of carbonate nodules, which indicated their entrapment by carbonate cementation leading to their death by suffocation and/or starvation. Alternatively, the carbonate could have cemented shell pavements after the bivalves died. In one of the core samples, especially for Site 173 (Bear's Paw), shell fragments of *Calyptogena* were found deep within the sediment column overlain with sandy silt without carbonate nodules. This indicates that the methane seepage had been active in the past but is presently waning or dormant. *Calyptogena* tends to be the main species that characterise many modern cold seep communities worldwide (e.g. North American continental margin) (Levin and Michener 2002; Sahling et al. 2002). Their presence, whether live or dead, provide some indications of different stages of seep developments (Olu et al. 1997).

4.4.4 *Provanna*

Provanna sp. are small gastropods that graze on organic matter (Waren and Ponder 1991) and filamentous sulfide-oxisiding bacteria (Levin and Michener 2002). In addition, *Alviniconcha ifrerneria* of the family Provannidae are large provannids that host sulfur-oxidising and methane-oxidising symbionts in their gills (Dubilier et al. 2008). Provannids depend on sulfide production and are sulfide tolerant (Cordes et al. 2005) and are endemic to hydrothermal vents (Waren and Ponder 1991) and seeps (Lewis and Marshall 1996; Cordes et al. 2009). All small, empty *Provanna* shells collected in this study (LM9: Sites 51, 66 and 96), were found among shell hash and bands of carbonate nodules, which indicates the level of sulphide in the sediments

was probably reduced. Moreover, there were holes in some of these shells resulting from bioerosion, which may be attributed to *Nassarius ephamillus.*

4.4.5   *Nassarius ephamillus*

In this study, *Nassarius ephamillus* appeared to be the most common species inhabiting all three habitats, in close association with seep bivalves and *Provanna*. In addition, all dead *Nassarius ephamillus* were found predominately in a parautochthonous position inhabiting sandy silts with or without carbonate nodules and shell debris. Some of them were buried within silty sediment near the burrow structures of *Spongeliomorpha* (Site #158A). Since they are not deep burrowers like the seep bivalves, their presence to 17 cm within the sediments may have resulted from rapid burial due to bioturbation activity by other organisms (Pillay et al. 2007) or they are fossils from an earlier time of sedimentation.

Nassarius are cosmopolitan gastropods inhabit a variety of substrates including sand, shell debris and mud in deep water, as well as in nearshore settings. They may be surface sediment grazers (Pillay et al. 2007), carnivores (Cernohorskey 1984), scavengers or deposit feeders (Southward et al. 1997) depending on the species based on morphological characters and geographical distribution. For example, *Cyclope neritea,* in the family Nassariidae, inhabits fine sands underlain by sulphidic brine seeps and have dual feeding behaviours. They ingest sediments containing bacteria and diatoms and also feed on dead animals (Southward et al. 1997). *Nassarius ephamillis* is widely distributed around New Zealand, including at bathyal depths (McKnight and Probert 1997).   Nothing is known about *Nassarius ephamillus'* feeding behaviour or their tolerance of a sulphidic environment. They are not deep burrowers like lucinids but glide horizontally through the upper layer of sediments with their siphon extended

into the water column above them (Morton 2004). They may be vagrant scavengers that use their chemosensory siphon to detect dead animals in the area. There was some evidence of holes in some of the shells collected from the box core samples, which may be attributed to *Nassarius'* feeding strategy. It is known that *Nassarius* use their radula to drill holes in shells and then use their proboscis to ingest animal flesh from inside the shells (Brown 1982). Based on these findings, it is assumed that *Nassarius ephamallis* are predators and are adapted to reduced environmental conditions which may include low oxygen and sulphidic sediments. Since *Nassarius ephamillus* is widely distributed and not restricted by geographical barriers, their dispersal abilities can be inferred by the shape of their protoconch (Gili and Martinell 1994); therefore it is assumed that they have planktonic larval development.

4.4.6 *Polychaetes*

Polychaetes are important bioturbators of marine environments and they were relatively common in all the sites studied. They are assumed to be non symbiont species that colonise organic-rich cold seeps (Sibuet and Olu 1998), and are also common in deep sea habitats and shallow water counterparts (Read 2004). Moreover, they are known to be tolerant of sulphidic sediments and obtain nutrients from microbial activities deep within sediments (Levin and Michener 2002). The polychaetes of vertical dwelling traces (e.g. *Skolithos*) include maldanids, chaetopterids, flabelligerids and siboglinids (Gingras et al. 2008). The polychaetes of dwelling-feeding traces (e.g. *Palaeophycus*) include maldanids (deposit-feeding bamboo worms), and for crawling-feeding traces (e.g. *Planolites*) include capitellids. The nephtyids are predators or detritivores that swim freely in the water column but do not produce burrow structures like other polychaetes. Instead, they inhabit burrow structures constructed by burrowing bivalves. In this study, these polychaetes were obtained through sorting and sieving of

sampled sediments. The general descriptions of the selected polychaetes from the study based on Read's (2004) diagnosis are summarised as follows. The chaetopterids are filter-feeding tube dwellers with transparent brown chitinous or white parchment-like tubes. The flabelligerids are cylindrical tapering worms with bright coloured head gills and their bodies are covered with mucus or encrusted with particles. The siboglinids are symbionts-containing species with thick chitinous tubes inhabiting sulphide-rich sediments in the deep sea, especially among hydrothermal vents, cold seeps, whale falls and shipwrecks (Schulze 2003 and references therein). In summary, polychaetes are most likely to be the main contributors of most traces studied.

4.4.7 *Epifauna of Rock Garden*

Carbonate rocks were exposed on the seafloor at the area known as the Rock Garden that lies above a subducting seamount. These rocks provide a habitat for non-seep epibenthic invertebrates including bryozoans, stylasterids, gorgonians, hydroids, sponges, holothurians and chitons. These epibenthic invertebrates were also reported inhabiting carbonate rocks in the vicinity of seep environments (Sellanes et al. 2008; Baco-Taylor et al. in press). A high diversity of colonial, sessile, filter feeding, bryozoan were also found in this location, as well as living and dead benthic foraminifera (forams) attached to the rocks or other organisms, and in rock crevices. The feeding strategies of these organisms vary, which include deposit feeding, filter or suspension feeding, and grazing. The forams feed on organic detritus (Jorissen 1999). Sponges, gorgonians and stylasterids are either filter or suspension feeders. Holothurian is a deposit feeder (Morton and Miller 1968). Deep-sea chiton graze on forams and encrusting organisms such as sponges and bryozoans (Kaas and van Belle 1987). This shows that hard substrate and food availability enable these epibenthic invertebrates to

exist in both seep and non-seep environments of the deep sea.

4.5   Ecologic interpretation

In this study, three distinctive ecological habitats were observed based on sedimentologic characteristics, ichnologic assemblages and benthic invertebrates association. These observations showed that there was great variety of environmental conditions among habitats, which affected the ecology of benthic invertebrates occupying those habitats.

4.5.1   *Habitat 1*

Habitat 1 is seep-related and has its own unique environmental conditions that set it apart from the 'normal' deep-sea habitat. The upward expulsion of fluids or gas bubbles containing methane from deeper sediments asserts control on the construction of the seep ecosystem, which makes seep-related habitats unique. It is known that upward fluid flow and its duration vary greatly between sites, locally, regionally and globally (Sahling et al. 2002; Campbell 2006). Furthermore, seepage activity associated with subduction zones tends to be more diffusive, short-lived and cyclic (Gage and Tyler 1991).

 There are two criteria that distinguish seep-related from other deep-sea habitats. These are the presence of carbonates, and the type of benthic invertebrates typically found there. In this study, it became clear that the formation of carbonates were microbially mediated by methanotrophic archaea and sulphate reducing bacteria involving the anaerobic oxidation of methane. The source of methane is most likely derived from hydrate dissociation commonly associated with subduction. The longevity of the seep ecosystem is dependent on a steady supply of methane. The death assemblages of bivalves and gastropods deep within the stratified layers and the rarity of living

162

chemosymbiotic benthic invertebrates in Habitat 1 group suggests that these sites are relict seep habitats, and that the methane seepage must be either waning or dormant. A change in environmental conditions may have altered the ichnological patterns within the stratified layers, resulting in changes in sediment characteristics. It was noted that most dwelling traces were associated with finer grained sediments containing no carbonate nodules; whereas, most crawling-feeding traces were associated with coarser grained sediments containing carbonate nodules. Small traces indicated that the sediments were probably poorly oxygenated and the sedimentation rate was low (Wetzel 1991). The apparent low number of burrow structures in these habitats may be the result of their low preservation potential in unconsolidated sediments, or their overprinting by accumulation of carbonates.

4.5.2 *Habitat 2*

Habitat 2 is most likely to be non-seep related, as examples are situated on the outskirts of seep vents. This inference was based on the absence of carbonate nodules, and the mineral content and stable isotopic signatures of the carbonates in the sediments sampled. In addition, living bivalves, *Acharax* and *Lucinoma*, were observed in these habitats, which are known to host bacterial symbionts and are not restricted to seep habitats. Furthermore, most sites assigned to Habitat 2 groups contained a layer of shell hash comprising shell fragments deep within the sediment column overlain with sandy silt. These shell fragments are relict.

4.5.3 *Habitat 3*

Habitat 3 is non-seep related, which is based on the mineral content and stable isotopic signature of carbonates in the sediments sampled. Furthermore, the sampled sites were associated with finer-grained sediments with high TOC and the dwelling traces were

dominant. Since they were in close proximity to land (~ 30 km) and in the path of two main currents converging, high depositional environment is likely, which promotes quick burial of organic matter, thus increasing the sediment TOC and food availability for benthic invertebrates. Benthic invertebrates associated with Habitat 3 were sedentary polychaetes and mobile, predatory gastropod families.

4.6 Comparison with Northern Hemisphere modern seep counterparts

The findings reveal some basic similarities between the Hikurangi Margin's cold seeps and their associated benthic invertebrates and the northern counterparts. Most taxa studied are representative of seep environments worldwide (e.g. Sibuet and Olu 1998 and references therein) and they are indicative of the presence of methane seepage and sulphidic sediments (Olu et al. 1997). In addition, some non-seep taxa studied, such as polychaetes and non-symbiotic gastropods, which are tolerant of deep-sea reducing environments, were found at these seep sites.

4.7 Limitations of the study

Concentrations of methane and sulphide are the two main factors which control the abundance and distribution of benthic invertebrates that depend on microbial primary production (Bergquist et al. 2003). In future studies, measurements of pore-water sulphate and methane concentrations, and measurement of sulphate reduction and methane oxidation rate (Arvidson et al. 2004) may assist in further our understanding of the interaction between benthic invertebrates and biogeochemistry of sediments at the seep environments. Furthermore, the dating of carbonate nodules and seep sediments using ^{234}Uranium and ^{230}Thorium determination methods (Godoy et al. 2006) may fill in the gap of knowledge on the formation of seep habitats through time.

4.8 X-ray radiography appraisal

X-ray radiography is a useful tool, which is used by both sedimentologists/geologists and ecologists for the assessment of burrow structures and bioturbation in core samples of fresh, unconsolidated sediments by benthic invertebrates (Bouma 1964; Howard 1968). Furthermore, this method revealed structures that are otherwise invisible on the surface of the cores (e.g. Figure 49) and shell orientation within the core (e.g. Figure 43). Also, it is useful for discerning the stratified layers of sediment properties such as seep sediments containing bands of carbonate nodules (e.g. Figure 13). However, there was one disadvantage with X-ray radiography that became apparent while analysing the distinguished burrow structure of *Solemyatuba*, which was visible on the surface of the core but was not detected in the X-ray image (Figure 49).

CT scanning with high resolution of the sediment cores for the three-dimensional view of burrow structures would be a better option compared with the traditional method of X-ray radiography. The advantages of using this method includes the ability to detect small burrow structures accurate, measuring of three-dimensional burrow structures, and determining the spatial distribution of burrows and organic matter in the sediments (Dufour et al. 2005; Gagnoud et al. 2009). Moreover, the core samples remain intact. This method may be a useful tool for enabling scientists to construct a three-dimensional view of seep sediment ecosystems. Furthermore, combining this method with the conventional sedimentological analysis may provide a better ecological interpretation of the seep environments.

5 CONCLUSION

Sediment core samples, invertebrate collections and carbonate rock samples obtained during the RV SONNE SO191 to the Hikurangi Margin provided some valuable insights into how cold seep ecosystems evolve in the deep-sea and provided parallels with the Northern Hemisphere modern cold seep counterparts. Amalgamation of the analytical results for the aforementioned samples revealed three distinctive ecological habitats based on sediment characteristics and benthic invertebrate associations. These habitats reflected local and/or regional variations of environmental conditions as well as relative proximity to land. The abundance and distribution of seep benthic invertebrates for the Hikurangi Margin's cold seeps was low compared with the northern counterparts. This may be in part, attributed to sampling methods. Alternatively, the localised diffuse nature of methane seepage and low supply of sulphide may be responsible for the low abundance of seep fauna observed.

Only one of these ecological habitats is recognised as seep-related, based on the stable isotopic signature of carbonates sampled from seep-related Habitat 1 group sites. The carbon source for the carbonates sampled derived from gas hydrate dissociation. It is assumed that the carbonates, formed near the sediment surface, were mediated by a consortium of methanotrophic archaea and sulphate-reducing bacteria involving in anaerobic oxidation of methane. Living and/or dead assemblages of benthic invertebrates hosting bacterial symbionts inhibiting those seep-related habitat included *Calyptogena*, *Acharax, Lucinoma* and siboglinids and their presence in those habitat are an indication of the existence of passive seeps. Thus, these findings are consistent with those of Northern Hemisphere counterparts.

Carbonate rocks exposed on the seafloor at the Rock Garden provide hard substrate for epibenthic invertebrates to colonise. Since most of these are filter feeders, they do not rely on the chemosynthesis process for food. Therefore, their presence in the deep-sea depends largely on substrate and food availability.

The composition of both symbiont-containing species and non-symbiont-containing species (e.g. polychaetes, gastropods, brittle stars and decapods) varied between three types of habitats studied, which are likely influenced by food availability and sediment characteristics (e.g. grain size diversity, TOC and carbonate contents). These three habitat groups displayed distinctive traces and ethologies: habitat 1 (seep-related setting) with dominant crawling, feeding and minor dwelling traces; habitat 3 with dominant dwelling traces with minor crawling traces; and habitat 2 with traces and ethologies lying between the two end-members reflecting local and/or regional variations of environmental conditions (e.g. grain size diversity, total organic content, carbonate content) as well as relative proximity to land. In addition, the low diversity of traces and ethologies reflected oxygen-poor environmental conditions; however oxygen was not a limiting factor for the sites studies. While the *Skolithos* and *Cruzianna* ichnofacies that characterize the deep-seafloor are well known, the recognition of the ethological patterns, ichnotaxa and ichnofacies of the cold seep settings in the deep-sea are believed to be new to science. This may be of ongoing significance to our understanding of ichnology.

The use of X-ray imagery enabled a means of peering inside the sediment core samples and locating various features, providing a picture of deep-sea benthic processes within each habitat. The pictures obtained may be useful for future studies by providing comparisons and a means of measuring changes within seep sites over time.

For future studies, pore-water chemistry analysis is recommended to assess the biogeochemistry of the seep sediments in order to establish further relationships between benthic invertebrates and seep habitats, especially for New Zealand.

REFERENCES

Abrams MA (1996) Distribution of subsurface hydrocarbon seepage in near-surface marine sediments. In: Schumacher D, Abrams MA (eds) Hydrocarbon migration and its near-surface expression. AAPG Memoir 66, pp 1-14

Aitken JJ (1996) Plate Tectonics for curious Kiwis. Institute of Geological & Nuclear Sciences information series 42: 78

Aller JY, Aller RC (1986) Evidence for localized enhancement of biological activity associated with tube and burrow structures in deep sea sediments at the HEBBLE site, western North Atlantic. Deep Sea Research 33: 755-790

Aller RC, Blair NE (2004) Early diagenetic remineralization of sedimentary organic C in the Gulf of Papua deltaic complex (Papua New Guinea): net loss of terrestrial C and diagenetic fractionation of C isotopes. Geochimica et Cosmochimica Acta 68: 1815-1825

Arvidson RS, Morse JW, Joye SB (2004) The sulfur biogeochemistry of chemosynthetic cold seep communities, gulf of Mexico, USA. Marine Chemistry 87: 97-119

Baco-Taylor A, Rowden AA, Levin LA, Smith CR, Bowden DA (in press) Initial characterization of cold seep faunal communities on the New Zealand Margin. Marine Geology

Baker PA, Burns SJ (1985) Occurrence and formation of dolomite in organic-rich continental-margin sediments. American Association of Petroleum Geologists 69: 1917-1930

Barry JP, Whaling PJ, Kochevar RK (2007) Growth, production, and mortality of the chemosynthetic vesicomyid bivalve, *Calyptogena kilmeri* from cold seeps off central California. Marine Ecology 28: 169-182

Bauer JE, Montagna PA, Spies RB, Prieto MC, Hardin D, Limno (1988) Microbial biogeochemistry and heterotrophy in sediments of a marine hydrocarbon seep. Limnology and Oceanography 33: 1493-1513

Beninger PG, Le Pennec M (1997) Reproductive characteristics of a primitive bivalve from a deep-sea reducing environment: giant gametes and their significance in Acharax alinae (Cryptodonta: Solemyidae). Marine Ecology Progress Series 157: 195-206

Bennett BA, Smith CR, Glaser B, Maybaum HL (1994) Faunal community structure of a chemoautotrophic assemblage on whale bones in the deep northeast Pacific Ocean. Marine Ecology Progress Series 108: 205-223

Berger WH (1974) Deep-sea sedimentation. In: Burk CA, Drake CL (eds) The geology of continental margins. Springer-Verlag, New York, pp 213-241

Berger WH, Ekdale AA, Bryant PP (1979) Selective preservation of burrows in deep-

sea carbonates. Marine Geology 32: 205-230

Bergquist DC, Ward T, Cordes EE, McNelis T, Howlett S, Kosoff R, Hourdez S, Carney R, Fisher CR (2003) Community structure of vestimentiferan-generated habitat islands from Gulf of Mexico cold seeps. Journal of Experimental Marine Biology and Ecology 289

Berner RA (1980) Early diagenesis: a theoretical approach. Princeton University Press, Princeton

Blott S (2000) GRADISTAT Version 4.0. A grain size distribution and statistics package for the analysis of unconsolidated sediments by sieving or laser granulometer. Surface Processes and Modern Environments Research Group, Department of Geology, Royal Holloway, University of London, Surrey

Blott S, Pye K (2001) GRADISTAT: a grain size distribution and statistics package for the analysis of unconsolidated sediments. Earth Surface Processes and Landforms 26: 1237-1248

Boetius A, Ravenschlag K, Schubert CJ, Rickert D, Widdel F, Giesecke A, Amann R, Jorgensen BB, Witte U, Pfannkuche O (2000) A marine microbial consortium apparently mediating anaerobic oxidation of methane. Nature 407: 623-626

Boetius A, Suess E (2004) Hydrate Ridge: a natural laboratory for the study of microbial life fueled by methane from near-surface gas hydrates. Chemical Geology 205: 291-310

Bohrmann G, Greinert J, Suess E, Torres M (1998) Authigenic carbonates from the Cascadia subduction zone and their relation to gas hydrate stability. Geology 26: 647-650

Bouma AH (1964) Notes on X-ray interpretation of marine sediments. Marine Geology 2: 278-309

Bromley RG (1996) Trace fossils: biology, taphonomy and applications. Chapman & Hall, London

Brown AC (1982) The biology of sandy-beach whelks of the Genus Bullia (Nassariidae). In: Barnes M, Bonnett R, Barnes H (eds) Oceanography and Marine Biology: An annual review. Aberdeen University Press, UK, pp 309-361

Bruun AF (1956) Animal life of the deep sea bottom. In: Bruun AF, Greve SV, Mielche H, Sparck R (eds) The Galathea Deep Sea Expedition. George Allen & Urwin Ltd, London, pp 149-195

Burd AB, Jackson GA (2009) Particle Aggregation. Annual Review of Marine Science 1: 65-90

Burton EA (1993) Controls on marine carbonate cement mineralogy: review and reassessment. Chemical Geology 105: 163-179

Butman CA, Carlton JT, Palumbi SR (1995) Whaling effects on deep-sea biodiversity. Conservation Biology 9: 462-464

Callender WR, Powell EN, Staff G, Davies DJ (1992) Distinguishing autochthony, parautochthony and allochthony using taphofacies analysis: can cold seep assemblages be discriminated from assemblages of the nearshore and continental shelf? Palaios 7: 409-421

Campbell KA (1992) Recognition of a Mio-Pliocene cold seep setting from the Northeast Pacific Convergent Margin, Washington, U.S.A. Palaios 7: 422-433

Campbell KA (2006) Hydrocarbon seep and hydrothermal vent paleoenvironments and paleontology: past developments and future research directions. Palaeogeography, Palaeoclimatology, Palaeoecology 232: 362-407

Campbell KA, Bottjer DJ (1995) Brachiopods and chemosymbiotic bivalves in Phanerozoic hydrothermal vent and cold seep environments. Geology 23: 321-324

Campbell KA, Francis DA, Collins M, Gregory MR, Nelson CS, Greinert J, Aharon P (2008) Hydrocarbon seep-carbonates of a Miocene forearc (East Coast Basin), North Island, New Zealand. Sedimentary Geology 204: 83-105

Campbell KA, Nelson CS, Alfaro AC, Boyd S, Greinert J, Nyman SL, Grosjean E, Logan GA, Gregory MR, Cooke S, Linke P, Milloy S, Wallis I (in press) Geological imprint of methane seepage on the seabed and biota of the convergent Hikurangi Margin, New Zealand: survey of core and grab carbonates. Marine Geology

Campbell KA, Nesbitt EA, Bourgeois J (2006) Signatures of storms, oceanic floods and forearc tectonism in marine shelf strata of the Quinault Formation (Pliocene), Washington, USA. Sedimentology 53: 945-969

Canfield DE (1994) Factors influencing organic carbon preservation in marine sediments. Chemical Geology 114: 315-329

Carney RS (1994) Consideration of the oasis analogy for chemosynthetic communities at Gulf of Mexico hydrocarbon vents. Geo-Marine Letters 14: 149-159

Carter L (1975) Sedimentation on the continental terrace around New Zealand: a review. Marine Geology 19: 209-237

Carter L, Manighetti B, Elliot M, Trustrum N, Gomez B (2002) Source, sea level and circulation effects on the sediment flux to the deep ocean over the past 15 ka off eastern New Zealand. Global and Planetary Change 33: 339-355

Cernohorskey WO (1984) Systematics of the family Nassariidae (Mollusca: Gastropoda). Bulletin of the Auckland Institute and Museum 14: 21

Chiswell SM (2000) The Wairarapa Coastal Current. New Zealand Journal of Marine and Freshwater Research 34: 303-315

Cordes EE, Bergquist DC, Fisher CR (2009) Macro-ecology of Gulf of Mexico cold seeps. The Annual Review of Marine Science 1: 143-168

Cordes EE, Hourdez S, Predmore BL, Redding ML, Fisher CR (2005) Succession of hydrocarbon seep communities associated with the long-lived foundation species *Lamellibrachia luymesi*. Marine Ecology Progress Series 305: 17-29

Corliss JB, Dymond J, Gordon LI, Edmond JM, von Herzen RP, Ballard RD, Green K, Williams D, Bainbridge A, Crane K, van Andel TH (1979) Thermal springs on the Galapagos Rift. Science 203: 1073-1083

D'Alessandro A, Bromley RG (1995) A new ichnospecies of Spongeliomorpha from the Pleistocene of Sicily. Journal of Paleontology 69: 393-398

Dando PR, Ridgway SA, Spiro B (1994) Sulphide 'mining' by lucinid bivalve molluscs: demonstrated by stable sulphur isotope measurements and experimental models. Marine Ecology Progress Series 107

Dando PR, Southward AJ, Southward EC (1986) Chemoautotrophic symbionts in the gills of the bivalve mollucs *Lucinoma borealis* and the sediment chemistry of its habitat. Proceedings of the Royal Society of London. Series B, Biological Sciences 227: 227-247

Davies DJ, Powell EN, Stanton jr RJ (1989) Taphonomic signature as a function of environmental process: shells and shell beds in a hurricane-influenced inlet on the Texas Coast. Palaeogeography, Palaeoclimatology, Palaeoecology 72: 317-356

Dell RK (1995) New species and records of deep-water Mollusca from off New Zealand. Tuhinga: Records of the Museum of New Zealand Te Papa Tongarewa 2: 1-26

Desbruyeres D, Alayse-Danet A, Ohta S (1994) Deep-sea hydrothermal communities in Southwestern Pacific back-arc basins (the North Fiji and Lau Basins): composition, microdistribution and food web. Marine Geology 116: 227-242

Desbruyeres D, Biscoito M, Caprais JC, Colaco A, Comtet T, Crassous P, Fouquet Y, Khripounoff A, Le Bris N, Olu K, Riso R, Sarradin PM, Segonzac M, Vangriesheim A (2001) Variations in deep-sea hydrothermal vent communities on the Mid-Atlantic Ridge near the Azores plateau. Deep Sea Research I 48: 1325-1346

Dubilier N, Bergin C, Lott C (2008) Symbiotic diversity in marine animals: the art of harnessing chemosynthesis. Nature Reviews Microbiology 6: 725-740

Dufour SC, Desrosiers G, Long B, Lajeunesse P, Gagnoud M, Labrie J, Archambault P, Stora G (2005) A new method for three-dimensional visualization and quantification of biogenic structures in aquatic sediments using axial tomodensitometry. Limnology and Oceanography: Methods 3: 372-380

Dufour SC, Felbeck H (2003) Sulphide mining by the superextensile foot of symbiotic

thyasirid bivalves. Nature 426: 65-67

Duperron S, Halary S, Lorlon J, Sibuet M, Gaill F (2008) Unexpected co-occurrence of six bacterial symbionts in the gills of the cold seep mussel *Idas* sp. (Bivalvia: Mytilidae). Environmental Microbiology 10: 433-445

Duperron S, Nadalig T, Caprais JD, Sibuet M, Fiala-Medioni A, Amann R, Dubilier N (2005) Dual symbiosis in a *Bathymodiolus* sp. mussel from a methane seep on the Gabon Continental Margin (Southeast Atlantic): 16S rRNA phylogeny and distribution of the symbionts in gills. Applied and Environmental Microbiology

Dworschak PC, Cunha MR (2007) A new subfamily, Vulcanocalliacinae n.subfam., for Vulcanocalliax arutyunovi n.g., n.sp. from a mud volcano in the Gulf of Cadiz (Crustacea, Decapoda, Callianassidae). Zootaxa 1460: 35-46

Edmonds SJ (2000) Phylum Sipuncula. In: Beesley PL, Ross GJB, Glasby CJ (eds) Polychaetes & Allies: The Southern Synthesis. Fauna of Australia. CSIRO Publishing, Melbourne, pp 375-400

Ekdale AA (1988) Pitfalls of paleobathymetric interpretations based on trace fossil assemblages. Palaios 3: 464-472

Ekdale AA, Berger WH (1978) Deep-sea ichnofacies: modern organism traces on and in pelagic carbonates of the western equatorial Pacific. Palaeogeography, Palaeoclimatology, Palaeoecology 23: 263-278

Faure K, Greinert J, Pecher IA, Graham IJ, Massoth GJ, De Ronde CEJ, Wright IC, Baker ET, Olson EJ (2006) Methane seepage and its relation to slumping and gas hydrate at the Hikurangi margin, New Zealand. New Zealand Journal of Geology and Geophysics 49: 503-516

Faure K, Greinert J, von Deimling JS, McGinnis DF, Kipfer R, Linke P (in press) Methane seepage along the Hikurangi Margin of New Zealand: geochemical and physical evidence from the water column, sea surface and atmosphere. Marine Geology

Faure K, McGinnis DF, Schneider von Deimling J, Greinert J (2008) Submarine flatulence along the Hikurangi Margin of New Zealand: linking geochemical methane anomalies in the water column with hydroacoustic evidence of bubble transport European Geosciences Union General Assembly 2008, Vienna, Austria

Fiala-Medioni A, Boulegue J, Ohta S, Felbeck H, Mariotti T (1993) Source of energy sustaining the *Calyptogena* populations from deep trenches in subduction zones off Japan. Deep Sea Research I 40: 1241-1258

Folk RL (1954) The distinction between grain size and mineral composition in sedimentary-rock nomenclature. Journal of Geology 62: 344-359

Folk RL (1957) Brazos River bar: a study in the significance of grain size parameters. Journal of Sedimentary Petrology 27: 3-26

Frey RW (1968) The Lebensspuren of some common marine invertebrates near

Beaufort, North Carolina. I. Pelecypod burrows. Journal of Paleontology 42: 570-574

Froelich PN, Klinkhammer GP, Bender ML, Luedtke NA, Heath GR, Cullen D, Dauphin P (1979) Early oxidation of organic matter in pelagic sediments of the eastern equatorial Atlantic: suboxic diagenesis. Geochimica et Cosmochimica Acta 43: 1075-1090

Futterer D (2006) The solid phase of marine sediments. In: Schulz HD, Zabel M (eds) Marine geochemistry. Springer, Berlin, pp 1-25

Gage JD, Tyler P (1991) Deep-sea biology: a natural history of organisms at the deep-sea floor. Cambridge University Press, Cambridge

Gagnoud M, Lajeunesse P, Desrosiers G, Long B, Dufour S, Labrie J, Mermillod-Blondin F, Stora G (2009) Litho- and biofacies analysis of postglacial marine mud using CT-Scanning. Engineering Geology 103: 106-111

Gaillard C (1991) Recent organism traces and ichnofacies on the deep-sea floor off New Caledonia, Southwestern Pacific. PALAIOS 6: 302-315

Gibert JM, Robles JM (2005) Firmground ichnofacies recording high-frequency marine flooding events (Langhian transgression, Valles-Penedes Basin, Spain). Geologica Acta 3: 295-305

Gieskes J, Mahn C, Day S, Martin JB, Greinert J, Rathburn T, McAdoo B (2005) A study of the chemistry of pore fluids and authigenic carbonates in methane seep environments: Kodiak Trench, Hydrate Ridge, Monterey Bay, and Eel Basin. Chemical Geology 220: 329-345

Gili C, Martinell J (1994) Relationship between species longevity and larval ecology in nassariid gastropods. Lethaia 27: 291-299

Gingras MK, Dashtgard SE, MacEachern JA, Pemberton SG (2008) Biology of shallow marine ichnology: a modern perspective. Aquatic Biology 2: 255-268

Godoy MLDP, Godoy JM, Kowsmann R, dos Santos GM, da Cruz RP (2006) [234]U and [230]Th determination by FIA-ICP-MS and application to uranium-series disequilibrium in marine samples. Journal of Environmental Radioactivity 88: 109-117

Goldring R, Cadee GC, Pollard JE (2007) Climatic control of marine trace fossil distribution. In: Miller WI (ed) Trace fossils concepts, problems, prospects. Elsevier, Amsterdam, pp 159-195

Greinert J, Bialas J (2008) An overview of latest cold seep research around New Zealand (2006 and 2007) European Geosciences Union General Assembly 2008, Vienna, Austria

Greinert J, Bohrmann G, Suess E (2001) Gas hydrate-associated carbonates and methane-venting at Hydrate Ridge: classification, distribution, and origin of authigenic lithologies. In: Paul CK, Dillon WP (eds) Natural gas hydrates:

occurrence, distribution, and detection. The American Geophysical Union, Washington, pp 99-113

Haeckel M, Sommer S, Linke P (2008) Porewater geochemistry and methane fluxes of cold seeps at the Hikurangi Margin, offshore New Zealand European Geosciences Union General Assembly 2008, Vienna, Austria

Hashimoto J, Ohta S, Gamo T, Chiba H, Yamaguchi T, Tsuchida S, Okudaira T, Watabe H, Yamanaka T, Kitazawa M (2001) First hydrothermal vent communities from the Indian Ocean discovered. Zoological Science 18: 717-721

Hayward BW (1976) Lower Miocene bathyal and submarine canyon ichnocoenoses from Northland, New Zealand. Lethaia 9: 149-162

Henrys SA, Ellis S, Uruski C (2003) Conductive heat flow variations from bottom-simulating reflectors on the Hikurangi Margin, New Zealand. Geophysical Research Letters 30

Hensen C, Zabel M, Schulz HD (2006) Benthic cycling of oxygen, nitrogen and phosphorus. In: Schulz HD, Zabel M (eds) Marine geochemistry. Springer-Verlag, Berlin, pp 207-240

Hessler RR, Kaharl VA (1995) The deep-sea hydrothermal vent community: an overview Seafloor Hydrothermal Systems: Physical, Chemical, Biological, and Geological Interactions. Geophysical Monograph 91. The American Geophysical Union, pp 73-82

Howard JD (1968) X-ray radiography for examination of burrowing in sediments by marine invertebrate organisms. Sedimentology 11: 249-258

Hyland J, Baptiste E, Campbell J, Kennedy J, Kropp R, Williams S (1991) Macroinfaunal communities of the Sanda Maria Basin on the California outer continental shelf and slope. Marine Ecology Progress Series 78: 147-161

Imhoff JE, Sahling H, Suling J, Kath T (2003) 16S rDNA-based phylogeny of sulphur-oxidising bacterial endosymbionts in marine bivalves from cold-seep habitats. Marine Ecology Progress Series 249: 39-51

Iversen N, Jorgensen BB (1985) Anaerobic methane oxidation rates at the sulfate-methane transition in marine sediments from Kattegat and Skagerrak (Denmark). Limnology and Oceanography 30: 944-955

Jones AT, Greinert J, Bowden DA, Klaucke I, Peterson J, Netzeband G, Weinrebe W (in press) Acoustic and visual characterization of methane-rich seabed seeps at Omakere Ridge on the Hikurangi Margin, New Zealand. Marine Geology

Jones AT, Greinert J, Klaucke I, Petersen J, Netzebund G, Weinrebe W (2008) Integrated side-scan, sub-bottom profiler and seismic signatures of methane seepage from Omakere Ridge on New Zealand's Hikurangi Margin European Geosciences Union General Assembly 2008, Vienna, Austria

Jorissen FJ (1999) Benthic foraminiferal microhabitats below the sediment-water

interface. In: Sen Gupta BK (ed) Modern Foraminifera. Kluwer Academic Publishers, Dordrecht, pp 161-179

Judd A, Hovland M (2007) Seabed fluid flow. The impact on geology, biology, and the marine environment. Cambridge University Press, Cambridge

Julian D, Gaill F, Wood E, Arp AJ, Fisher CR (1999) Roots as a site of hydrogen sulfide uptake in the hydrocarbon seep vestimentifran *Lamellibrachia* sp. The Journal of Experimental Biology 202: 2245-2257

Kaas P, van Belle RA (1987) Monograph of living chitons (Mollusca: Polyplacophora): suborder Ischnochitonina - Ischnochitonidae - Schizoplacinae, Callochitoninae and Lepidochitoninae. Brill Academic Publishers, London

Keil RG, Montlucon DB, Prahl FG, Hedges JI (1994) Sorptive preservation of labile organic matter in marine sediments. Nature 370: 549-552

Klaucke I, Weinrebe W, Petersen CJ, Bowden DA (in press) Temporal variability of gas seeps offshore New Zealand: multi-frequency geoacoustic imaging of the Wairarapa area, Hikurangi Margin. Marine Geology

Klaucke I, Weinrebe W, Petersen J, Greinert J, Jones AT (2008) Temporal variability of gas seeps offshore New Zealand: multi-frequency geoacoustic imaging of the Wairarapa area, Hikurangi Margin European Geosciences Union General Assembly 2008, Vienna, Austria

Kvenvolden KA, Lorenson TD (2001) The global occurrence of natural gas hydrate. In: Paul CK, Dillon WP (eds) Natural gas hydrates: occurrence, distribution, and detection. The American Geophysical Union, Washington, pp 3-18

Leeder MR (1982) Sedimentology. George Allen & Unwin, London

Levesque C, Juniper SK, Limen H (2006) Spatial organization of food webs along habitat gradients at deep-sea hydrothermal vents on Axial Volcano, Northeast Pacific. Deep-Sea Research II 53: 726-739

Levin LA (2005) Ecology of cold seep sediments: interactions of fauna with flow, chemistry and microbes. Oceanography and Marine Biology: an Annual Review 43: 1-46

Levin LA, Huggett CL, Wishner KF (1991) Control of deep-sea benthic community structure by oxygen and organic-matter gradients in the eastern Pacific Ocean. Journal of Marine Research 49: 763-800

Levin LA, Michener RH (2002) Isotopic evidence for chemosynthesis-based nutrition of macrobenthos: the lightness of being at Pacific methane seeps. Limnology and Oceanography 47: 1336-1345

Lewis KB, Marshall BA (1996) Seep faunas and other indicators of methane-rich dewatering on New Zealand convergent margins. New Zealand Journal of Geology and Geophysics 39: 181-200

Li L, Kato C, Horikoshi K (1999) Microbial Diversity in Sediments Collected from the Deepest Cold-Seep Area, the Japan Trench Marine Biotechnology 1: 391-400

Liebetrau V, Eisenhauer A, Linke P (2008) Cold seep carbonates and cold water corals from the Hikurangi Margin, offshore New Zealand (Cruise SO191): growth structures, fluid pathways and first isotope geochemical results European Geosciences Union General Assembly 2008, Vienna, Austria

Luff R, Wallmann K, Aloisi G (2004) Numerical modeling of carbonate crust formation at cold vent sites: significance for fluid and methane budgets and chemosynthetic biological communities. Earth and Planetary Science Letters 221: 337-353

MacEachern JA, Pemberton SG, Gingras MK, Bann KL (2007) The ichnofacies paradigm: a fifty-year retrospective. In: Miller M (ed) Trace fossils concepts, problems, prospects

Martin RA, Nesbitt EA, Campbell KA (2009) The effects of anaerobic methane oxidation on benthic foraminiferal assemblages and stable isotopes on the Hikurangi Margin of eastern New Zealand. Marine Geology

Marwick J (1953) A Pliocene fossil found living by the Galathea Expedition. New Zealand Journal of Science and Technology, Section B 35: 109-112

McGinnis DF, Faure K, von Deimling JS, Greinert J (2008) Physical properties of methane-enriched plumes along the Hikurangi margin of New Zealand: thoughts on sources and life spans of water column methane anomalies European Geosciences Union General Assembly 2008, Vienna, Austria

McKnight DG (1969) Infaunal benthic communities of the New Zealand continental shelf. New Zealand Journal of Marine and Freshwater Research 3: 409-444

McKnight DG, Probert PK (1997) Epibenthic communities on the Chatham Rise, New Zealand. New Zealand Journal of Marine and Freshwater Research 31: 505-513

Miura T, Nedachi M, Hashimoto J (2002) Sulphur sources for chemoautotrophic nutrition of shallow water vestimentiferan tubeworms in Kagoshima Bay. Journal of Marine Biology 82: 537-540

Moran JJ, Beal EJ, Vrentas JM, Orphan VJ, Freeman KH, House CH (2008) Methyl sulfides as intermediates in the anaerobic oxidation of methane. Environmental Microbiology 10: 162-173

Morse JW (2005) Formation and diagenesis of carbonate sediments. In: Mackenzie FT (ed) Sedimentary, diagenesis and sedimentary rocks. Elsevier, Amsterdam, pp 67-86

Morton J (2004) Seashore Ecology of New Zealand and the Pacific. David Bateman Ltd, Auckland

Morton J, Miller M (1968) The New Zealand sea shore. Collins, London

Muralidhar K, Mazumdar A, Karisiddaiah SM, Borole DV, Ramalingeswara Rao B (2006) Evidences of methane-derived authigenic carbonates from the sediments of the Krishna-Godavari Basin, eastern continental margin of India. Current Science 91: 318-323

Murray J, Renard AF (1891) Report on deep-sea deposits based on the specimens collected during the voyage of H.M.S. Challenger during the years 1872 to 1876. Johnson Reprint Corporation, New York

Murray J, Thomson CW (1895) Report on the Scientific Results of the Voyage of H.M.S. Challenger During the Years 1873-76 under the Command of Captain George S. Nares and the Late Captain Frank Tourle Thomson: A summary of the scientific results. Printed for H. M. Stationery Office, London

Naehr TH, Eichhubl P, Orphan VJ, Hovland M, Paul CK, Ussler III W, Lorenson TD, Greene HG (2007) Authigenic carbonate formation at hydrocarbon seeps in continental margin sediments: a comparative study. Deep Sea Research II 54: 1268-1291

Naudts L, Greinert J, Poort J, Belza J, Vangampelaere E, Boone D, Linke P, Henriet JP, De Batist M (2008) Submeter mapping of methane seeps by ROV observations and measurements at the Hikurangi Margin, New Zealand European Geosciences Union General Assembly 2008

Niemann H, Treude T, Wegener G, Santillano D, Anrnds J, Boetius A, Pfannkuche O, Linke P (2008) Microbial methane consumption at cold seeps of the Hikurangi Margin (South-West Pacific, New Zealand) European Geosciences Union General Assembly 2008, Vienna, Austria

Olu-Le Roy K, Caprais JC, Fifis A, Fabri MC, Galeron J, Budzinsky H, Le Menach K, Khripounoff A, Ondreas H, Sibuet M (2007) Cold-seep assemblages on a giant pockmark off West Africa: spatial patterns and environmental control. Marine Ecology 28: 115-130

Olu K, Duperret A, Sibuet M, Foucher J-P, Fiala-Medioni A (1996) Structure and distribution of cold seep communities along the Peruvian active margin: relationship to geological and fluid patterns. Marine Ecology Progress Series 132: 109-125

Olu K, Lance S, Sibuet M, Henry P, Fiala-Medioni A, Dinet A (1997) Cold seep communities as indicators of fluid expulsion patterns through mud volcanoes seaward of the Barbados accretionary prism. Deep-sea Research I 44: 811-841

Orphan VJ, Ussler III W, Naehr TH, House CH, Hinrichs K-U, Paull CK (2004) Geological, geochemical, and microbiological heterogeneity of the seafloor around methane vents in the Eel River Basin, offshore California. Chemical Geology 205: 265-289

Paull CK, Hecker B, Commeau R, Freeman-Lynde RP, Newumann C, Corso WP, Golubic S, Hook JE, Sikes E, Curray J (1984) Biological Communities at the

Florida Escarpment Resemble Hydrothermal Vent Taxa Science 226: 965-967

Pecher IA, Henrys SA, Chiswell SM, Kukowski N (2005) Erosion of the seafloor at the top of the gas hydrate stability zone on the Hikurangi Margin, New Zealand. Geophysical Research Letters 32

Pemberton SG, Frey RW, Ranger MJ, MacEachern J (1992) The conceptual framework of ichnology. In: Pemberton SG (ed) Applications of ichnology to petroleum exploration. Society for Sedimentary Geology, Calgary, pp 1-32

Pemberton SG, Spila M, Pulham AJ, Saunders T, MacEachern JA, Robbins D, Sinclair IK (2001) Ichnology & sedimentology of shallow to marginal marine systems: Ben Nevis & Avalon Reservoirs, Jeanne D'Arc Basin. Short course volume 15. Geological Association of Canada, Newfoundland

Pillay D, Branch GM, Forbes AT (2007) The influence of bioturbation by the sandprawn *Callianassa kraussi* on feeding and survival of the bivalve *Eumarcia paupercula* and the gastropod *Nassarius kraussianus*. Journal of Experimental Marine Biology and Ecology 344: 1-9

Powell AWB (1979) New Zealand Mollusca: marine, land and freshwater shells. William Collins Publishers Ltd, Auckland

Probert PK, Grove SL (1998) Macrobenthic assemblages of the continental shelf and upper slope off the west coast of South Island, New Zealand. Journal of the Royal Society of New Zealand 28: 259-280

Probert PK, McKnight DG, Grove SL (1997) Benthic invertebrate bycatch from a deep water trawl fisher, Chatham Rise, New Zealand. Aquatic Conservation Marine and Freshwater Ecosystems 7: 27-40

Probert PK, Read GB, Grove SL, Rowden AA (2001) Macrobenthic polychaete assemblages of the continental shelf and upper slope off the west coast of the South Island, New Zealand. New Zealand Journal of Marine and Freshwater Research 35: 971-984

Proffitt F (2006) Voyage reveals extraordinary life around deep-sea gas seeps Media Release. Niwa Science Wellington

Pruski AM, Fiala-Medioni A (2003) Stimulatory effect of sulphide on thiotaurine synthesis in three hydrothermal0-vent species from the East Pacific Rise. The Journal of Experimental Biology 206: 2923-2930

Read GB (2004) Guide to New Zealand Shore Polychaetes

Rullkotter J (2006) Organic matter: the driving force for early diagenesis. In: Schulz HD, Zabel M (eds) Marine geochemistry. Springer, Berlin, pp 125-168

Sahling H, Galkin SV, Salyuk A, Greinert J, Foerstel H, Piepenburg D, Suess E (2003) Deep-related structure and ecological significance of cold-seep communities - a case study from the Sea of Okhotsk. Deep Sea Research I 50: 139-1409

Sahling H, Rickert D, Lee H, Linke P, Suess E (2002) Macrofaunal community structure and sulfide flux at gas hydrate deposits from the Cascadia convergent margin, NE Pacific. Marine Ecology Progress Series 231: 121-138

Savrda CE (2007) Taphonomy of trace fossils. In: Miller W, III (ed) Trace fossils: concepts, problems, prospects. Elsevier, Amsterdam, pp 93-109

Schulze A (2003) Phylogeny of Vestimentifera (Siboglinidae, Annelida) inferred from morphology. Zoologica Scripta 32: 321-342

Seibold E, Berger WH (1993) The sea floor. An introduction to marine geology. Springer-Verlag, Berlin

Seilacher A (2007) Trace Fossil Analysis. Springer, Berlin

Sellanes J, Quiroga E, Neira C (2008) Megafauna community structure and trophic relationships at the recently discovered Concepcion methane seep area, Chile, ~36 ºS. Journal of Marine Science 65: 1102-1111

Shank TM, Fornari DJ, Von Damm KL, Lilley MD, Haymon RM, Lutz RA (1998) Temporal and spatial patterns of biological community development at nascent deep-sea hydrothermal vent ($9^o50'$N, East Pacific Rise). Deep Sea Research II: 465-515

Sibuet M, Olu K (1998) Biogeography, biodiversity and fluid dependence of deep sea cold seep communities at active and passive margins. Deep Sea Research II 45: 517-567

Sommer S (in press) Benthic respiration in a noval seep habitat dominated by dense beds of ampharetid polychaetes at the Hikurangi Margin (New Zealand). Marine Geology

Sommer S, Linke P, Pfannkuche O, Bowden DA, Haeckel M, Greinert J, Thurber AR (2008) Novel cold seep habitat along the Hikurangi Margin (New Zealand) European Geosciences Union General Assembly 2008, Vienna, Austria

Southward AJ, Southward EC, Dando PR, Hughes JA, Kennicutt MC, Alcala-Herrera J, Leahy Y (1997) Behaviour and feeding of the nassariid gastropod *Cyclope neritea*, abundant at hydrothermal brine seeps off Milos (Aegean Sea). Journal of Marine Biology Association U.K. 77: 753-771

Suess E (1980) Particulate organic carbon flux in the oceans-surface productivity and oxygen utilization. Nature 288: 260-263

Tarasov V, Bogovski S, Muzkya V (2003) Biochemical characteristics of alga-bacterial mats and invertebrates from shallow-water hydrothermal fields of the West Pacific Ocean. Aquatic Science: 73-80

Taylor AM, Goldring R (1993) Description and analysis of bioturbation and ichnofabric. Journal of Geological Society, London 150: 141-148

Taylor JD, Glover EA (2006) Lucinidae (Bivalvia) - the most diverse group of

chemosymbiotic molluscs. Zoological Journal of the Linnean Society 148: 421-438

Thurber AR, Levin LA, Baco A, Smith CR, Rowden AA, Bowden DA, Kroeger K (2008) Metazoan use of chemosynthetic food sources at New Zealand cold seeps European Geosciences Union General Assembly 2008, Vienna, Austria

Treude T, Boetius A, Knittel K, Wallmann K, Jorgensen BB (2003) Anaerobic oxidation of methane above gas hydrates (Hydrate Ridge, OR). Marine Ecology Progress Series 264: 1-14

Treude T, Niggemann J, Kallmeyer J, Wintersteller P, Schubert CJ, Boetius A, Jorgensen BB (2005) Anaerobic oxidation of methane and sulfate reduction along the Chilean continental margin. Geochimica et Cosmochimica Acta 69: 2767-2779

Tucker M (1990) Carbonate depositional systems II: deeper-water facies of pelagic and resedimented limestones. In: Tucker ME, Wright VP (eds) Carbonate sedimentology. Blackwell Scientific Publications, Oxford, pp 228-283

Tunnicliffe V, Juniper SK, Sibuet M (2003) Reducing environments of the deep-sea floor. In: Tyler P (ed) Ecosystems of the deep oceans: ecosystems of the world 28. Elsevier Science B.V., Amsterdam, pp 81-110

Tyler PA (2003) Ecosystems of the world: ecosystems of the deep oceans. Elsevier, Amsterdam

Tyson RV (1995) Sedimentary organic matter. Chapman & Hall, London

Uchman A (2007) Deep-sea ichnology: development of major concepts. In: Miller W (ed) Trace fossils concepts, problems, prospects. Elsevier, Amsterdam, pp 248-267

Udden JA (1914) Mechanical composition of clastic sediments. Bulletin of the Geological Society of America 25: 655-744

Van Dover CL (2000) The ecology of deep sea hydrothermal vents. Princeton University Press, Princeton, N.J.

Van Dover CL (2002) Community structure of mussel beds at deep-sea hydrothermal vents. Marine Ecology Progress Series 230: 137-158

Van Dover CL, Aharon P, Bernhard JM, Caylor E, Doerries M, Flickinger W, Gilhooly W, Goffredi SK, Knick KE, Macko SA, Rapoport S, Raulfs EC, Ruppel C, Salerno JL, Seitz RD, Sen Gupta BK, Shank T, Turnipseed M, Vrijenhoek R (2003) Blake Ridge methane seeps: characterization of a soft-sediment, chemosynthetically based ecosystem. Deep Sea Research I 50: 281-300

Van Dover CL, Lutz RA (2004) Experimental ecology at deep-sea hydrothermal vents: a perspective. Journal of Experimental Marine Biology and Ecology 300: 273-307

von Cosel R, Marshall BA (2003) Two new species of large mussels (Bivalvia: Mytilidae) from active submarine volcanoes and a cold seep off the eastern North Island of New Zealand, with description of a new genus. The Nautilus 117: 31-46

Wallman K, Linke P, Suess E, Bohrmann G, Sahling H, Schluter M, Dahlmann A, Lammers S, Greinert J, von Mirbach N (1997) Quantifying fluid flow, solute mixing, and biogeochemical turnover at cold vents of the eastern Aleutian subduction zone. Geochimica et Cosmochimica Acta 61: 5209-5219

Waren A, Ponder W (1991) New species, anatomy, and systematic position of the hydrothermal vent and hydrocarbon seep gastropod family Provannidae fam.n. (Caenogastropoda). Zoologica Scripta 20: 27-56

Wentworth CK (1922) A scale of grade and class terms for clastic sediments. Journal of Geology 30: 377-392

Wetzel A (1991) Ecologic interpretation of deep-sea trace fossil communities. Palaeogeography, Palaeoclimatology, Palaeoecology 85: 47-69

Young DK, Jahn WH, Richardson MD, Lohanick AW (1985) Photographs of deep-sea lebensspuren: a comparison of sedimentary provinces in the Venezuela Basin, Caribbean Sea. Marine Geology 68: 269-301

Zobell CE, Morita RY (1956) Bacteria in the deep sea. In: Bruun AF, Greve SV, Mielche H, Sparck R (eds) The Galathea Deep Sea Expedition: 1950-1952. George Allen & Urwin Ltd, London, pp 201-210

Appendix 1. Statistics for grain size distribution for all core samples based on Folk and Ward method (Blotts, 2001).

Core No.	Horizon	Mean (M_G)	Sorting (σ_G)	Skewness (Sk_G)	Kurtosis (K_G)	Mode 1 (µm)	Mode 2 (µm)
51-1B	D	14.550	5.911	0.178	0.891	8.148	148.3
51-1B	C	19.040	6.974	0.226	0.746	8.148	224.4
51-1B	B	11.570	5.936	0.184	1.042	8.148	170.2
51-1B	A	8.632	5.252	0.134	1.098	7.097	112.5
51-2B	E	14.630	6.001	0.181	0.927	8.148	148.3
51-2B	D	19.390	6.126	0.191	0.758	8.148	170.2
51-2B	C	23.440	7.616	0.186	0.708	8.148	295.8
51-2B	B	10.880	5.480	0.164	1.033	8.148	129.1
51-2B	A	9.997	4.953	0.111	1.139	9.355	224.4
51-3B	C	15.730	5.148	0.154	1.097	10.74	170.2
51-3B	B	13.110	6.173	0.159	0.958	8.148	129.1
51-3B	A	12.000	6.145	0.204	1.054	8.148	112.5
51-4B	C	19.140	5.967	0.202	0.785	8.148	170.2
51-4B	B	22.410	7.233	0.192	0.708	8.148	224.4
51-4B	A	12.140	6.444	0.207	0.982	8.148	148.3
51-5B	C	19.720	6.124	0.201	0.808	9.355	148.3
51-5B	B	9.570	5.263	0.143	1.114	8.148	
51-5B	A	12.850	5.942	0.173	1.067	9.355	
66-1B	C	64.41	6.361	-0.417	0.754	257.7	9.355
66-1B	B	77.55	7.354	-0.509	0.732	390.0	9.355
66-1B	A	11.88	6.007	0.169	1.079	9.355	447.7
66-2B	C	46.54	7.447	-0.229	0.712	295.8	9.355
66-2B	B	15.87	6.995	0.214	0.969	8.148	390.0
66-2B	A	9.335	4.578	0.078	1.044	9.355	
96-1B	C	29.20	6.781	0.074	0.712	257.7	9.355
96-1B	B	22.16	6.606	0.179	0.723	8.148	224.4
96-1B	A	12.38	6.494	0.197	0.938	7.097	112.5
96-2B	C	21.14	7.321	0.215	0.743	8.148	224.4
96-2B	B	19.48	7.015	0.208	0.772	8.148	224.4
96-2B	A	10.37	5.752	0.160	0.943	7.097	56.37
98-1B	C	36.88	7.741	-0.020	0.684	390.0	9.355
98-1B	B	12.16	6.135	0.169	0.973	8.148	
98-1B	A	16.23	7.194	0.196	0.878	8.148	295.8
98-2B	B	26.13	7.387	0.192	0.702	8.148	339.7
98-2B	A	17.20	7.132	0.188	0.884	8.148	295.8
156	D	9.915	3.152	-0.047	1.116	10.74	
156	C	9.167	3.078	-0.073	1.122	10.74	
156	B	9.354	3.285	-0.033	1.092	9.355	
156	A	9.418	3.430	-0.074	1.012	10.74	
158A	B	9.869	3.230	-0.029	1.081	10.74	
158A	A	10.45	3.635	-0.012	1.032	9.355	
158B	C	8.357	3.093	-0.081	1.080	9.355	
158B	B	10.39	3.313	-0.013	1.082	9.355	
158B	A	9.129	3.513	-0.057	1.004	9.355	
173	B	22.57	7.050	0.218	0.732	8.148	257.7
173	A	25.30	7.403	0.150	0.707	8.148	224.4

Core No.	Horizon	Mean (M_G)	Sorting (σ_G)	Skewness (Sk_G)	Kurtosis (K_G)	Mode 1 (µm)	Mode 2 (µm)
232-1A	D	30.01	6.964	0.131	0.708	9.355	339.7
232-1A	C	16.76	6.392	0.215	0.901	9.355	195.5
232-1A	B	15.49	6.658	0.183	0.875	8.148	112.5
232-1A	A	10.76	5.914	0.145	0.990	9.355	390.0
232-1B	C	7.158	3.521	0.023	1.102	8.148	
232-1B	B	10.59	5.023	0.134	1.065	8.148	
232-1B	A	9.728	5.005	0.095	0.982	8.148	
242	C	12.89	6.005	0.213	1.033	8.148	295.8
242	B	11.15	5.384	0.167	1.065	8.148	447.7
242	A	10.95	6.731	0.194	0.971	7.097	390.0
242B	C	12.65	6.143	0.201	0.994	8.148	85.32
242B	B	12.29	5.466	0.146	0.997	8.148	
242B	A	11.01	5.463	0.142	0.976	8.148	
261	C	42.32	6.790	-0.025	0.705	339.7	10.74
261	B	18.76	6.903	0.259	0.842	8.148	339.7
261	A	9.664	6.172	0.201	1.138	7.097	447.7
262	B	7.107	3.337	-0.006	1.137	8.148	
262	A	7.584	3.707	0.004	1.042	9.355	
262B	C	7.283	3.406	0.007	1.100	8.148	
262B	B	7.094	3.302	-0.024	1.052	8.148	
262B	A	7.821	3.599	0.021	1.082	8.148	
305-4	D	8.689	3.303	-0.084	1.013	9.355	
305-3	C	8.469	3.296	-0.085	1.018	9.355	
305-3	B	8.474	3.152	-0.086	1.036	9.355	
305-3	B	8.723	3.435	-0.072	1.008	9.355	
305-2	B	8.839	3.497	-0.097	0.978	10.74	
305-1	A	8.567	3.317	-0.093	1.010	10.74	

Appendix 2. Ternary plots for all core samples. (Nomenclature of sediments: S = sand, C = clay, M = mud, Z = silt, CS = clayey sand, MS = muddy sand, ZS = silty sand, SC = sandy clay, SM = sandy mud, SZ = sandy silt.)

SO191-2/51

SO191-2/66

SO191-2/96

185
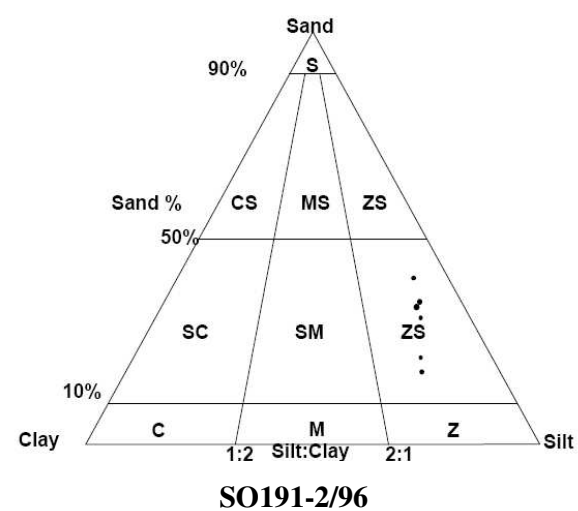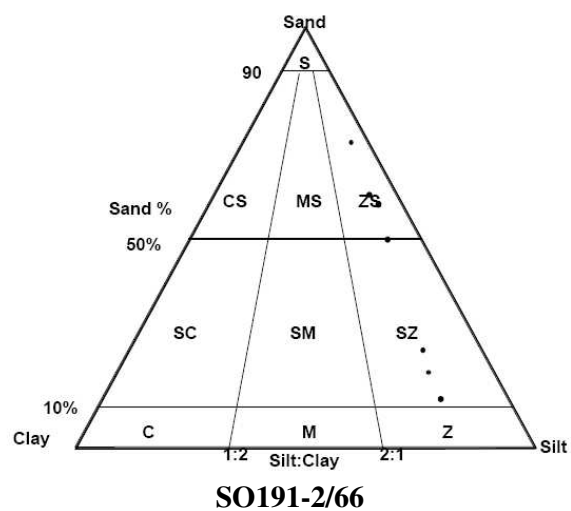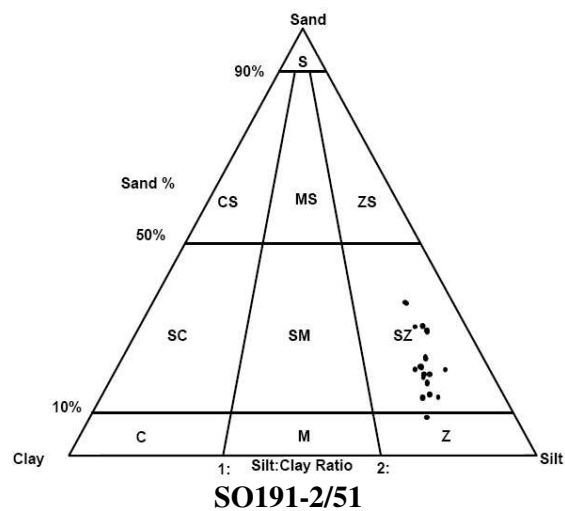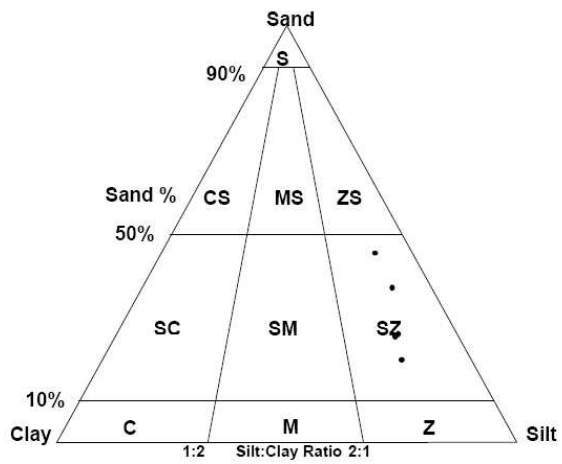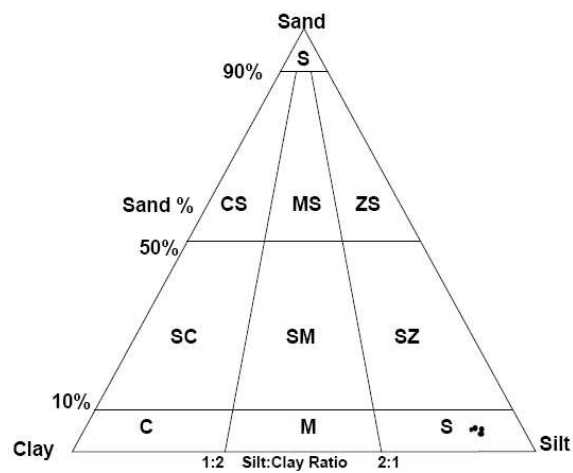
SO191-2/98
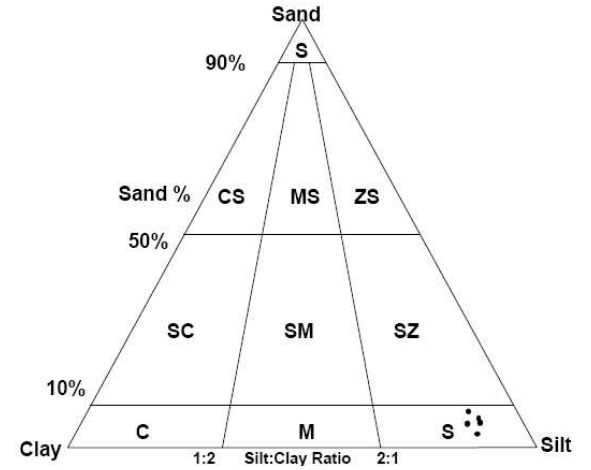
SO191-2/156

SO191-2/158
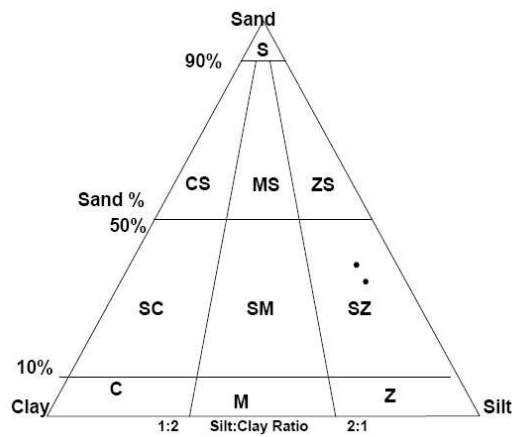
SO191-2/173
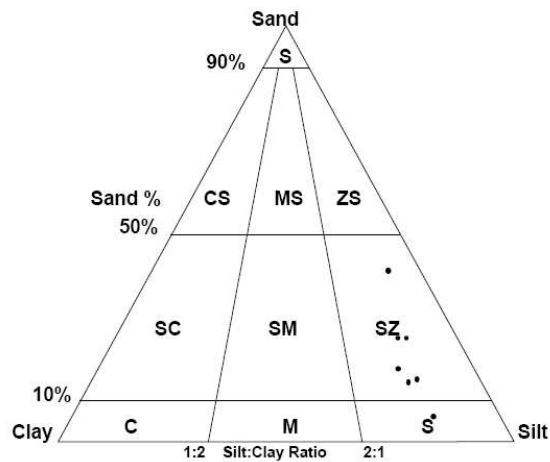
SO191-3/232
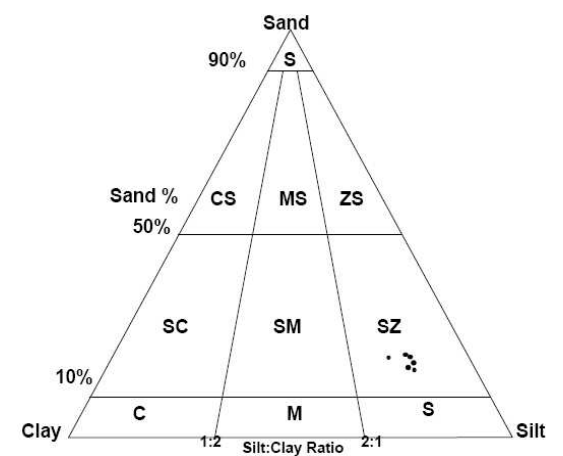
SO191-3/242
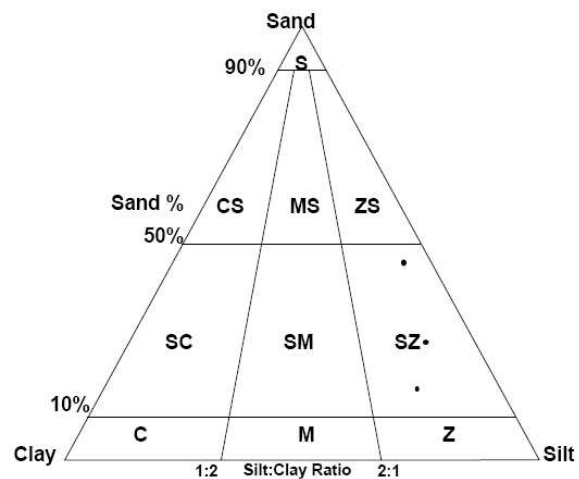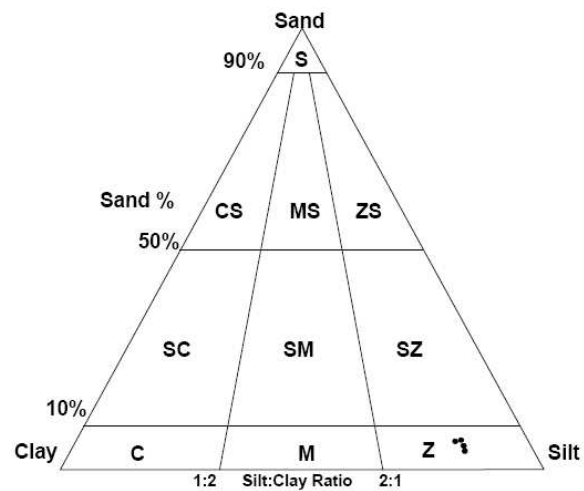
SO191-3/261   **SO191-3/262**   **SO191-3/305**
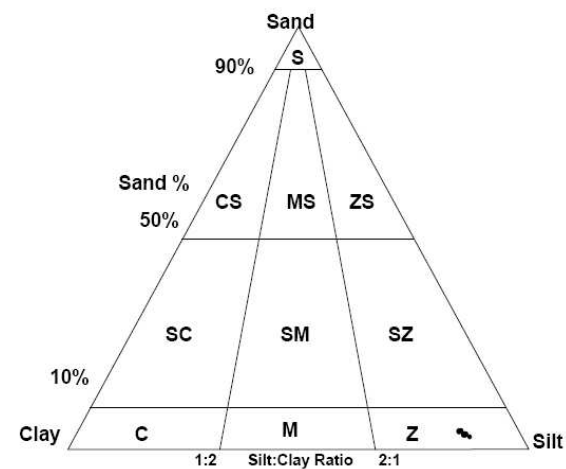
Appendix 3. Analytical results for core samples of nodular/banded carbonate and siliciclastic horizons in this study. Mineralogy: quartz (Qtz), plagioclase (plag), low Mg-calcite (LMC), high Mg-calcite (HMC), aragonite (Arag), K-feld (potassium-feldspar)(Courtesy of the Geology Department, University of Auckland)

Lab No.	Core No.	Horizon	Lithology	Carbonate wt%	TOC wt%	$\delta^{13}C$ ‰ PDB	$\delta^{18}O$ ‰ PDB	Mineralogy (Major; minor)
C29	51-1B	D	silt 1	10.8	0.566	−5.47	0.77	Qtz; plag, LMC
C73	51-1B	C	carbonate	64.7	0.659	−47.80	2.92	Arag; qtz
C30	51-1B	C	silt 1	17.6	0.355	−23.57	1.71	Qtz; plag, LMC, arag
C31	51-1B	B	silt 1	20.2	0.500	−24.80	2.02	
C32	51-1B	A	silt 1	23.8	0.497	-30.77	2.32	
C72	51-1B	A	carbonate	75.4	0.597	−46.68	2.70	Arag; LMC, HMC, qtz
C33	51-2B	E	silt 1	13.5	0.545	−16.92	1.54	
C34	51-2B	D	silt 1	11.7	0.517	−14.01	1.39	
C76	51-2B	C	carbonate	62.5	0.358	−49.14	2.94	Arag, Qtz; LMC, HMC
C35	51-2B	C	silt 1	19.8	0.452	−34.98	2.48	Qtz, Plag, Arag; LMC; HMC
C75	51-2B	B	carbonate	67.0	0.646	−50.29	3.21	Arag; qtz
C36	51-2B	B	silt 1	17.6	0.491	−22.03	1.96	Qtz; plag, LMC, HMC
C74	51-2B	A	carbonate	72.4	0.743	−49.14	3.14	Arag; qtz
C37	51-2B	A	silt 1	23.8	0.469	−29.67	2.43	Qtz; plag, L/HMC, arag
C38	51-3B	C	silt 1	10.7	0.550	−9.37	1.15	Qtz, Plag; LMC
C78	51-3B	B	carbonate	64.6	0.274	−48.43	2.99	Arag; LMC, qtz, plag
C39	51-3B	B	silt 1	27.1	0.406	−37.70	2.61	Qtz; plag, arag, L/HMC
C77	51-3B	A	carbonate	62.2	0.311	−47.78	3.01	Arag; LMC, HMC, qtz
C40	51-3B	A	silt 1	18.9	0.456	−22.55	1.97	Qtz; plag, LMC, HMC
C42	51-4B	C	silt 1	19.1	0.443	−29.34	2.17	Qtz, Plag; LMC, arag, HMC, K-feld
C43	51-4B	C	silt 1	20.8	0.504	−27.74	2.24	Qtz; plag, L/HMC, arag
C80	51-4B	B	carbonate	70.2	0.580	−49.34	3.05	Arag; LMC, qtz
C44	51-4B	B	silt 1	17.7	0.566	−20.49	1.85	Qtz; plag, LMC, HMC
C79	51-4B	A	carbonate	78.0	0.330	−49.96	3.20	Arag, Qtz; plag

Lab No.	Core No.	Horizon	Lithology	Carbonate wt%	TOC wt%	δ^{13}C ‰ PDB	δ^{18}O ‰ PDB	Mineralogy (Major; minor)
C45	51-4B	A	silt 1	18.3	0.489	–24.52	1.99	Qtz, Plag, LMC; HMC
C82	98-2B	B	carbonate	67.7	0.286	–48.73		Arag; qtz
C57	98-2B	B	silt 1	13.7	0.344	–24.49	1.90	Qtz; plag, arag, LMC
C81	98-2B	A	carbonate	76.6	0.701	–49.27	3.12	Aragonite; qtz
C58	98-2B	A	silt 1	14.6	0.420	–29.53	2.42	Qtz; plag, arag, L/HMC
C85	66-1B	C	carbonate	67.7	0.288	–48.28	3.08	Aragonite; qtz, plag
C46	66-1B	C	silt 1	4.6	0.46			Qtz; plag, LMC
C47	66-1B	B	silt 1	33.6	0.419	–44.39	2.92	Qtz, Plag, Arag; LMC, HMC
C84	66-1B	B	carbonate	71.2	0.115	–49.16	3.17	Arag, Qtz; plag
C48	66-1B	B	silt 1	10.1	0.329	–36.56	2.22	Qtz, Plag; arag, LMC
C83	66-1B	A	carbonate	75.4	0.253	–50.30	3.10	Arag; qtz
C49	66-1B	A	silt 1	14.1	0.457	-28.78	2.02	
C50	66-1B	A	silt 1	10.8	0.236	–36.48	2.61	Plag; qtz, arag
C59	158A	B	silt 1	4.1	0.923			Qtz; plag, LMC, HMC
C60	158A	A	silt 1	5	0.83	–0.63	0.99	Qtz, Plag; LMC
C51	96-2B	C	silt 2	8.9	0.45	–0.28	0.69	Qtz; plag, LMC, HMC
C52	96-2B	B	silt 2	8.9	0.412	–0.17	0.43	Qtz, LMC; plag
C53	96-2B	A	silt 2	10.6	0.447	–0.11	0.54	Qtz, LMC; plag
C54	98-1B	C	silt 2	13.5	0.337	–25.32	1.88	Plag; qtz, LMC, arag
C55	98-1B	B	silt 2	17.3	0.36	–34.52	2.23	Qtz; plag, arag, LMC
C56	98-1B	A	silt 2	14.3	0.398	–26.40	2.00	Qtz; plag, LMC, arag, HMC
C61	173-B	B	silt 2	9.7	0.481	–6.88	0.91	Qtz; plag, LMC
C62	173-B	A	silt 2	13.6	0.362	–14.10	1.58	Plag, Qtz; LMC
C63	261	C	silt 2	0.8	0.479	–0.52	1.44	
C64	261	B	silt 2	10.2	0.338	–26.97	2.66	
C65	261	A	silt 2	6.9	0.548	–2.18	0.04	Qtz, Plag; LMC, K-feld

Lab No.	Core No.	Horizon	Lithology	Carbonate wt%	TOC wt%	$\delta^{13}C$ ‰ PDB	$\delta^{18}O$ ‰ PDB	Mineralogy (Major; minor)
C66	305-D	D	silt 2	6	0.788	1.50	0.88	Qtz; plag, LMC, HMC
C67	305-C	C	silt 2	6.1	0.742	1.51	0.89	Qtz; plag, LMC, HMC
C68	305-B	B	silt 2	6.2	0.791	1.19	0.94	Qtz, Plag; LMC, HMC
C69	305-B	B	silt 2	5.9	0.765	1.49	0.84	Qtz; plag, LMC
C70	305-B	B	silt 2	8	0.777	1.38	0.73	Qtz, Plag; LMC, HMC
C71	305-A	A	silt 2	6.1	0.748	1.38	0.83	Qtz; plag, LMC, HMC

Appendix 4. Data of shell specimens from core samples

X-Ray Shell No.	AU No.	AUT No.	Leg	Station No.	Sub-sample	Gear Method	Family	Genus	Species	Height (mm)	Length (mm)	Width / tumidity (mm)	Horizon	Found at depth (cm) bsf
S1	19104	80	2	51	51-1B	TV-BC	Lucinidae	*Lucinoma*	*galathea*	35	41	11.25	C	4 cm bsf
S2	19104	113	2	51	51-1B	TV-BC	Lucinidae	*Lucinoma*	*galathea*	31.5	36	10.1	C	5.5 cm bsf
S3	19121	261	2	51	51-1B	TV-BC	Naticidae	*Falsilunatia*		11		8	C	6.5 cm bsf
	19123	91	2	51	51-2B	TV-BC	Vesicomyidae	*Calyptogena*		12	19.4	3.4	C	4-6 cm bsf
	19123	91	2	51	51-2B	TV-BC	patelliform			2.9	5		C	4-6 cm bsf
S4	19104	110	2	51	51-2B	TV-BC	Lucinidae	*Lucinoma*	*galathea*	21.1	24	6	B	21-23 cm bsf
	19122	263	2	51	51-2B	TV-BC	Solemyidae	*Acharax*	*clarificata*				D	3 cm bsf
S5	19123	264	2	51	51-2B	TV-BC	Vesicomyidae	*Calyptogena*		24			C	4 cm bsf
S6	19123	266	2	51	51-2B	TV-BC	Nassariidae	*Nassarius*	*ephamillus*	15.3		9.1	C	11 cm bsf
S7	19123	267	2	51	51-2B	TV-BC	Vesicomyidae	*Calyptogena*		23.26	48.36	10.35	C/D contact	3.5-7.8 cm bsf
S8	19124	268	2	51	51-2B	TV-BC	Nassariidae	*Nassarius*		15		9	B	20 cm bsf
S9	19125	269	2	51	51-2B	TV-BC	Provannidae	*Provanna*		3.5		1.9	A	29 cm bsf
S10	19126	137	2	51	51-3B	TV-BC	Lucinidae	*Lucinoma*	*galathea*	40.17	47.21	11.95	B	5-8 cm bsf
S11	19126	138	2	51	51-3B	TV-BC	Lucinidae	*Lucinoma*	*galathea*	28.45	33	13.2?	B	7-9 cm bsf
S12	19126	139	2	51	51-3B	TV-BC	Lucinidae	*Lucinoma*	*galathea*	26	29		B	9-10 cm bsf
S13	19126	140	2	51	51-3B	TV-BC	Lucinidae	*Lucinoma*	*galathea*	31.02	33.49	7.62	B	4.5-6 cm bsf
S14	19127	141	2	51	51-3B	TV-BC	Lucinidae	*Lucinoma*	*galathea*	33.9	37.22	21.37	A	23-25 cm bsf
		133	2	51	51-4B	TV-BC							B	2 cm bsf
	19128	274	2	51	51-4B	TV-BC	unidentified						B	10 cm bsf
	19128	275	2	51	51-4B	TV-BC	unidentified						B	10 cm bsf
	19129	107	2	51	51-5B	TV-BC	Nassariidae	*Nassarius*	*ephamillus*	15.5			B	4-12 cm bsf
S15	19129	278	2	51	51-5B	TV-BC	Vesicomyidae	*Calyptogena*					B/C contact	3-7.5 cm bsf
S16	19130	279	2	51	51-5B	TV-BC	Solemyidae	*Acharax*	*clarificata*				A	28.6 cm bsf
	19131	149	2	66	66-1B	TV-BC	unidentified						C	0-5 cm bsf

X-Ray Shell No.	AU No.	AUT No.	Leg	Station No.	Sub-sample	Gear Method	Family	Genus	Species	Height (mm)	Length (mm)	Width / tumidity (mm)	Horizon	Found at depth (cm) bsf
	19132	153	2	66	66-1B	TV-BC	unidentified						B	5-14 cm bsf
	19133	159	2	66	66-1B	TV-BC	unidentified						B	8-12cm bsf
S17	19131	283	2	66	66-1B	TV-BC	Vesicomyidae	*Calyptogena*		25.7	55.1	13	C	4-8 cm bsf
S17	19131	283	2	66	66-1B	TV-BC	Vesicomyidae	*Calyptogena*		19.5	44.1	6.4	C	4-8 cm bsf
S17	19131	283	2	66	66-1B	TV-BC	Vesicomyidae	*Calyptogena*		12	35	5	C	4-8 cm bsf
S18	19131	284	2	66	66-1B	TV-BC							C	7-9 cm bsf
S19	19131	287	2	66	66-1B	TV-BC	Vesicomyidae	*Calyptogena*		23.9	49.2	7.5	B	8-9 cm bsf
S20	19132	288	2	66	66-1B	TV-BC	Nassariidae	*Nassarius*	*ephamillus*				B	8-9 cm bsf
	19132	288	2	66	66-1B	TV-BC	unidentified						B	8-9 cm bsf
	19132	289	2	66	66-1B	TV-BC	Vesicomyidae	*Calyptogena*		21.8	45	6.5	B	7-13/17 cm
	19134	146	2	66	66-2B	TV-BC	Vesicomyidae	*Calyptogena*					C	0-5 cm bsf
S21	19134	291	2	66	66-2B	TV-BC	Vesicomyidae	*Calyptogena*		11	18.7	3.4	C	8 cm bsf
	19134	319	2	66	66-2B	TV-BC	Vesicomyidae	*Calyptogena*		18.3	35.5	5.3	C	
	19134	319	2	66	66-2B	TV-BC	Provannidae	*Provanna*		5.8		3.9	B	
		164	2	96	96-1B	BC	unidentified						C	0-3 cm bsf
	19135	294	2	96	96-1B	BC	Nassariidae	*Nassarius*	*ephamillus*	10.8		7.2	C	2 cm bsf
S23	-	15	2	98	98-1B	BC	Solemyidae	*Acharax*	*clarificata*					
		70	2	98	98-1B	BC	unidentified						A	11 cm bsf
S24		70	2	98	98-1B	BC	Nassariidae						A	11 cm bsf
	19137	95	2	98	98-1B	BC	Nassariidae	*Nassarius*	*ephamillus*	8.4		5.3	?	?
		116	2	98	98-1B	BC							C	2 cm bsf
		117	2	98	98-1B	BC							C	3 cm bsf
S25	19136	297	2	98	98-1B	BC	Vesicomyidae	*Calyptogena*		25.3	56.2	9.3	C	1.6-2.7 cm bsf
S26	19138	298	2	98	98-1B	BC	unidentified						A	22.5 cm bsf
	19136	317	2	98	98-1B	BC	Vesicomyidae	*Calyptogena*		12.9	21.8	3.35		
S27	19140	5	2	98	98-2B	BC	Vesicomyidae	*Calyptogena*			56.8		A	10-14 cm bsf
S28	19140	6	2	98	98-2B	BC	Vesicomyidae	*Calyptogena*		25	52.9		A	14-30 cm bsf

X-Ray Shell No.	AU No.	AUT No.	Leg	Station No.	Sub-sample	Gear Method	Family	Genus	Species	Height (mm)	Length (mm)	Width / tumidity (mm)	Horizon	Found at depth (cm) bsf
S29	19139	300	2	98	98-2B	BC	Vesicomyidae	*Calyptogena*		33.1	73.2		B	6 cm bsf
	19140	318	2	98	98-2B	BC	Vesicomyidae	*Calyptogena*		25	54.1			
S30	19141	301	2	156	156	TV-MUC	Naticidae			12.4		10	A	8-9 cm bsf
	19142	302	2	156	156	TV-MUC								
	19144	188	2	158	158A	TV-MUC	?						A	12-23 cm bsf
	19144	188	2	158	158A	TV-MUC	Naticidae	*Friginatica*					A	12-23 cm bsf
	19144	188	2	158	158A	TV-MUC	Nassariidae	*Nassarius*					A	12-23 cm bsf
	19144	188	2	158	158A	TV-MUC	Nassariidae	*Nassarius*					A	12-23 cm bsf
	19144	188	2	158	158A	TV-MUC	Nassariidae	*Nassarius*					A	12-23 cm bsf
	19144	188	2	158	158A	TV-MUC	?						A	12-23 cm bsf
	19144	188	2	158	158A	TV-MUC	?						A	12-23 cm bsf
S31	19143	304	2	158	158A	TV-MUC	Nassariidae	*Nassarius*	*ephamillus*	14		8.5	B	9 cm bsf
S32	19144	306	2	158	158A	TV-MUC	Nassariidae	*Nassarius*	*ephamillus*	17.2		9.4	A	14 cm bsf
	19144	307	2	158	158A	TV-MUC							A	17 cm bsf
S33	19144	308	2	158	158A	TV-MUC	Nassariidae	*Nassarius*	*ephamillus*	14.5		9.2	A	17 cm bsf
	19145	192	2	158	158B	TV-MUC	Vesicomyidae	*Calyptogena*					A	18-25 cm bsf
	19145	310	2	158	158B	TV-MUC								
	19146	311	2	158	158B	TV-MUC								
S34	19146	312	2	158	158B	TV-MUC		*Flabellum*					A	19 cm bsf
S35	19146	313	2	158	158B	TV-MUC	Nassariidae	*Nassarius*	*ephamillus*	14		8	A	19.8-20.6 cm
S36	19146	313	2	158	158B	TV-MUC	Nassariidae	*Nassarius*	*ephamillus*	8		7	A	19.8-20.6 cm
S37	19146	313	2	158	158B	TV-MUC	Naticidae	*Friginatica*	*conjuncta*	13.5		11	A	19.8-20.6 cm
	19146	313	2	158	158B	TV-MUC							A	19.8-20.6 cm
	19148	176	2	173	173	TV-MUC							A	12.8-14.6
	19147	177	2	173	173	TV-MUC							B	2 cm bsf
	19148	178	2	173	173	TV-MUC							A	6.5-8.5 cm bsf
	19147	196	2	173	173	TV-MUC							B	0-5 cm bsf
	19147	196	2	173	173	TV-MUC	Nassariidae	*Nassarius*	*ephamillus*				B	0-5 cm bsf

X-Ray Shell No.	AU No.	AUT No.	Leg	Station No.	Sub-sample	Gear Method	Family	Genus	Species	Height (mm)	Length (mm)	Width / tumidity (mm)	Horizon	Found at depth (cm) bsf
19147		196	2	173	173	TV-MUC							B	0-5 cm bsf
19148		316	2	173	173	TV-MUC	Lucinidae	*Lucinoma*	*galathea*	22.1	25.1	5.4		
19148		316	2	173	173	TV-MUC	Vesicomyidae	*Calyptogena*						
19149		203	2	186	186	TV-MUC	Vesicomyidae	*Vesicomya*			9.6			
19149		203	3	186	186	TV-MUC	Provannidae	*Provanna*						
19151		209	3	232	232-1A	TV-MUC							B	13 cm bsf
19150		241	3	232	232-1A	TV-MUC	Vesicomyidae	*Calyptogena*					D	0-6 cm bsf
19151		247	3	232	232-1A	TV-MUC	unidentified						B	20-24 cm bsf
19151		209	3	232	232-1A	TV-MUC								
19152		206	3	232	232-1B	TV-MUC								
19153		254	3	232	232-1B	TV-MUC	unidentified						B	14-27 cm bsf
19154		226	3	242	242	TV-MUC							C	0-3 cm bsf
19155		229	3	242	242	TV-MUC	?Solemyidae	*?Acharax*	*?clarificata*				B	3-10 cm bsf
19156		231	3	242	242	TV-MUC	unidentified						A	10-18 cm bsf
-		256	3	242	242	TV-MUC	Solemyidae	*Acharax*	*clarificata*				B	6 cm bsf
19156		259	3	242	242	TV-MUC	unidentified						A	12-15 cm bsf
19157		205	3	242	242B	TV-MUC	Lucinidae	*Lucinoma*	*galathea*				A	20-22 cm bsf
19157		239	3	242	242B	TV-MUC	unidentified						A	12 cm bsf
	19104-17(7)		2	51		TV-BC	Vesicomyidae	*Calyptogena*		25.1	52.3	10		
	19104-17(7)		2	51		TV-BC	Solemyidae	*Acharax*	*clarificata*	24.2	66.9	5.5		
	19104-17(7)		2	51		TV-BC	Naticidae	*Friginatica*		21.2		20.4		
	19104-17(7)		2	51		TV-BC	Naticidae	*?Fasilunatia*		22.2		17.4		
	19104-17(7)		2	51		TV-BC	Turridae	*Splendrillia*		21.3		8.7		
	19104-17(7)		2	51		TV-BC	Nassariidae	*Nassarius*	*ephamillus*					
	19104-17(7)		2	51		TV-BC	Nassariidae	*Nassarius*	*ephamillus*					
	19104-17(7)		2	51		TV-BC	Nassariidae	*Nassarius*	*ephamillus*					
	19104-17(7)		2	51		TV-BC	Nassariidae	*Nassarius*	*ephamillus*					
	19104-17(7)		2	51		TV-BC	Vesicomyidae	*Vesicomya*		10	14	4		
	19104-17(7)		2	51		TV-BC			*ephamillus*					